Akilesh Ananth

ELECTRICAL AND OPTICAL DETECTION OF STREAMERS IN TRANSFORMER INSULATION

T̃U Delft

Electrical and optical detection of streamers in transformer insulation

By

Akilesh Ananth

to obtain the degree of **Master of Science,** in Electrical Engineering

at the Delft University of Technology,

to be defended publicly on Wednesday April 17, 2019 at 09:00 AM.

Student Number	4739892	
Supervisor:	Dr. ir. Armando Rodrigo Mor	
	Ir. Luc Dorpmanns	Royal Smit Transformer
	Ing. Radek Heller	TU Delft
Thesis committee:	Prof. Dr. ir. Rob Ross,	TU Delft
	Dr. ir. Armando Rodrigo Mor	TU Delft, supervisor
	Dr. ir. Marjan Popov	TU Delft

This thesis is under embargo

An electronic version of this thesis is available at http://repository.tudelft.nl/.

TUDelft

Acknowledgements

Akilesh Ananth

Delft, April 2019

Abstract

The use of esters as transformer insulation has been gaining increasing interest over the past few years because of their better environmental performance, higher resistance to the influence of moisture and for some particular liquids, higher flash point as well. However, in order to completely replace the traditional mineral oil and be considered as a viable insulating fluid for high voltage equipments, these liquids must have comparable responses to mineral oil under DC,AC, lightning impulse as well as switching impulse waveforms. The study of pre-breakdown phenomenon(streamer activity) under different stresses has proven to be crucial in determining the breakdown process taking place in transformer insulations.

To study the streamer characteristics in ester (MIDEL 7131) and mineral oil (Shell Diala Transformer oil), both electrical and optical techniques have been used in this thesis. Significant research was conducted in identifying the parameters for the selection of the optical sensor suitable for this application. Various diagnostic techniques were employed for accurate detection of streamers electrically as well as optically. Streamers were initially studied in the highly non uniform needle-plane geometry under DC and lightning impulse stress. This configuration represents the situation of a defect in the transformer. Pressboard was introduced at the needle tip to simulate the effect of triple point as a source of discharge. Experiments conducted in Lodz University of Technology proved to be crucial in understanding the optical detection of streamers under this configuration.

The main goal of this thesis was to detect streamers originating from transformer winding. For the first time, electrode arrangements involving transformer windings were tested in ester and mineral oil under lightning impulse for streamer activity. The thesis presents the various streamer signals obtained under different configurations and provides important analysis regarding the characteristics of streamers in transformer insulation. The possible effect of spacers between transformer windings and wooden blocks used in transformer coils in also analyzed. The tests performed in this thesis can contribute to the ultimate goal of understanding the difference in streamer propagation in real life electrode arrangements between ester and mineral oil.

Table of Contents

LIST OF FIGURES

11

14

15

LIST OF TABLES

1. Introduction

This chapter provides an overview of the investigations and experiments conducted in this thesis. The chapter begins with the use of the ester as transformer insulation and provides some background information about esters. Further, important terminologies used in this research are defined and the motivation behind the research is discussed. The chapter concludes with the research objectives, followed by the main research questions and the final outline of the research which will guide the readers through the rest of the thesis.

1.1 Ester as an alternate for transformer insulation

Transformer oil is one of the most important components in power transformers as they provide electrical insulation and act as a thermal coolant[4]. According to various statistics, most of the transformer failures have been found to be caused by insulation problems. The dielectric strength and performance of the oil directly affect the safety level of the transformer insulation. Oils used in the transformer insulation can get degraded as a result of the decomposition of hydrogen molecules after several years of use. This long term aging could result in the formation of various byproducts which are hazardous to the efficient operation of the transformer.

The use of synthetic and natural ester as transformer insulation has attracted significant attention over the past years with the increasingly strict environmental rules and regulations. Esters show a much better environmental performance when compared to mineral oils. These liquids are biodegradable and nontoxic, thereby present a very low threat to the aquatic life as well as the earth ground. Mineral oils contain various compounds such as petroleum, silicone, naphthene ,and aromatics that do not biodegrade and may also contain traces of carcinogens.

Higher flash point and fire points result in better fire safety characteristics for the esters when compared to mineral oils. The frequency and impact of fire during the operation of transformers is significantly lesser and provides better safety. It has also been shown that the hygroscopic nature of ester based oils helps in keeping the insulation paper dry for longer periods of time by absorbing the moisture and in the long run improve its lifetime. A more uniform distribution of the electric field is resulted in the paper dielectric insulating system due to the higher permittivity of esters when compared to mineral oils[5]. Electrical investigations on esters have shown that in terms of AC strength, both ester and mineral oil exhibit similar breakdown voltages. Moreover, esters are more resistant to the influence of moisture content on its electrical breakdown strength.

Also, the price of products based on mineral oils over the past 15 years has been continuously on the rise. The use of ester oils has proven to lead to long term economic benefits and promote longer transformer life.

At the same time, esters also have their drawbacks which can be summarized as follows:

- They can be easily oxidized and hydrolyzed and thus require the help of additives while being used in free breathing power transformers.
- The viscosity of esters is around 4 times that of mineral oils and hence, the use of esters will require attention to the oil gaps between the adjacent pressboards.

- Higher pour points could limit their use in cold climates
- Further, several researchers in the past have found out that the propagation of streamers is much faster in esters, thereby resulting in lower impulse breakdown strengths. Thus, the substitution of mineral oils with esters require a thorough understanding of the dielectric performance of esters and their impact on transformer design.

This thesis aims to analyze the propagation of streamers in ester under DC, AC ,and lightning impulse voltages. Since, the pre breakdown phenomenon is strongly linked to the breakdown phenomenon of dielectrics, investigating the streamer activity in ester and mineral oil could provide important differences with respect to their performance in different conditions.

1.2 Background- Ester

Esters are chemical compounds derived from acids(usually carboxylic acid) and alcohols. There are two main types of esters:

1.2.1 Natural Ester

These types of esters are refined from vegetable oil such as sunflower, cottonseed, olive, soya, etc. These vegetable oils are chemically very similar to polyesters and hence share their excellent environmental properties. Natural esters can be derived from single, double or triple unsaturated fatty acids. For example, natural ester FR3 is refined from soya bean with its primary molecular component being triglyceride which is a fatty acid ester. The optimal condition for natural esters involves the use of fluids with high concentrations of single unsaturated fatty acids[1]. Figure 1.1 depicts the chemical structure of triglyceride which contains a mixture of saturated and unsaturated fatty acids with up to 22 carbon length chains[2]

Figure 1. 1 : Chemical structure of triglyceride [3]

1.2.2 Synthetic Ester

Few of the most commonly used synthetic ester for transformer insulation include MIDEL 7131 and Elantas BecFluid 9902. MIDEL 7131 is categorized as a type T1, a halogen free pentaerythritol ester. Figure 1.2 shows the molecular structure of the ester where the four ester groups are depicted by the '-COOR' group. These esters show a very high

electronegative performance because of the oxygen atoms and as a result, possess higher relative permittivity. These esters are very environment friendly due to their biodegradable nature.

Table 1.1 compares the key physical, chemical and electrical properties of natural(FR3) and synthetic ester(MIDEL 7131)[3].

Figure 1. 2: Chemical structure of synthetic ester [3]

Property	Synthetic Ester	Natural Ester
PHYSICAL PROPERTIES		
Density at 20°C(kg/dm^3)	0.97	0.92
Viscosity at 40°C(mm^2/s)	28	34
Pour Point (°C)	-60	-21
Flash Point(°C)	275	316
CHEMICAL PROPERTIES		
Acidity(mg)	<0.003	0.004
Water Content(mg/kg)	50	30
ELECTRICAL PROPERTIES		
Breakdown voltage AC(kV)	**>**75(IEC 2.5mm)	56 (ASTM 2.0mm)
Dielectric Dissipation factor (90°C)	<0.03	0.03

Table 1. 1: Properties of natural and synthetic esters

1.3 Terminologies

This section provides the reader with a brief introduction about the terminologies and keywords that appear in this thesis. They are mentioned in a tabular form in alphabetical order.

BREAKDOWN VOLTAGE	The minimum voltage which causes a portion of the insulator to conduct electricity.
CORONA	Electrical discharges causing ionization of the fluid around the conductor due to high electric fields
COUPLING CAPACITOR	Device which helps to sense the PD pulse by blocking the power frequency signal and allowing the high frequency signals from the PD to reach the detection equipment.
ELECTRON AFFINITY	Energy released or absorbed on the addition of an electron to a neutral molecule to form a negative ion
ESTER	A class of organic compounds derived from acids(organic or inorganic) and alcohols.
FLASH POINT	Lowest temperature at which a liquid can form an ignitable mixture in air near the surface of the liquid
PARTIAL DISCHARGE PULSE	The voltage(or current) pulse that results during a partial discharge from the test object
POUR POINT	Temperature below which a liquid loses its flow characteristics
PULSE REPETITION RATE	The ratio of the total number of PD pulses for a particular time with the duration of this time interval
PRPD(PHASE RESOLVED PD) PATTERN	Very widely used to analyze the PD data by displaying the pulses generated in sync with the phase of the sine wave
PENTAERERYTHITOL	White, crystalline organic compound(polyol-$C_5H_{12}O_4$) which is the building block for the synthesis for various chemicals such as paints, explosives etc.

STREAMER CHANNEL	Channel through which the streamers propagate after its inception
STREAMER DISCHARGE	Transient electrical discharge characterized by a highly conductive channel of plasma which can eventually lead to breakdowns
SRS	Secondary reverse streamers are back discharges observed due to the reverse electric field induced during the falling (tail) period of the impulse voltage
TRIGLYCERIDE	Ester derived from glycerol and three fatty acids. It is the primary constituent of animal and vegetable fat

Table 1. 2: Definition of important terminologies used in the thesis

1.4 Motivation

Over the past decades, significant knowledge on the design and manufacture of transformer insulation has been gained in conjunction with the use of mineral oil. The use of ester as an alternate for power and distribution transformer insulation will considerably affect stress distribution between the various insulating components as shown in figure 1.3. Here, the voltage drop and electric field experienced in each material are a function of the width(d1 and d2) and the permittivity of the material. During AC fields, the stress distributes inversely proportional to the permittivity of the materials.
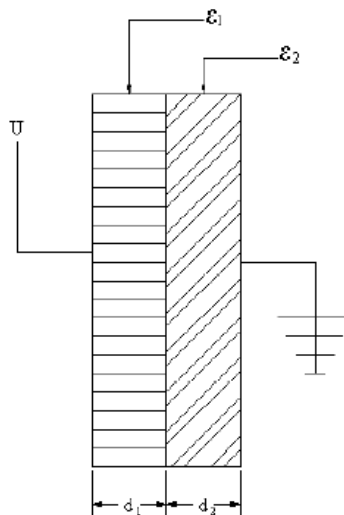
Figure 1. 3: Variation of electric field due to mediums with different permittivity [4]

Apart from providing an adequate level of dielectric strength in fluid filled transformers, the insulation structure used in the transformer should ensure a sufficient level of cooling and heat transfer from the windings. High levels of forces generated during various types of faults should be endured by the insulation without any failure. One of the most important

parts of the insulation system is the intern turn insulation. Short circuits in the inter turn insulation could result in serious damages to the transformer. Furthermore, the influence of the tangential component of the electric field on the insulation structure should also be investigated in order to ensure protection against creepage discharges

Transformers constantly experience both homogenous and inhomogeneous field configurations during their life time. Onload tap changers in regulated power transformers show many different electrode configurations as a result of their functional requirement[5]. Previous studies have shown that esters may have a lower withstand capability when compared to mineral oil in inhomogeneous field configurations. Furthermore, these tap changers have triple junction points(electrode-laminated PB-oil), which are the weakest point of the insulation and experience the highest fields. Such arrangements require in-depth investigation in order to ensure proper shielding to such points where creep discharges are likely to occur. Figure 1.4 shows the creepage discharge on the pressboard surface in mineral oil causing breakdown

Figure 1. 4: Creepage discharge in mineral oil [5]

1.5 Research Objectives

The ultimate goal of the research is to be able to test ester and mineral oil under various electrode configurations with and without the presence of solid interfaces. The results obtained from the investigations performed in this thesis will serve as a guideline to achieve the final goal. One such configuration is the Weidman curve. As previously stated, stress along the interface of the solid/liquid should always be within the specified limits for the safe operation of the transformer. EHV Weidman developed a design curve for the same which provides the safety margin for the tangential stress. Figure 1.5 shows a possible winding arrangement for tests to verify and develop creep design curves.

Figure 1. 5: Sample winding- Royal Smit Transformers

24

Though this thesis aims at the study of the lightning impulse tests, the final goal of the research is to obtain the design criteria for the following tests. These tests are conducted according to the IEC 60076-3 standard[6].

1.5.1 Line Terminal AC Withstand Test

This test is arranged in such a way that the test voltage appears between the terminal in test and earth. Testing of each phase takes place in turns. Depending upon the insulation of the low voltage winding, the tap position for the test is chosen. The procedure of the test time, frequency and voltage is similar to the induced voltage withstand test.

1.5.2 Lighting impulse test

These tests are performed in accordance with IEC 60060-1. For transformers which are liquid immersed, tests are performed with negative polarity generally in order to avoid external flashover in the test circuit. Sufficient time should be given before applying impulses of opposite polarity for the residual charges to decay. The test impulse for the full wave lightning impulse is 1.2/50us with a tolerance of 30% on the front time and 20% on the tail.

Chopped lightning impulse tests(LIC) are also performed on transformers with and without non-linear elements. The time to chopping of the impulse should be between 3us and 6us. The chopping circuit should be devoid of any additional resistance unless the swinging observed during the voltage application is greater than 30%.

1.5.3 Switching impulse test

During the SI tests, the voltage developed across the windings is proportional to the number of turns. The SI voltage test is specified to the winding with the highest U_m. For 3 phase transformers, the line terminal voltage should be approximately 1.5 times the line to neutral terminal voltage.

This thesis aims to provide a better understanding of the withstand capabilities of cellulosic insulation impregnated with ester. The investigations performed will be the first step towards the understanding of the performance of esters as an insulation medium in high voltage transformers. The thesis attempts to answer various questions regarding partial discharges and pre breakdown phenomenon in ester under AC, DC as well as lightning impulse voltages. These experiments and observations will assist transformer manufacturers to choose between different insulation oils used for power transformers. Further, a better understanding of the use of optical detection methods can be obtained from the studies done in this thesis. Through these measurements and statistical analysis, it is aimed to contribute to the environment by researching on the suitability of esters in power transformers and enable sustainable development. These objectives are summarized below to provide a clear picture of the thesis.

1.5.4 Partial Discharge in ester under AC stress

As mentioned earlier in the chapter, PDs are one of the major contributors to insulation failure in power transformers. Due to the difference in intrinsic properties and chemical composition between esters and mineral oils, evaluation of partial discharges in esters is vital to understand its performance as transformer insulating liquid. For this purpose, experiments related to partial discharge inception voltage, PD repetition rate have been performed along with the measurements of charge as well as current. IEC 61294 test procedure has been used as a reference for the same. Surface discharges and creepage discharges have been analyzed in this thesis using AC divergent field set up. The characteristics of PDs play an important role in determining the breakdown process in transformer insulations. This thesis uses the typical approach of stressing the dielectric with

divergent fields under AC field for 2 different configurations. Though the main focus of the thesis is recording streamers in oil under lighting impulse, tests performed initially to measure PD in ester provided useful information about the current signals to be expected during streamer measurement.

1.5.5 Prebreakdown phenomenon in ester and mineral oil under DC stress

Increased interest in High Voltage Direct Current(HVDC) application in transmission of energy over long lines has resulted in depth investigations of HVDC converter transformers which are essential components in the system. Understanding the discharge phenomenon in these transformers under DC and DC biased AC stress could provide important information about the performance of the system as a whole. Investigation of the pre breakdown phenomenon of transformer insulation under DC stress is a crucial aspect to understand the breakdown mechanism and dielectric performance in transformers. Investigations have been performed using electrical and optical methods to help analyze the streamer propagation in ester under DC stress.

1.5.6 Prebreakdown phenomenon in ester and mineral oil under lighting impulse stress

In order to be considered as a suitable option for high voltage transformers as an insulating liquid, esters(and other alternate liquids) need to exhibit a similar response to lightning impulses as compared to mineral oils. Pre breakdown phenomenons are characterized by streamer channels which can eventually lead to the breakdown of the insulation. Previous studies concerning streamer propagation and breakdown under lightning impulse (LI) voltage have indicated that esters may behave worse than mineral oils at such types of voltage stresses, but the number of studies and knowledge in this area is still very limited. With the help of electrical detection techniques as well as advanced optical detection equipment such as photomultipliers and optical fibers, various investigations have been performed in this thesis to identify the pre breakdown phenomenon in ester and mineral oil under lightning impulse fields.

The electrical detection of streamers involves the analysis of several test set ups in order to ensure accurate measurements are recorded. This research aims to provide the diagnosis involved in the electrical detection and measurement of streamers under lightning impulse originating in the needle-PB arrangement as well as from transformer windings. The results obtained during these tests will then have to be compared to the ones obtained with the optical sensor in order to have a better understanding of the phenomena. For this purpose, several optical sensors have to be compared and the optimal one should be selected based on multiple factors. This thesis also discusses the steps involved in selecting such optical sensors and the methods involved in ensuring a working test set up for optical detection of streamers.

1.5.7 Breakdown of ester and mineral oil under DC and impulse stress

Several research workers in the past have studied the breakdown voltages of esters in quasi-uniform and non-uniform fields under lightning impulse. In order to perform the impulse tests, different methods such as the rising voltage method, up-down method, constant voltage method have been proposed by previous investigations. The experiments performed in this thesis will attempt to provide a suitable test set up for lightning impulse testing as well as DC testing of esters and mineral oil for different configurations. The use of esters are alternate liquids for transformer insulation can lead to a dispersion in breakdown voltages which has a significant effect on its performance and safety margin required in transformers. Moreover, the presence of triple point could also have a significant effect on the breakdown voltage. Hence, this thesis also conducts statistical analysis of the breakdown voltages to better understand the dielectric response of esters to lighting impulse voltages.

1.6 Research Questions

The following section summarizes the important research questions answered in this thesis.

- **DESIGN OF TEST CELL FOR STREAMER INITIATION**: Streamer propagation in transformer insulation is detected with the help of a divergent field set up with discharge on the surface of a pressboard. Streamers originating from needle tip as well as transformer winding are discussed in this thesis.
- **CHOOSING THE RIGHT OPTICAL AND ELECTRICAL DETECTION TECHNIQUE**: Several electrical detection techniques have been used in the past to detect partial discharge. Similarly, various optical detection systems are available, but the right kind should be adopted to clearly detect streamers. This thesis aims to provide a guide during the selection of measurement devices for optical and electrical detection of streamers.
- **DIFFERENCE IN STREAMER PROPAGATION IN ESTER AND MINERAL OIL UNDER NEEDLE-PB-PLANE ARRANGEMENT:** In order to be considered as a suitable high voltage transformer insulation, ester should have comparable AC, DC and lightning impulse voltage strengths. Study of streamer phenomenon in ester and comparison with streamer signals in mineral oil will shed more light on this topic.
- **POSSIBILITY OF USE OF ELECTRICAL AND OPTICAL DETECTION FOR DIFFERENT ELECTRODE ARRANGEMENT:** As mentioned in the earlier section, the final goal of this research is to implement the streamer detection techniques to more real life winding arrangements. This would help in assessing the viability of ester as a dielectric in high voltage applications. Experiments performed in this thesis aim to provide crucial information for the final research.

1.7 Research Outline

Table 1.3 represents the outline of the thesis and provides brief a description of the contents covered in each of the chapters. Though the thesis focusses more on the detection of pre breakdown phenomenon in ester under lightning impulse voltage, a brief discussion of the effect of AC and DC voltage has also been discussed. This proved to be a useful starting point to understand the discharge phenomenon in ester under different needle plane configurations and also the testing procedures involved in the high voltage laboratory. The needle plane configuration used in this thesis is only the starting point to completely understanding the effect of ester as transformer insulation in the windings.

Chapter Number	Chapter Name	Description
1	**Introduction**	This chapter provides a brief background of the thesis, research objectives and outline of the thesis
2	**Literature Review**	This chapter highlights the literature study conducted beginning with the partial discharge phenomenon, breakdown phenomenon, streamer theory, different techniques for detection of discharges, previous

		experimental works and different statistical techniques used.
3	**PD analysis in AC field distribution**	This chapter provides a brief introduction of the terminologies used in PD tests and presents the findings of the PD performance of ester using electrical detection under divergent field- corona and creepage discharges.
4	**Diagnosis of electrical test setup for streamer detection**	This chapter explains the process involved in preparing and tuning the test set up for the electrical detection of streamers under impulse and DC voltages.
5	**Diagnosis of optical test setup for streamer detection**	This chapter highlights the steps involved in preparing the test set up for the optical detection streamers. It discusses the optical sensor used in the thesis and the procedure involved in designing the set up to obtain accurate results
6	**Measurements and analysis of results**	This chapter presents the findings of the electrical and optical detection. The results obtained are further compared and interpreted to analyze the performance of ester and mineral under lightning impulse voltages as well as DC voltages. Measurement of streamer signals produced by transformer windings are also discussed.
7	**Conclusion and future work**	The outcomes and conclusion of the observations made in the various experiments presented in the thesis are discussed in this chapter. The chapter concludes by providing suggestions for future work to be carried.

Table 1. 3: Research outline

2. Literature Review

To understand the breakdown mechanism in esters and mineral oil, a thorough review of pre-breakdown phenomenons such as partial discharge activities and streamer propagation is important. This chapter begins with an introduction to the basics of the partial discharge phenomenon, its appearance and detection. This is followed by a discussion on the streamer theory to understand its initiation, occurrence, propagation as well as the polarity effect. After that, detection of streamers through optical techniques is reviewed. Following that, the various aspects of statistical analysis of breakdown voltages has been studied and discussed. Lastly, different procedure and arrangements that have been adopted in the past for testing esters as a suitable replacement for mineral oils as transformer insulation has been explained.

2.1 Breakdown in liquid dielectrics

When compared to solids and gases, the knowledge on electrical breakdowns in liquids is far less. One of the first theories about breakdown in liquids claims that ions are produced in liquids by the collision between liquid molecules and electrons. These ions move towards the cathode, resulting in field enhancement at that point and further emitting more electrons. When this feedback process becomes unstable, breakdown follows(established in 1953 by Goodwin and McFadyen). A major objection to the ionization theory was that inelastic collisions of electrons cannot provide sufficient momentum for ionization.

The theories that followed investigated the dependency of the liquid dielectric strength on suspended particles and other weak links which exists in the bulk or the surface of the liquid. Dissolved gasses, water droplets, ionic impurities, carbon particles etc. polarize in the presence of electric field and experience a force. The theory suggests that these particles could align due to the forces and form a stable chain bridging the electrode gap eventually causing breakdown.

Development in the field of high speed imaging techniques helped better understand the breakdown phenomenon. This led to the theory of streamer propagation in liquids which was further explained after investigating the behavior of liquids in divergent fields. These experiments have been discussed in the final section of the chapter. The streamer theory is one of the more widely accepted theories explaining the breakdown phenomenon in liquids comprising of streamer initiation, propagation and final breakdown. In divergent fields, streamer propagation is more dominant while in quasi uniform fields, the process comprises of streamer initiation as well as weak links in the liquid.

2.2 Partial Discharge

A classical definition of partial discharge is the name given to electrical discharges involving only a portion of a dielectric between two electrodes and which does not bridge the gap[7].In general terms, partial discharges are a result of a high level of local electrical stress concentration in the insulation or on its surface. The insulation may be comprised of solids, liquids, gaseous materials or a combination of these. Generally, such discharges appear as pulses having duration of much less than 1 μs.
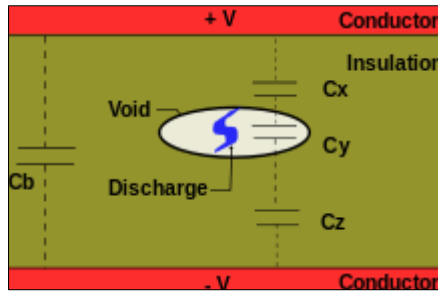
Figure 2. 1: Partial discharge in solid insulation

2.2.1 Partial Discharge classification

PD's are mostly restricted to the part of the dielectric material in use. In other words, they only partially bridge the electrodes between which the voltage is applied. From physical point of view self-sustaining electron avalanches may be created only in gases[8]. As a result, discharges are more likely to occur in gaseous voids or bubbles in both solid and liquid dielectrics. PD can be distinguished as follows:

INTERNAL DISCHARGE:

These types of discharges are a consequence of imperfections in the insulating medium such as gas filled cavities in solid dielectrics or gas bubbles in liquid insulations. Due to the fact that gases have a much lower dielectric strength than the insulation, the electrical stress inside the defect is equal to or greater than that in the surrounding medium. The enhancement of field in the defect also depends on its dimensions as well as the pressure inside. This will lead to the gradual deterioration of the insulation and further development of PD's will result in electrical treeing as shown in figure 2.2.

Figure 2. 2: Electrical treeing [9]

SURFACE DISCHARGES:

Such discharges arise along the dielectric interface as a result of substantial tangential field strength [10]. When compared to the internal discharges, field strengths to initiate surface discharges are lower. Surface discharges are very harmful to HV equipments and generally, thin layers are used to prevent them. When PDs are detected near their inception voltage, they show very little difference between internal and surface discharge. Hence, care has to be taken while distinguishing the two.

CORONA:

Corona is defined as a partial breakdown of insulation due to intensification of the electric stress at sharp edges or due to increased stress in one component of different insulating

30

materials in series [11]. They may occur at the HV electrode or the earth side or even between the electrodes. They result in a lot of interference during the measurements of PD's and hence it must be ensured that the test area is devoid of sharp points at all times.

2.2.2 Recurrence of discharges

PDs are recurrent in nature and constantly disrupt the output voltage. This can be explained with the help of a simple test circuit comprising a solid dielectric material between 2 electrodes(here, A and B) and a gaseous inclusion as shown in figure 2.3 [12].
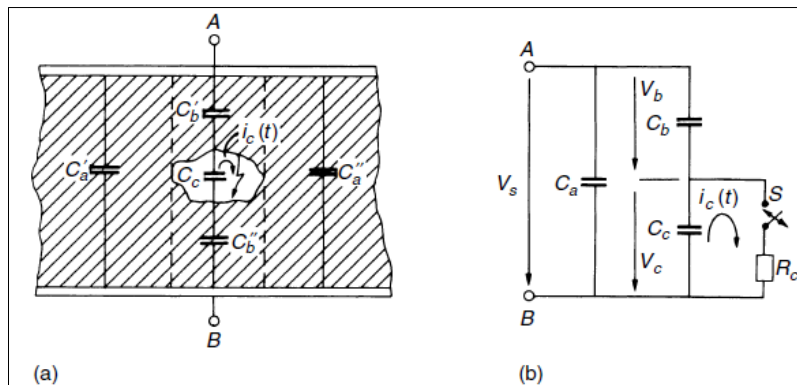
Figure 2. 3: Typical PD test object a) insulation with cavity b) equivalent circuit [12]

Field lines within the cavity are shown by C_c while those starting and ending at the cavity walls are represented by C_b' and C_b'' respectively. Field lines outside the cavity are represented by C_a.

When AC voltage is applied and the discharge occurs, the capacitance (C_c) gets charged and reaches the cavity's voltage breakdown and it is then recharged, repetitively. This is represented in figure 2.4 where U is the breakdown voltage and ΔV is the voltage drop limit [13]. This disruption of voltage output may also result in the potential rise of the total harmonic distortion. Through this model, it can also be seen that discharges, once ignited, can persist even below the inception voltage. In other words, the extinction voltage is lower than the inception voltage.
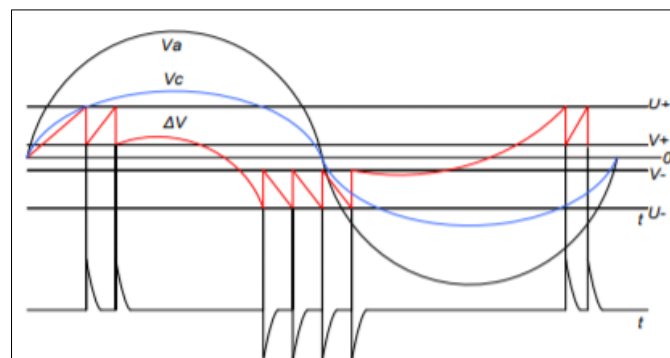
Figure 2. 4: Recurrence of Discharge [13]

31

2.2.3 Discharge detection

PD occurrences always results in various types of signals such as electromagnetic waves, sound and light. Chemical reactions in the transformer can lead to the evolution of gases. PD incidence on solid dielectrics as also produced ionizing rays [14]. This section reviews some methods of detecting and measuring PD's.

2.2.3.1 Electrical detection

This method includes conventional as well as the unconventional measurement of PDs. The conventional PD measurement is based on the standard for partial discharges IEC60270. This standard is used for measuring PD's that occur in electrical components, and associated systems when tested with alternating voltages up to 400 Hz or with direct voltage. Figure 2.5 depicts the typical measurement set up [15].
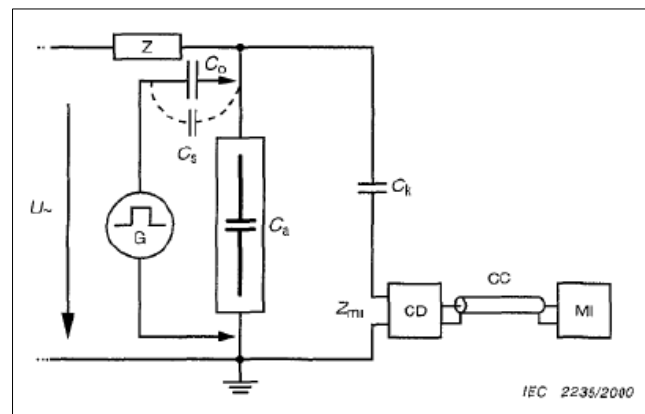
Figure 2. 5: PD Test Circuit

The set up consists of a high voltage source, which is preferably free of PDs, supplying voltage to the test object (shown as a capacitor). The coupling capacitor (CK) is connected in parallel and the measuring impedance is placed in series with this capacitor. The measuring impedance or coupling device (CD) measures the input PD current pulse and transforms it into an output voltage. The HV supply is provided with a blocking inductor in order to prevent discharges from the supply, if any, to interfere with the measurements. The signal is then measured by the oscilloscope after it passes through the transmission system (CC) which can be a coaxial cable or optical fibers.

The signal received from the PD source is optimized by the CD and CK, which often form a single unit. While measuring PDs according to the IEC standard, there are 2 different bandwidths specified:

- Wide Band: $100kHz \leq \Delta f \leq 400kHz$

- Narrow Band: $9kHz \leq \Delta f \leq 30kHz$

Δf stands for the width of the band. To obtain accurate measurement values, it is recommended that the bandwidth of the sensor is overlapping completely the bandwidth of the IEC filter. Z_{mi} comprises of LCR network where the inductance measures the low

32

frequency current during 50Hz voltage while the RC combination is capable of capturing the high frequency PD pulses. Conventional measurements suffer from electromagnetic interference which makes on site application difficult. Moreover, the sensitivity of measurements is influenced by the size and complexity of the object.

In the recent years, detection of EM pulses from PD activity has attracted more interest [16]. This type of unconventional measuring techniques is based on the very high frequency (VHF) band or the ultra-high frequency (UHF) band from 30 MHz to 300 MHz and 301 MHz to 3 GHz respectively. Un-conventional PD detection is used to provide result with suppressed noise or high signal to noise ratio. Moreover, they enable distributed measurements and evaluation of synchronous PRPD patterns [17]. These kinds of measurements replace the traditional quadrupole or CD with high frequency sensors (capacitive or inductive) which are capable of detecting the high frequency current pulses that occur during the PD. The signal is then sent to a computer with the PD software through coaxial cable and amplifier after spectral analysis.

2.2.3.2 Optical detection

Optical detection involves the detection of light which is a part of the EM emission due to partial discharge activities. Detection of light is applicable to external discharges. During the entire process of PDs, light radiations are constantly emitted. Thus, these radiations are considered as intrinsic property of PD activities, thus making optical detection a very intuitive means to study the various discharge properties [18].

PD detection using light has several advantages such as its high frequency response, immunity to EM interference and can also contribute to measuring various physical parameters and chemical elements. Latest techniques of detecting X rays and beta rays during PD activities in electrical cables, power lines and other equipments have also helped in the optical measurement of PDs.

2.2.3.3 Gas presence method

PD activity could alter the chemical composition of liquid dielectric and in the process, produce certain gases. Dissolved gas analysis is one of the reliable and sensitive techniques to identify the composition and diagnose the transformer without any interruption to its normal operation. DGA has been considered as a very effective means to indicate a developing fault in the transformer. Over the years, online monitoring version of DGA such as Hydrogen on line detection and photoacoustic spectroscopy (PAS) have been developed and used extensively. With the use of fiber optic sensors inside the transformer, online hydrogen detection could be implemented [19].

Another technique used in transformers is the hydrogen oil detector for monitoring the hydrogen concentration at regular intervals with the help of portable gas chromatograph [20]. Current research on highly sensitive fiber Bragg grating (FBG) sensor has found out that oil immersed sensors are very fast in detecting PD-related gaseous emissions [21]. Though a lot of techniques for chemical detection of PDs exists, the main disadvantage is that these methods are unable to locate the position of the PD source accurately. Hence, their use for online monitoring of HV equipments is still limited.

2.2.3.4 Acoustic emission method

As the PDs propagate in oil, vaporization is caused around the hot stream of current. This creates mechanical explosions, thereby producing acoustic emissions which propagate through the dielectric as pressure wave signals. Mechanical vibrations and electrical arcing are also main sources of acoustic emissions. One of the main advantages of this method is

its invulnerability to EM interferences. It has also proven to be a very economic method. Detection of pressure waves are done with the help of microphones, piezoelectric transducers (PZT) as well as accelerometers [22].

Due to the incapability of calibrating acoustic signals accurately, this method is often combined with other techniques to detect PDs. Moreover, the AE-based technique is unable to locate PD source that comes within the transformer's winding due to rapid signal attenuation when passing through different mediums [21].

2.2.3.5 Combinational methods

Over the years, research has produced several good results for combinational methods to create a robust technique and overcome the challenges of on-site PD detection. For example. The combination of optical and acoustic techniques has been investigated for better location and inspection of PD. Using the acoustic signals to locate the PD source and confirming the origin of the signal with the help of fluorescent optical fibers has been proposed in this scheme [23].In order to obtain an in depth understanding of the insulation condition, a combination of electrical, acoustic and DGA methods have been explored [24]. Further research on combining the common PD detection techniques with the uncommon ones has been proposed for the better inspection of PD in transformers.

2.3 Streamer ('Kanal') mechanism

The deviations from Townsend theory was initially observed during the investigation of avalanche growth using Wilson cloud chambers by Raether, Loeb and Meek [25]. This experiment showed that as the length of the avalanche increased, there was a distortion in the electric field caused by the negative and positive ions in the avalanche as shown in figure 2.7. The figure depicts the spherical representation of space charge at the head of the avalanche where the negative charges are ahead due to higher electron mobility. Right in front of the head of the avalanche, the field is enhanced
with field lines from the anode terminating at the head. Further back in the avalanche, the field is reduced due to the electrons and ions.
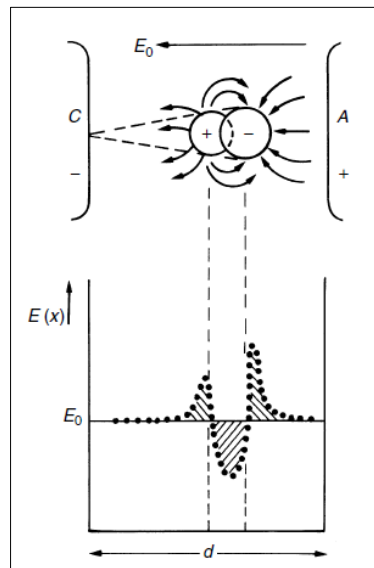
Figure 2. 6: Field distortion due to space charge distribution of an electron avalanche [12]

The increase in electric field causes the ionization coefficient to rise to such an extent that new avalanches are formed at the head of the original avalanche ,eventually bridging the gap. When the ion concentration exceeds 10^8, the critical number of ions will be reached. As a result, there is a steep rise in the avalanche current leading to breakdown.

2.3.1 Streamers in liquids

Streamers are luminous tree like figures which generally originate from a highly stressed electrode and eventually lead to breakdown. They are facilitated more easily in divergent fields, but their propagation is more restricted than in the uniform field. The velocity of streamers usually increases with voltage but in some cases can remain a constant until large overvoltages are applied. Positive streamers are faster than the negative streamers for a given liquid[20]. This can be attributed to the factor of diameter of the streamers. Diameter of negative streamer channels are 5-10 times the positive ones [27]. Due to a difference in direction of flow of charged particles, electric field in positive and negative streamer heads are found to be different. Typical values of electrical field in the positive streamer heads are around 2-4 times that of the negative streamer heads [49]. These weaker fields lead to a higher expenditure of energy in order to produce the initial electron pair. As a result of this, a larger expenditure of energy leads to a thicker and larger streamer. In other words, the positive streamer channels have a sharper tip ,leading to a higher field enhancement and more ionization in the liquid. This intrinsic difference between the radius stability of the positive and negative streamers enables the positive ones to propagate in lower electric fields.

Depending upon the liquid and applied voltage, streamers can propagate in a slow or fast mode. The slow mode comprises of the 1st and 2nd mode (few mm/us) while the fast mode constitutes the 3rd and 4th mode(tens of mm/us) of propagation. Generally, it is known that the 1st and 2nd mode are related to streamers with lower energies while the 3rd and 4th mode concern the higher energies [28].

The slow subsonic streamers are bush like while the fast ones are filamentary. Negative streamers of the lower modes respond to the addition of electron scavengers to the liquid with a marked increase in their velocities, while positive streamers are not responsive [26]. The propagation of streamers is associated with the production of current and light , both having similar shapes. They can be a continuous emission or can be observed as discrete pulses.

2.3.2 Streamer optical emission

Streamers are precursors of spark discharges. The high speed propagation of electrons in the streamers results in the excitation of species to higher levels in the streamer head. On falling back to lower excitation levels or ground states, energy is released in the form of photons. This phenomenon is used in streamer imaging and optical spectroscopy [48].

Various techniques including sub-nanosecond spectroscopic measurements have been used to determine properties such as electron density and electric field at the streamer head. For the investigations in optical detection of discharges, the following sensors have been used by researchers:

AVALANCHE PHOTODETECTOR

Avalanche photodiode (APD) is a highly sensitive light detecting sensor that converts light into electricity using photoelectric effect. This semiconductor electronic device is designed to work in the reverse breakdown region. When a high reverse bias voltage is applied, APD provides an internal current gain of up to 100 due to the avalanche effect. The high reverse voltage results in the amplification factor of 10^6 in the APD. Figure 2.7 depicts the working of the APD sensor.
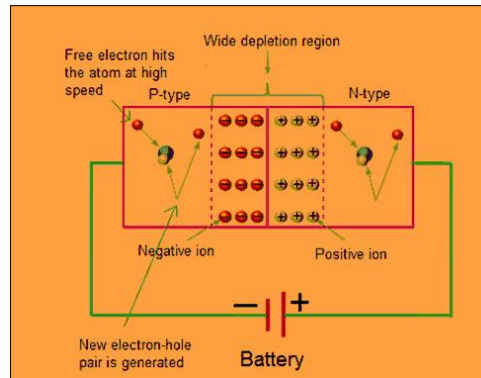
Figure 2. 7: Working of APD sensor [33]

SILICON PHOTOMULTIPLIER

SiPM are solid state single photon sensitive devices which feature low voltage operation, low sensitivity to magnetic interference, mechanical stability and highly uniform response[52]. They are a very attractive solution for optical detection of discharges owing to their high intrinsic gain and minimal excess noise. SiPM is an array of microcells where each microcell is connected in parallel with each other as shown in figure 2.8. When the microcell in the photomultiplier absorbs a photon, it fires and initiates a Geiger avalanche causing photocurrent to flow through the cell. The bias voltage is reduced below the breakdown value due to the voltage drop across the quench resistor and further Geiger avalanches are prevented. As recent as in 2017, silicon photomultipliers have been used by researchers in [31] for the optical detection of partial dischargers. In 2018, PD diagnosis in SF6 insulated systems have been carried out by [32] using SiPM based sensor arrays.
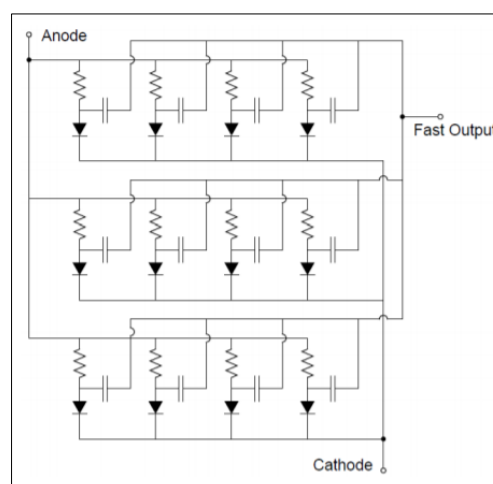
Figure 2. 8: Silicon photomultiplier [52]

36

PHOTOMULTIPLIERS(PMT):

PMTs are one of the most widely used optical sensors for the detection of dischargers and streamers in previous researches. In the past, several works have been carried out to investigate streamers with the help of PMTs. For example, as early as in 1961, fast photomultiplier techniques were used to study the streamer mechanism in breakdowns in Argon[34]. [35] used the Phillips 56AVP PMT to study the emission from Nytro10X when stressed at high fields. PMTs have also been successfully used to observe streamer activities in transformer insulations. Streamer propagation was investigated in 2016 in ester liquids under lightning impulse voltages using PMT by [28]. Chapter 4 discusses the working principle of the PMT in greater depth.

2.3.3 Streamer Breakdown

Studies on the prebreak down phenomenon under AC voltages in large air gaps has characterized the breakdown modes as either direct or streamer burst [29].

Lower distances are generally concerned with direct breakdowns where a single positive streamer leads to the bridging of gaps without being affected by the presence of impurities. Furthermore, the field in front of the head of the streamers are not affected by the electrode geometry. Direct breakdowns of oils are associated with the development of leader discharges extending from the stressed electrode as shown in the figure 2.9. They are characterized by recurring illuminations terminated by its extinction across the electrode gap [30].
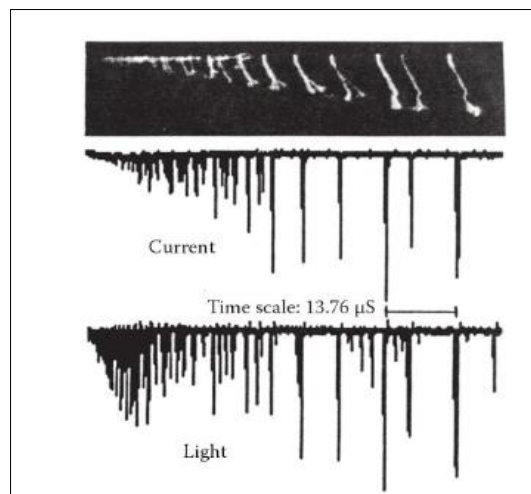
Figure 2. 9: Leader direct breakdown under positive polarity in oil in 60cm gap at 380 kV [30]

Streamer burst modes are specific to AC voltages, where low values of breakdown fields(<10 kV/cm) [29] are observed in addition to degradation of performance of oil insulation at large gaps. During bursts, the polarity of streamers changes corresponding to the AC cycle. Most of the times the bursts begin with positive streamers and end with positive or negative streamers.

Previous investigations have detected such events with the help of photomultipliers as shown in figure 2.10. The propagation of streamers corresponds to the impulses observed on the luminous signal. Breakdown was preceded by a burst of streams with the maximum duration of 20 bursts.
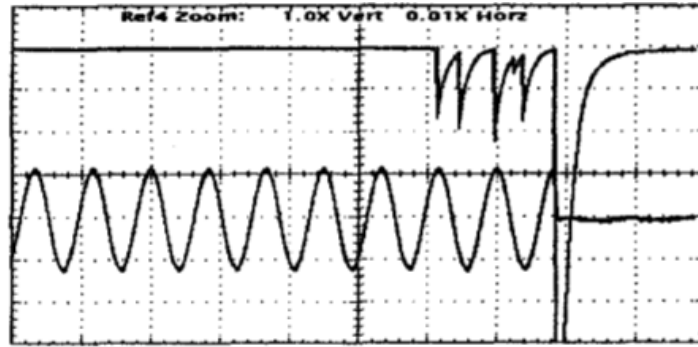
Figure 2. 10: Streamer burst leading to breakdown [29]

2.4 Statistical analysis

Several researchers over the past have investigated the breakdown voltage as well as partial discharge inception voltage and analyzed the data using statistical distribution. After performing statistical analysis on 100 AC breakdown voltages of ester and mineral oil, it was seen that at low probabilities, the breakdown performance of ester was similar to that of mineral oil [36]. Further, it was seen that for calculating withstand voltages at low levels, Weibull distribution is far more accurate than the Gaussian Distribution. Statistical analysis of the partial discharge inception voltage in natural esters by [37] concluded that variation of shape parameter, skewness and kurtosis are closely related to the type of oil and the aging conditions. Weibull distribution fitting of the breakdown voltages of esters under lightning impulse voltage in quasi uniform fields revealed that the withstand voltages at 1% breakdown probability of the ester liquids were close to that of the mineral oil [38]. Different statistical techniques have been used for understanding dielectric breakdown. Among all of them, Weibull distribution is the most widely used method.

2.4.1 Weibull Distribution

Mathematically, Weibull distribution is defined as follows: a random variable x is said to be Weibull distributed if its probability density function is given by [39]:

$f(x;\ \alpha, \beta)$

$$= \left(\frac{\alpha}{\beta^{\alpha}}\right) * x^{\alpha-1} * \exp\left(-\left(\frac{x}{\beta}\right)^{\alpha}\right), when\ x > 0;\ \alpha, \beta > 0$$

$$= 0, \qquad\qquad elsewhere$$

where α and β are the shape and scale parameter respectively.
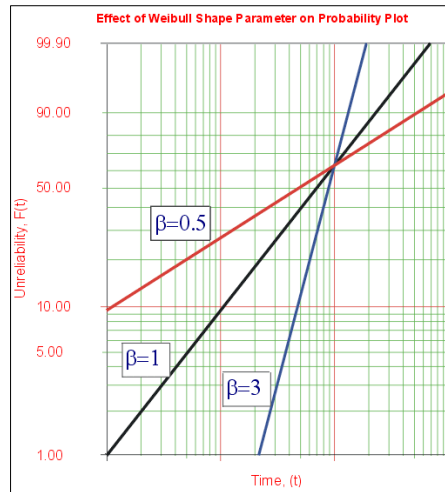
Figure 2. 11: Weibull plot for different scale parameters [40]

While performing the duration test, the Weibull distribution is based on the probability ΔP that a sample that is unbroken at time t will break down before t+Δt. This can be mathematically represented by using the double logarithmic function as:

$$\ln\{-\ln[1 - P(t))]\} = m * \ln(t) - m * \ln(t_o)$$

where m is the shape parameter and t_o is the scale parameter. For the probability curve P(t), time is projected in the horizontal scale as x=ln(t) while the vertical scale uses $\ln\{-\ln[1 - P(t))]\}$. The slope of this line is given by m, and the time constant t_0 is found at 63.2% probability. Weibull distribution is also used for endurance tests where the breakdown voltage (or electric field strength) is represented on the horizontal scale and the expression becomes:

$$P(u) = 1 - \exp\left[-\left(\frac{u}{u_o}\right)^b\right],$$

where u_o is the 63.2 % breakdown strength and slope *b* represent the scatter in results as shown in the figure 2.12 [10]
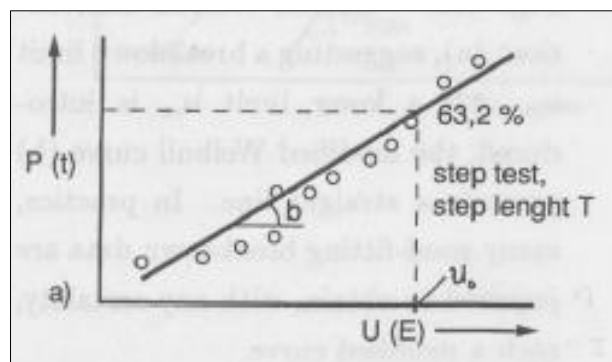
Figure 2. 12: Weibull plot for endurance test

39

Weibull distribution is used widely for comparing different design samples while checking for improvements in designs. Different design samples undergo breakdown tests and their Weibull curves are compared to see which design is better. In some cases when the endurance tests are performed at different levels, the Weibull distribution can be used to compare the results. Similarly, tests performed with different number of samples and volume can also be compared and analysed through Weibull plots. When a series of endurance tests are performed at different levels, the Weibull distribution can be used to estimate the slope of the life time curve of the sample.

In 1990, [41] showed that in some cases, Gumbel distribution, rather than Weibull distribution is a more appropriate form as its parameters could be better related to certain physical processes. Gumbel distribution, also referred to as the log-Weibull distribution is a type of generalized extreme value distribution that is used to model the distributions of maximum or minimum of a number of samples of various distributions.
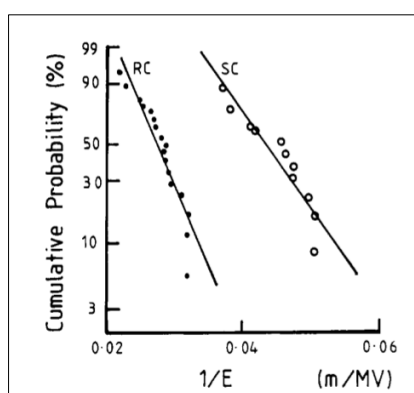
Figure 2. 13: Gumbel plot for BDV associated with Radiation cured (RC) and Steam cured (SC) XLPE cable [41]

2.5 Previous research on performance of transformer insulations under different configurations

This section reviews the different tests that have been performed on ester as transformer insulation to evaluate its performance based on its breakdown voltage, PDIV, streamer properties under lightning as well as AC stress. By highlighting some of the important experiments, it is hoped to present an overview of the performance of ester under different tests. This is an important section as it provides an outline to be followed to obtain significant results.

2.5.1 Breakdown voltage tests

Breakdown tests have been conducted based on different standards by several researchers. Based on the IEC 60156 (2.5mm gap) and ASTM 1816 (2mm gap), the breakdown voltage of ester liquids was found to be greater than 35 kV [42].Furthermore, the presence of moisture content in the liquid was investigated by [43]. It was found that the BDV of ester was not affected even with significant amount of moisture content. While for shorter gap lengths, the BDV of ester is similar to that of mineral oil, higher gap length shows a drastic reduction of BDV in case of esters [44].

2.5.2 Partial discharge test- AC stress

Several PD tests have been carried out in the past for both ester and mineral oils. The most common test setup involves the use of divergent field with the help of needle-plane or rod-plane configuration. Schematic diagram of the experimental setup for needle-plane electrode configuration PD test is shown in figure 2.14.
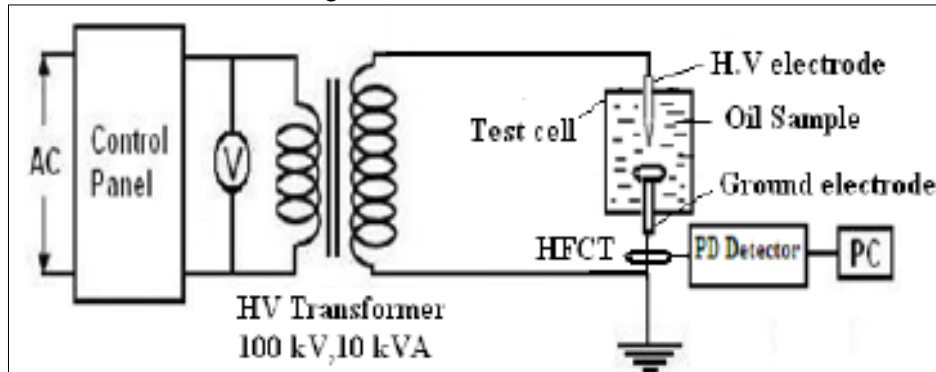
Figure 2. 14: PD detection test set up for needle plane configuration [37]

PD tests are regarded as quality control tests and their inspection can give details about the problems with the design and materials. Table 2.1 summarizes the PD behaviour of ester liquids as observed by several researchers over the past decade [42].

PD Characteristics	Performance of ester
PDIV(kV) (as per IEC 61294)	34 (similar to that of mineral oil)
PD Patterns(voltage is twice the PDIV)	Significant discharge activity in both cycles
PDIV- needle to plane	Performance of natural ester is slightly better voltages closer to PDIV
PDIV- point to plane with pressboard	Performance of natural esters is better at smaller gaps
Repetition rate	Slightly higher when compared to mineral oil

Table 2. 1: Performance of ester liquid under PD tests

2.5.3 Streamer characteristics under lighting impulse stress

Previous experiments of lightning impulse on different insulation liquids suggests that streamers propagate at lower voltages in esters when compared to mineral oils thus inducing lower breakdown voltages and lower time to breakdown in the liquid. In order to understand the streamer characteristics such as propagation velocity, stopping length, propagation modes. [28] used the experimental set up as shown in figure 2.15 and found

out that streamer channels formed in esters are much more energetic and propagate with higher velocity.

[45] performed polarity tests with lightning impulse on ester liquids and concluded that positive polarity appears to be the more unfavourable one for industrial applications. For quasi uniform fields it was concluded that impulse strength of esters is comparable to that of mineral oils [38].
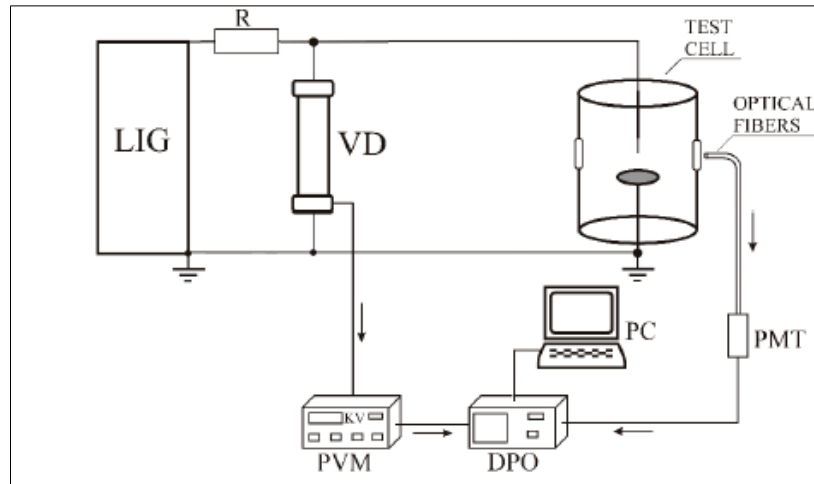
Figure 2. 15: Optical detection of streamers under LI stress in transformer insulation- Lodz University[28]

A summary of the different lightning impulse test procedures(non-uniform fields) and their findings is given in table 2.2 [42]:

Liquid characteristics under impulse	Performance of ester
Streamer propagation in long gaps	Lower BDV of ester for both polarity
Accelerating voltage	Lower for ester
Effect of pressboard on the ground electrode under lightning impulse	No significant effect
Empirical equation for BDV(kV)-positive polarity at gap distance d(mm)	$11.630 * d^{0.549}$

Table 2. 2: Performance of ester liquid under lightning impulse tests

Other lightning impulse tests suggest that the shape and propagation velocity of streamers is influenced by the rise time of the impulse. Impulses with shorter rise times have created faster streamers with larger diameters as compared the ones formed due to longer rise times around the needle electrode. Furthermore, it was seen that increasing the impulse voltage above a certain level caused a drastic rise in the streamer velocity due the high ionization energy of the molecules above the threshold electric field[47].

2.6 Summary

The desire to use safer and greener insulation liquids in transformer has led to several research works in the last few decades. Laboratory test set ups and investigations suggests that mineral oils behave better than ester liquids in extremely divergent field under impulse voltages. Difference in streamer propagation has been recorded to indicate higher probability of breakdown in ester under these conditions. However, experiments with slightly more realistic electrode arrangements suggest that ester liquids can be used at high voltages [46]. But designers have to take care to provide extra safety margins to compensate the faster streamer propagation in ester liquids. Though electrical and optical methods have been used in the past to detect streamers in transformer insulation in a small-scale set up, study of the pre-breakdown phenomenon for different electrode arrangements is yet to be conducted. This thesis aims to provide better understanding regarding the test set up and measurements related to streamer detection in small scale set up as well as in more real-life arrangements.

3. Partial discharge analysis of ester liquids

3.1 Introduction

Partial discharge activities in oil gaps and creepage discharges along the oil/pressboard interfaces are major causes of insulation failure in power transformers. As mentioned in the previous chapter, PDs are localized electrical discharges that only bridge a part of the insulation between two electrodes. These activities occur at points where the electric field is very high or enhanced due to material defects such as contaminants, sharp protrusions ,etc. These discharges play a significant role in the acceleration of thermal ageing and the chemical and physical degradation of the insulation oil.

Partial discharges are important signs of insulation faults in power transformers. Inter-turn insulation defects develop very fast and eventually lead to short circuits which can be highly dangerous. The close relationship between PD's and insulation defects make online PD monitoring a very crucial task [50]. Moreover, PD pulses lead to the development of streamers which can eventually lead to breakdown and formation of sludge in the insulation liquid. Barriers made out of pressboard in used in power transformers between the windings. Creepage discharges causes significant damage to the pressboard insulation. Investigation of creepage discharges is also very crucial for understanding PD behaviors in dielectric liquids.

Thus, degradation of the dielectric safety margin can be very harmful to the performance and life time of power transformers. Appropriate diagnostic techniques can help predict transformer failures and rectify them at early stages. Partial Discharge inception voltage(PDIV) is the voltage at which the ionization process begins, and partial discharges can be observed. To evaluate the intrinsic dielectric property of an insulation, the PDIV tests, evaluating corona and creepage dischargers in the insulation are all very relevant [57].

This chapter provides a useful insight about the partial discharge performance of ester liquids in divergent fields using different needle plane configurations. The chapter begins with a brief description of the various terminologies used for evaluating PDs, followed by the description of the sample preparation and test procedure. This thesis uses two different arrangements to simulate surface discharges as well as creepage discharges. The chapter concludes with the results and observations obtained during the tests along with their analysis.

3.2 Basic information about PD

3.2.1 Partial discharge inception voltage

With respect to industrial and laboratory tests, the definition of PDIV is different. As a result, the measurement of the inception voltage is significantly dependent on the definition. IEC 60270 and IEC 61924 have defined PDIV for industrial purposes. For laboratory tests, some

researchers have suggested that these specifications should be reviewed according to the latest detectors and sensors that are available for tests [52].

While IEC 60270 describes a conventional PD test technique for high voltage equipments in general, IEC 61924 introduces PDIV technique for liquid insulation. According to this standard, PDIV is the lowest voltage which first detected PD whose magnitude is greater than 100pC. IEC 60270 also defines PDIV as the voltage at which the PD pulse becomes greater than a specified threshold, but these measurements rely majorly on the choice of threshold value.

During this test according to IEC 61924, the voltage is increased at a constant rate of 1 kV/s, starting from zero until PD is detected. For the test procedure, the background noise level is required to be less than 50pC. While these prescriptions are reasonable for industrial testing, laboratory conditions have a sensitivity much better than 100pC. Research by [53] have found out that PDIV obtained using this procedure is much higher than those obtained using procedures which involve higher sensitivity and lower rate of voltage rise. For these tests, the background noise level is below 2pC and the detected charge for the first PD is much smaller.

Measurement of PDIV in ester using IEC 61294 suffers from few shortcomings as investigated by [54]. According to this research, the PDIV of ester under different ramping rates show no difference in AC voltage. Thus, the PDIV is measured by increasing in the voltage in steps of 1 kV with the duration of each step being sufficiently long enough to produce sufficient number of PDs at the same time not damage the needle tip due to erosion. In this chapter, PD signals are recorded continuously with step time of 1 minute and the lowest voltage at which the recorded PD pulse is greater than 100pC is chosen as the PDIV.

3.2.2 Creepage Discharges

Creepage discharges at the oil pressboard interface can be seen as the gradual development of conducting path associated with white and carbonized marks in transformers [55]. These white marks are a result of the heat from the discharges causing the oil and moisture to evaporate and decompose. Such discharges can cause significant damage to the pressboard insulation and thereby leading to the complete destruction of the transformer. Pressboards are manufactured by compressing several layers of cellulose paper and drying them. Excessive moisture content on the surface pf pressboard is one of the major causes of the discharges. Creepage discharges result in tracking on the surface of the pressboard on sustained AC stress as shown in figure 3.1. In some cases, high stress can cause instant flashover on the surface of the board and burn it due to high currents. Creepage discharges are minimized by controlling the tangential electrical field on the pressboard.
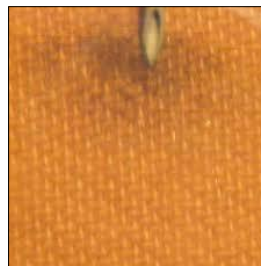
Figure 3. 1: Creepage discharges on pressboard [56]

3.3 Test set up and experimental procedure

3.3.1 Sample preparation

The ester used for the experiments was obtained from Royal Smit Transformers and was industry clean. The pressboard was processed according to the procedure suggested by [28]. It was first dried for 24 hours in a vacuum oven at a temperature of 105°C. This was followed by impregnation with the ester liquid in a vacuum oven at a temperature of 85°C for 24 hours and finally was placed in vacuum at ambient temperature for another 24 hours. Figure 3.2 shows the preparation of the pressboard in vacuum through drying and impregnation.
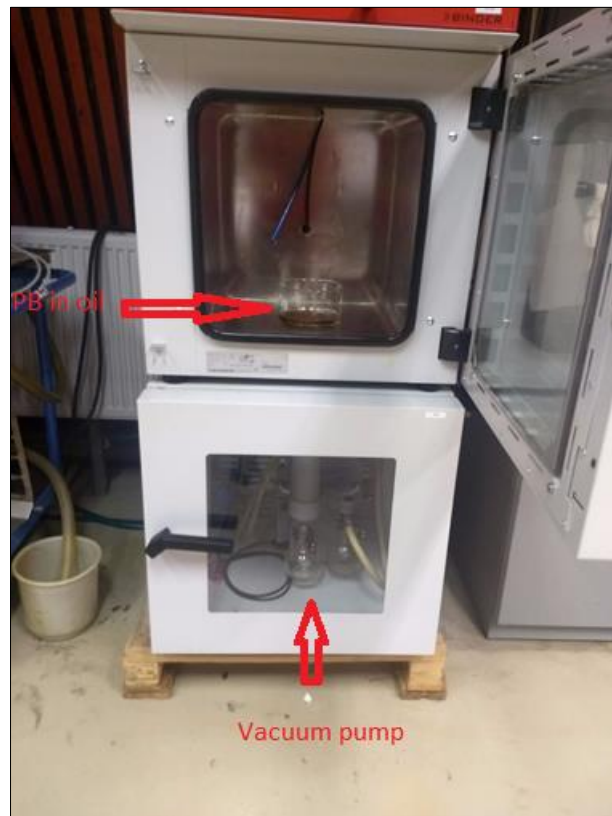
Figure 3. 2: Preparation of PB using vacuum pump

3.3.2 Experiment

The experimental set up is shown in figure 10. The HV supply is obtained from a 500V/200 kV Haefely supply transformer. A 1MΩ resistor is connected between the HV source and test cell to limit the current during breakdowns. To further protect the circuit against the high energy during flashovers and prevent damage to the test cell, overcurrent relay at the low voltage side is set to trip the power supply. A coupling capacitor of 1200pF was used in parallel to the test set up and connected to the PD detector through a measuring impedance. The background noise level was checked before the start of the experiment to ensure that it does not influence the measurements. The circuit diagram of the set-up is shown in figure 3.3.
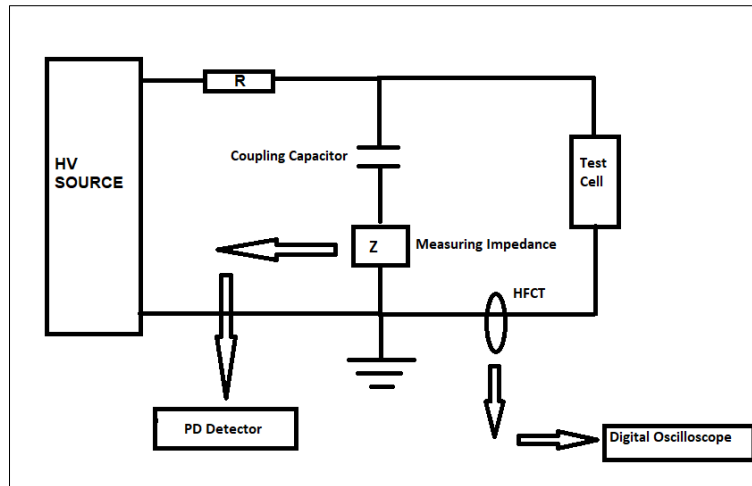
Figure 3. 3: Schematic diagram of PD measurement

For measuring corona discharges in oil, a needle-plane configuration is chosen as shown in figure 3.4(a). The cylinder test cell is made out of hard plastic and has a capacity of 4L. The test cell is fitted with a ground electrode inside on top of which the pressboard is placed. The needle is made out of tungsten and has a sharp tip in order to create high electric fields for initiating the discharges in oil. The tip radius is measured to be 50um and the length of the needle is 10mm. The distance between the needle tip and pressboard is fixed at 2.5cm. The pressboard is 5mm thick with a radius of 4.5cm.

The simulation of creepage discharges is performed by using the needle plane configuration in a glass aquarium as shown in figure 3.4(b). The aquarium was insulated from the ground in order to prevent the influence of the surrounding objects at ground potential. The adjustable arm of the HV needle is positioned such a way that the needle was at an acute angle with respect to the pressboard. Copper plate is chosen as the ground electrode in this investigation. The gap between the ground plate and the needle tip is fixed at 2.5cm. The short duration of the tests ensured that no tracking damage could be observed on the pressboard.

a)   b)

Figure 3. 4: a) Simulation of corona discharges in ester b) Simulation of creepage discharges in ester

47

3.3.3 Current measurement

High Frequency current sensors are very useful in detecting PDs and other transient signals. They consist of an induction coil with a ferromagnetic core , generally clamped in the ground wire of the earthing network. As shown in figure, the HFCT measures the induced voltage over the measuring impedance when the PD current pulse flows through It.
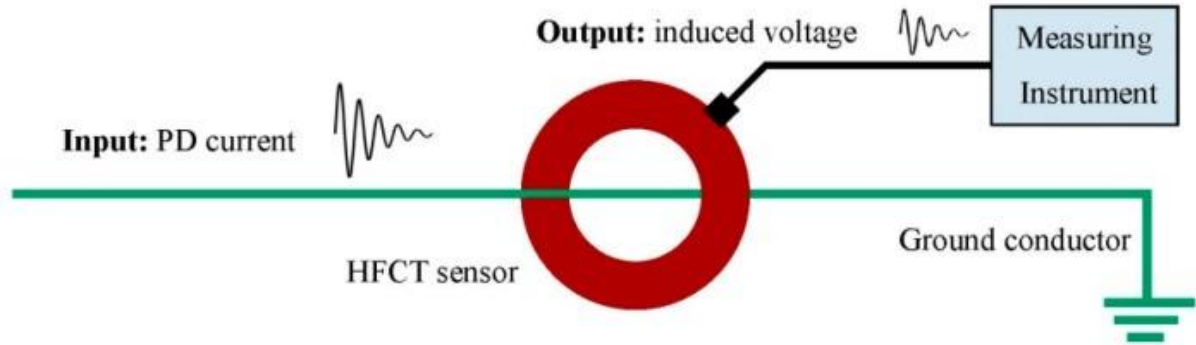
Figure 3. 5: Working principle of HFCT [57]

The induced voltage in the secondary of the HFCT is proportional to the rate of change of current in the primary and this is given by

$$e = M * \frac{di}{dt}$$

where M is the constant of proportionality and represents the mutual inductance between the secondary and earth. In this thesis, HFCT is used to measure the PD current pulse and the measurements are recorded on DPO 3034B.

3.3.4 Charge measurement

PD signals were monitored with the help of the commercially available PD detector DDX 9101 by Haefely Hipotronics. Further, the PD signals were measured through the Techimp software which enables high speed PD recording and processing. The online PRPD Pattern, frequency response as well as classification map can be obtained using this software. Both the detection methods were calibrated to 50pC as per the IEC standard by a PD calibrator.

3.4 FEM model

A mathematical model was developed in 1995 by [58] while examining the breakdown of solid dielectrics in divergent fields. According to this, the field at the tip of the needle is given by

$$E = v * \left(\frac{2}{\ln \left(4 * \left(\frac{d}{r} \right) + 1 \right) * r} \right)$$

where r is the radius tip, d is the gap length and V is the applied voltage. While this equation does suggest that the breakdown channel is most likely to develop at the tip of the needle and is dependent on the radius of the tip, it does not take into account the presence of

48

dielectric. Further, it is seen that space charge accumulation reduces the field near the tip to lower values than the those calculated by geometry.

In order to have an idea about the electric field experienced by the needle tip during the needle plane configuration in ester, a comsol model of the same was developed in 2D axis symmetry based on research by [58] where the needle geometry was created with a parametric curve. Figure 3.6 represents the 3D model of the needle to pressboard configuration in ester as mentioned in the previous section with a voltage of 30 kV applied to the needle.
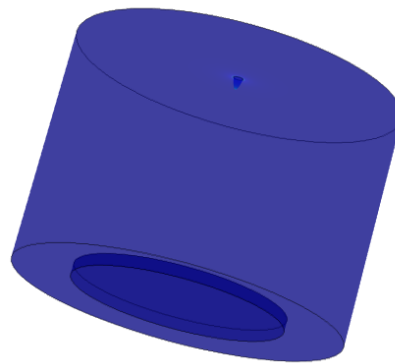
Figure 3. 6: 3D model of needle-ground arrangement in Comsol

On examining the tip of the needle, it was seen that the electric field at this point is highest, as expected, with $3.3*10^7$ V/m. Figure 3.7 shows the electric field experienced by the needle for the above mentioned configuration.
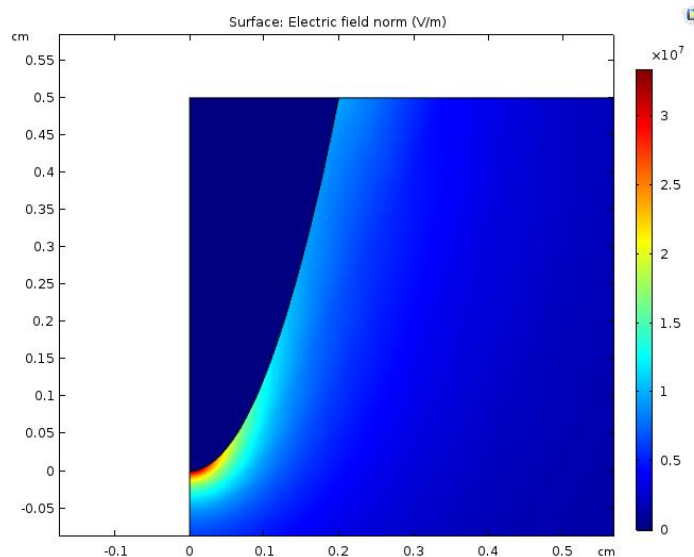
Figure 3. 7: Electric field distribution at needle tip using Comsol

49

3.5 Observations and discussions

The following section provides an overview of the typical PD pattern and associated current pulse observed during AC stress in ester insulation. Under AC stress, PD's of both polarities can appear, positive PD's appearing during the positive cycle while the negative PD's appearing during the negative cycle. The pulse duration is in the range of few hundred ns to few us with the amplitude ranging between few mA. The PD pulse is shaped and fed to the PD instrument in PD measurement circuits. This allows for the measurement of the apparent charge during the PD activity, expressed in pC. The waveforms and behavior of PD varies depending upon the insulation due to different electron affinities and other physical properties such as boiling point. While positive pulses appear in the form of high frequency oscillations superimposed on low frequency ones, negative PD's are generally recorded in the form of pulse bursts.

PD frequency, phase angle and apparent charge are expressed using PD patterns. Phase resolved PD Patterns are the most common technique used to obtain PD patterns. The pulse repetition rate and phase distribution of discharges can vary depending upon the type of electrode arrangement and medium in which they are generated.

3.5.1 Phase resolved PD pattern analysis

As mentioned in the previous sections, PDIV is obtained by increasing the voltage in steps of 1 kV per minute and recording the voltage at which the PD pulse magnitude reached 100pC. In the PRPD patterns recorded below, the PD's are measured as voltage pulses. During the positive cycle, a discharge or partial short circuit results in negative(downward oriented) pulse and this is represented during the first quarter cycle of the applied voltage. PD of positive polarity is measured during the third quarter of the cycle when increasing negative voltage is applied. For the needle pressboard configuration simulating corona discharges, the PDIV was observed to be 40 kV. Figure 3.8 shows the PRPD pattern for this configuration at the PDIV. The phase resolved PD pattern represents the amplitude and phase of the entire number of PD pulses obtained during the test. Under the divergent field, PD's exhibit phase angles ranging from 30 -150° at lower voltages. Towards the onset of the PD inception, the phase angle detected is from 5-10° with negative PD's also recorded .
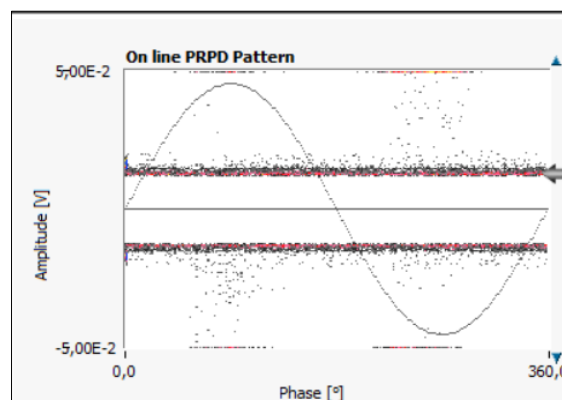
Figure 3. 8: PRPD pattern at PDIV- Corona discharge in ester

50

Figure 3.9 represents the PRPD pattern observed for the creepage discharges where the PDIV was lower than the NG configuration and recorded to be 31 kV. It can be clearly observed that the PD activity is significantly higher for the creepage discharges when compared to the corona discharges. PD's are detectable at lower voltages with a significantly different PRPD pattern. While the corona discharges are more spread-out, the creepage discharges are highly confined to the 90° and 270° phase which represent the voltage peaks with some PD's also detected close to 0° and 180° phase. Moreover, figure suggests that the creepage discharges have a higher PD repetition rate. This could further suggest that the PB surface tends to promote the development of discharges, especially those occurring in the negative cycle as shown. This enhancement of discharges could lead to the increased probability of breakdown in liquid PB composite insulation systems.
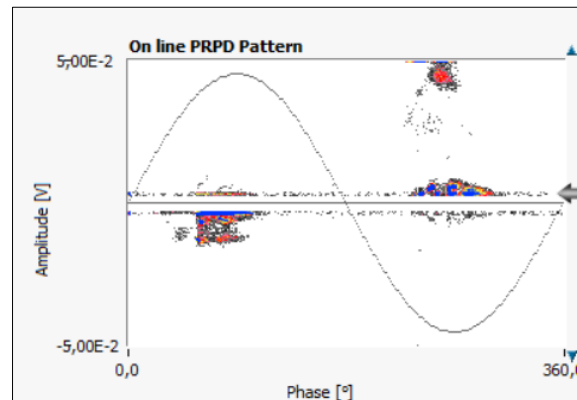
Figure 3. 9: PRPD pattern at PDIV- Creepage discharge in ester

It can also be noticed that the PD activity for the configuration emulating corona discharges are more symmetric when compared to the creepage discharges. This is because the electric field at the surface of the pressboard is not symmetrical during positive and negative cycles during the creepage discharges. Creepage discharges in ester shows a higher magnitude and higher repetition rate in the negative cycle, however, corona discharges show a higher magnitude of discharges in the positive cycle. During the creepage discharges, electrons are more easily generated from the needle when negative voltage is applied and hence, the electron avalanches are developed faster. As the electric field builds up along the avalanche path, the avalanches grow longer causing a higher magnitude of negative discharge[62]. This the maximum PD is observed at 270° for creepage discharges. Generally speaking, the PDs are present in both cycles but are more intense in the negative cycle(180°-360°) for creepage discharges. Since the PDIV value varies significantly with the radius of the needle tip and distance between the needle and ground plate, these parameters must be taken into consideration while analysand stress enhancement sites likely to be encountered in ester filled electrical equipments[57].

PD repetition rate is another important parameter to analyze the PD response of insulating liquids such as ester. Figure 3.10(a) shows the PD repetition rate of creepage discharges with the applied voltage. It was observed that the recurrence of PD pulses increased with the increase in voltage. Figure 3.10(b) represents the variation of the PD magnitude with applied voltage during creepage discharges. It is evident that the PD magnitude gradually increases with the voltage but as the voltage approaches the PDIV, the magnitude of the PD pulses rises drastically.

a)

b)
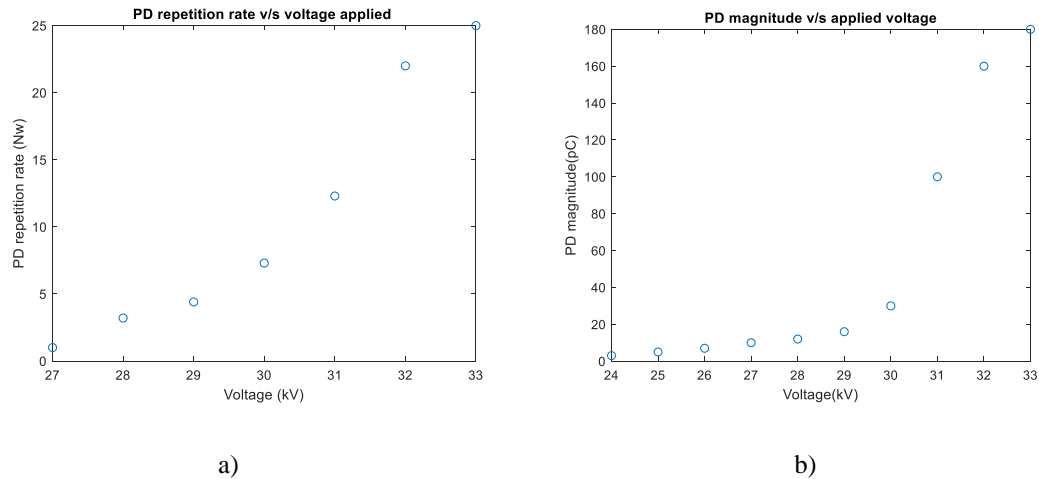
Figure 3. 10: a) variation of PD repetition with voltage- Creepage discharges b) Variation of PD magnitude with voltage-Creepage discharges

3.5.2 Frequency domain analysis

Frequency spectrum and equivalent time length are important parameters usually used to understand the time frequency characteristics of PD signals, which in turn may provide crucial information about the insulation liquid conditions [37].

a)

b)
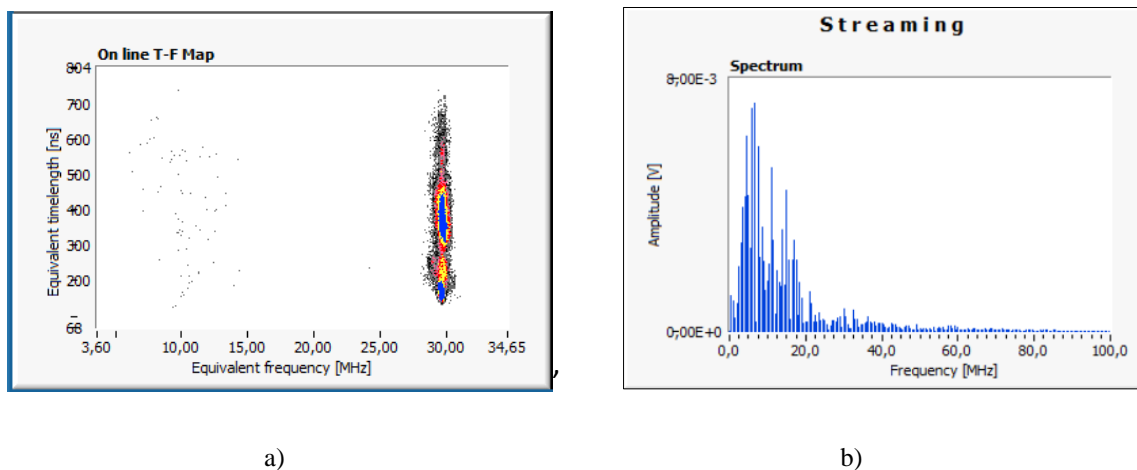
Figure 3. 11: a) Classification map- corona discharges in ester b) Frequency spectrum- corona discharges in ester

The frequency spectrum of the PD pulses during the partial discharge inception voltage for the needle to pressboard configuration in ester (corona discharge) is shown in figure 3.11(b). From this frequency spectrum, it is evident that the frequency component of the pulses lies in the 5-15MHz frequency range with peaks around 10MHz. On increasing the PD pulse beyond the PDIV, no significant change in the frequency response was noticed. The frequency spectrum during PDIV is further confirmed by figure 3.11(a) which represents the classification map(time - frequency) of the PD pulses. Two significant clusters are recorded, initially before the PDIV, most of the pulses recorded are noise signals and PD activity of low magnitude. These activities are noticed in the higher frequency range of 30MHz. The lower

52

frequency group corresponds to the PD pulses around the PDIV with an equivalent frequency of around 10MHz as confirmed by the frequency spectrum.

Figure 3.12 depicts the frequency spectrum of the PD pulses during the PDIV for creepage discharges in ester. It is evident from this spectrum that majority of the PD pulses recorded during PDIV are in the 5-10MHz frequency range, which is lower than the range observed previously for the corona discharges. The amplitude of the PD pulses recorded were however lower for the creepage discharges.
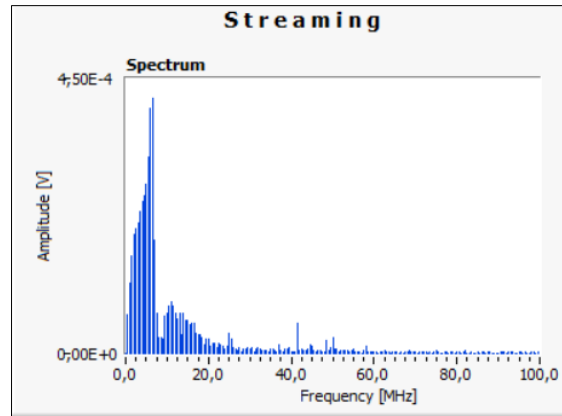
Figure 3. 12: Frequency spectrum- creepage discharge in ester

Furthermore, this is confirmed by the classification map as shown in figure 3.13. The PD activity during the PDIV is represented by the cluster with a lower frequency range and this range was seen to be from 5-10MHz. On closer examination, it can be observed that for PD pulses around the PDIV, the TF(time-frequency) map highlights the presence of two groups of pulses having different frequency content. The higher frequency cluster(10MHz-13MHz) is characterized by discharges of smaller magnitude and time length. Moreover, the discharges with higher frequency component had a smaller repetition rate as compared to the ones with a lower frequency component(5MHz-8MHz). This clearly shows us that the repetition rate for PD pulses is much higher for the creepage discharges in ester as compared to the corona discharges. It is also observed that the PD pulses have a much steadier pattern during creepage discharges unlike the ones recorded for the corona discharges.
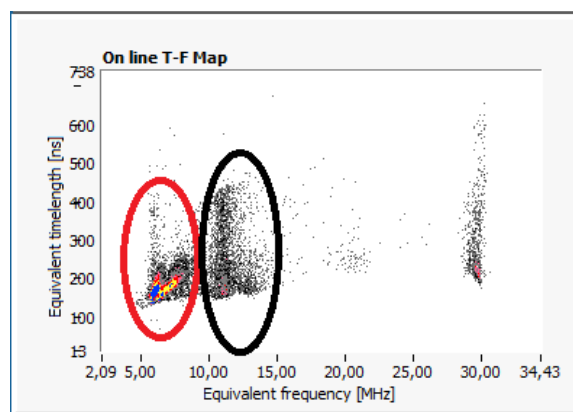
Figure 3. 13: Classification map- creepage discharge in ester

3.5.3 PD pulse characteristics

Figure 3.14 shows the voltage(current) characteristics of the PD pulses recorded at the partial discharge inception voltage with different step times during the simulation of corona and creepage discharges in ester. As previously suggested, the PD pulses increased in magnitude with the increase in voltage as seen in figure 3.14. Also, the sustaining time which represents the duration time for which the PD signal lasts, increases with the increase in voltage applied.

a)   b)
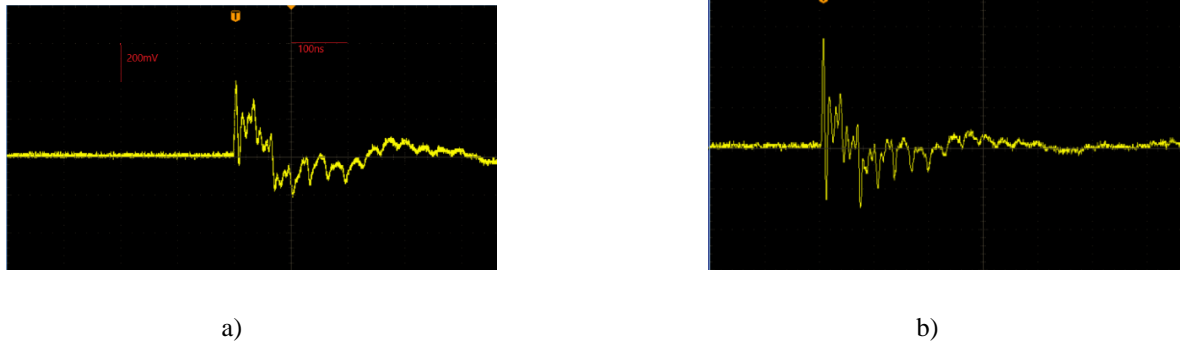
Figure 3. 14: a) PD pulse at 40 kVduring corona discharges in ester(200mV/div; 100ns/div) b) PD pulse at 45 kVduring corona discharges in ester(1V/div; 100ns/div)

On examining with figures which show the PD pulse characteristics during creepage discharge at PDIV as shown in figure 3.15, it can be observed that the PD activity is significantly higher when compared to corona discharges. It is evident that the PD pulses have a higher recurrence during creepage discharges as discussed earlier.
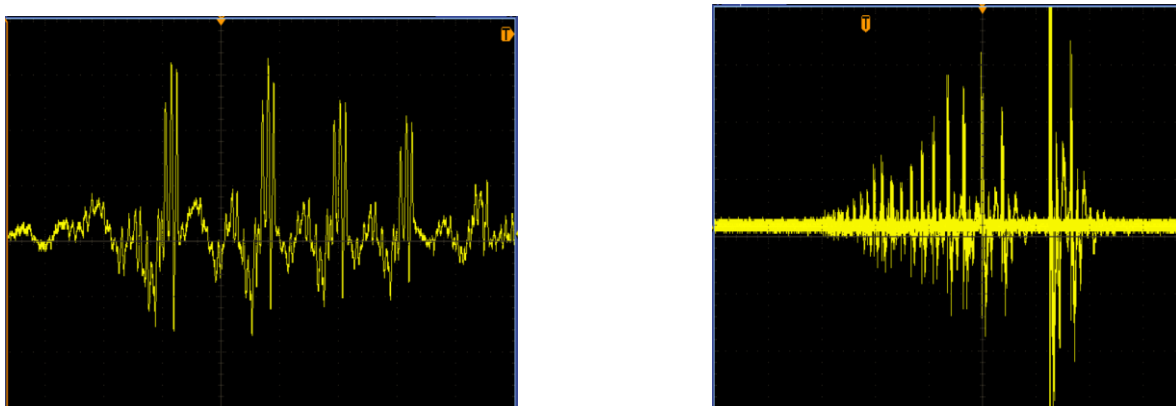
Figure 3. 15: a) PD pulse at 35 kVduring creepage discharges in ester(1V/div; 200ns/div) b) PD pulse at 35 kVduring corona discharges in ester(1V/div; 1μs/div)

PD signals recorded for the creepage discharges denote a train of high frequency pulses. At the start of each pulse train, the interval between the pulses are smaller, as the signal grows in magnitude, the pulses ae larger, and more widely spaced. The role of the pressboard in promoting discharges during creepage activities is higher for the negative discharges as these kinds of discharges are highly significant in terms of their pulse magnitude and sustaining time [61]. In the coming chapters, the use of different methods to detect the discharge activities in oil is presented in depth.

3.6 Summary

The characteristics of PD activities in ester for different types of discharges including corona discharges and creepage discharges were studied in the AC divergent field. Measurements were made using multiple techniques such as HFCT, PD detector as well as the Techimp software for better analysis and results. Ester shows a high resistance to partial discharge and could prove to be a viable substitute for mineral oil as the transformer insulating liquid. Based on the experiments conducted, it can be concluded that corona discharges have a lower repetition rate as compared to creepage discharges. Also, corona discharges are much more symmetric and spread out throughout the voltage waveform unlike creepage discharges which occur mainly at the positive and negative peaks with higher discharges in the negative cycle.

Frequency response analysis suggests that creepage discharges occur at slightly lower frequency ranges and are characterized by two groups of PD pulses having different frequency spectrum. The higher recurrence of PD pulses during creepage discharges could be attributed to the role of the pressboard surface which tends to promote the development of discharges especially during the negative cycle. The increase in PD activity and enhancement of negative discharges during the negative cycle can trigger failures due to flashover and damage the insulation liquid in use for the transformer. The presence of high tangential field can result in the propagation of discharges along the surface of the insulation towards the low voltage point. Such discharges are more common in cable terminations, coil heads rotary machines, outdoor insulators and bushings.

However, further research on the oil/pressboard interface as well as better standardization in the PDIV measurements is needed to fully understand the response of ester and other insulating liquids to PD activity. Increased transmission voltages have opened the possibilities for the use of new insulating liquids which necessitates new dielectric testing techniques. While PD analysis focuses majorly on the charge transfer between the dielectric and external circuit, streamer characteristics represents the physical phenomenon and conductive channels formed in the medium. The investigations of theses phenomenons are conducted in depth in the coming chapters and provide a basis for understanding the breakdown process in insulations.

4. Electrical diagnosis of measurement set-up for streamer detection

This chapter provides the description of the test set up used for electrically detecting streamers in the transformer insulation under DC and lightning impulse. The results obtained using the electrical detection were simultaneously compared with the optical measurements during the final measurements. Different techniques for streamer signal measurement and the high voltage diagnostics involved in improving the set-up have been discussed in this chapter. The chapter provides the general description of the test set up followed by the different methods and results involved in tuning the test set up. The chapter also presents the analysis of the test set up using the ATP-EMTP and COMSOL software.

4.1 Measurement set-up

Over the duration of the thesis, several experimental analyses were conducted to understand the properties of the test set up and the results of the measurements recorded. During this process, the test set up was modified several times due to various reasons that will be discussed in the following sections. The first sub section provides an overview of the experimental investigations carried out initially for the detection of streamers in a divergent field using a needle, pressboard and ground plate. This is followed by explanation of the shortcomings of certain aspects of the measurements and the modifications made to the set up. Finally, the section concludes with discussion on the test set up that has been used for the streamer detection for the winding arrangement for the first time.

4.1.1 PART 1- Initial test set-up

The initial experimental test set up for lighting impulse testing consisted of a 20 stage Haefely impulse generator capable of producing voltages up to 4000 kV with a storage energy of 300kJ .The impulse voltage waveform generated was according to the IEC standard of 1.2/50us. It was supplied by a testing transformer of ratio 230:110000 and high voltage solid state rectifiers. Resistive voltage divider, along with a capacitive load was used to measure the voltage signal as shown in figure 4.1 and both current as well as voltage measurements were recorded on the Haefely lightning impulse measurement system DIAS 744.

A similar test set up with a 40 kV DC source was used for testing with DC voltages. The test set up was installed in the faraday cage and measurements were done in dark as optical detection of streamers were also performed simultaneously. Testing with the high voltage DC source proved to be a good starting point for the electrical and optical diagnosis of the test set up.

Figure 4. 1: Initial test set up for electrical streamer detection in ester under LI voltage

The needle plane configuration was used to produce the streamers in ester under lightning impulse voltages as shown in figure 4.2. Tungsten needle with the tip radius of 50mm was used as the point electrode. The needle tip was monitored after every few tests to ensure the tip remains sharp. The length of the needle was 20mm and the needle was fixed to a brass holder of length 150 mm. The plane electrode was made of brass and fixed to the base of the acrylic test cell. The diameter of the electrode was 100 mm. The distance between the needle tip and the plane electrode was 60mm. The pressboard was placed inclined to the point plane electrode and in firm contact with the needle tip. This was done to simulate a triple point which is the weakest point in the transformer insulation and will more likely initiate the streamers. A pressboard was placed on top of the ground electrode to detect streamers during partial breakdowns as seen in figure 4.2.

a)   b)

Figure 4. 2 a), b): Simulation of creepage discharges in ester using needle-PB arrangement for the initial set up

Measurement of current was initially done with the help of a non-inductive shunt of 1Ω. These shunts use a coaxial construction in order to reduce the stray inductances which can have a drastic t effect at high frequencies. The self-inductance of these shunts is very low because of the significant reduction of the magnetic flux. In order to reduce the effect of the electromagnetic radiation of the lightning impulse generator, the shunt was shielded by a metallic case as shown in figure 4.3.

a)   b)

Figure 4. 3 a): 1Ω shunt enclosed by a metal case b): Metal case used for shielding the shunt from EM disturbances

This was done to ensure that the noise signals and radiation produced during the charging and discharging in the impulse generator would not affect the measurements of the shunt.

As mentioned before, the amount of charge developed during steamers is in the order of few picocoulombs. This can result in currents of hundreds of mA depending upon the voltage applied. In order to ensure that the current shunt of 1Ω can pick these signals up, a test set up according to the circuit diagram shown in figure 4.4 was created.
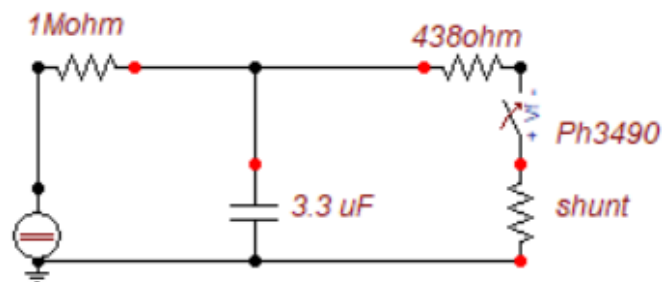
Figure 4. 4: Circuit diagram of test set up to verify the sensitivity of the 1Ω shunt

The circuit consists of the voltage supply capable of providing up to 300V. This was used to charge the 3.39uF capacitor through a 1MΩ resistor. Across the capacitor is a Phillips 3490 spark gap which is designed to breakdown at a voltage range of 150-200V. The capacitance

of the spark gap was calculated according to $C = A\varepsilon/d$ and was found to be 1pF with a breakdown voltage of 200V. Hence, the charge measured by the shunt is in the range of that produced during streamer activities in lightning impulse. Also, the current measured by the shunt was ensured to be a few mA, as expected during streamer activity, by inserting a 478Ω resistor in series with the spark gap as seen in figure 4.5(a). Figure 4.5(a) shows the experimental set up of the same. A voltmeter was added in parallel to the spark gap to record the voltage at which breakdown is observed.
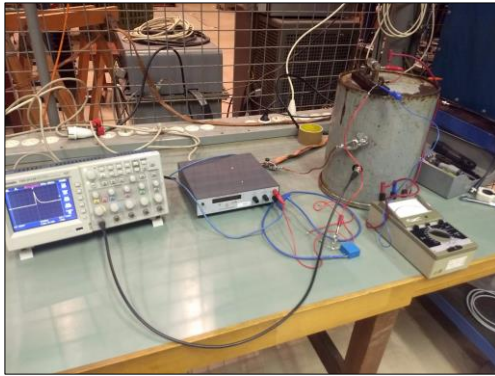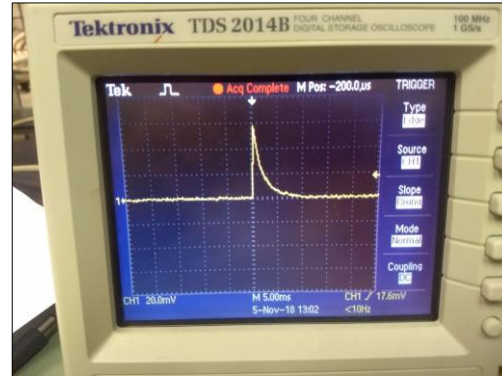
a)   b)

Figure 4. 5 a): Test set up to verify the shunt sensitivity b): Output waveform recorded on the oscilloscope

The output from the shunt was recorded on a Tektronix TDS 2014B digital oscilloscope and is shown in figure 4.5(b). Here, it can be seen from the figure that the shunt is capable to capturing the signal released during the breakdown. Hence, the 1Ω shunt can be used to detect the streamer signals during lightning impulse voltages. The current detected by the shunt was found to be 60mA.

4.1.2 PART 2- Modified test set-up

Table 4.1 presents the different techniques used in the initial test set up for impulse and DC testing and possible improvements that can be made. The following sections discuss some of these improvements and their effect on the measurement of streamer signals.

Initial test configuration	Shortcomings	Possible improvements
Measurement of current signal using Haefely system during impulse testing	Unable to capture the streamer signals accurately as the current magnitude of streamers are significantly lesser than the initial disturbance	Using oscilloscope of high sampling rate to focus on a smaller sclae

Use of 1Ω shunt for DC and impulse testing	Oscillations in the current signal during streamer measurement	Measurement of current signals using 10Ω shunt to damp the oscillations
Test set up during impulse testing comprised of large loop including additional structures such as capacitive load ,support insulators, and leads between shunt and test cell	Large oscillations due to stray inductance and capacitance in the set up	Making the test set up more compact to reduce the effect of parasitic elements
Testing during DC voltage did not include coupling capacitor	Low sensitivity of current measurements	Introducing blocking inductor and coupling capacitor
Using pressboard on the ground electrode	Breakdown voltage was much higher with more energy, causing damage to the test cell. Moreover, streamer activity is disrupted due to the presence of the PB on the ground	Using a single PB to create surface discharges with reduced needle- ground distance simulating the effect of triple point.

Table 4. 1: Possible improvements to the initial test set up for electrical detection of streamers

4.1.2.1 Diagnostics- DC testing

After performing measurements with the previous set up, it was observed that the current signal detected during streamer activity has several oscillations(or ringing). These are electrical oscillations that arise due to stray capacitances and inductances in the circuit. An under damped circuit can allow such oscillations to occur thereby preventing an accurate current signal measurement. By introducing a limiting resistor and making the test set up more compact along with the reduction in the inductance of the leads and stray capacitances, the current signal recorded was improved for analysis. In order to obtain an accurate electrical signal, suitable components for the electrical detection should be installed. The circuit should compose of right values of resistors and capacitors in order to ensure that the streamer signal can circulate in the loop. The introduction of relevant resistors and inductors can smoothen the current signal from the shunt as well as the HFCT. Figure 4.6 shows the circuit diagram for the modified test set up.
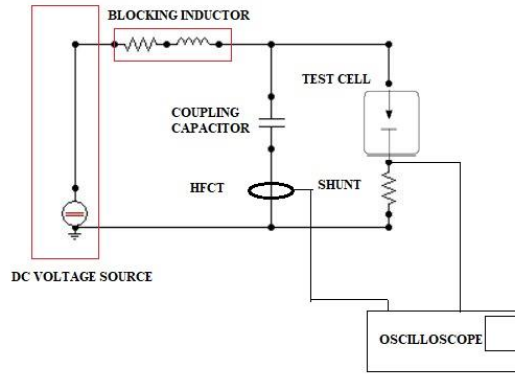
Figure 4. 6: Circuit diagram of the modified test set up for electrical detection of streamers under DC

The test set up included a coupling capacitor which provided a closed circuit for the discharge during the application of the voltage and improve the current measurement. The value of the coupling capacitor was chosen to be 50pF as higher values of the coupling capacitor would lead to large currents during breakdowns. A series resistor is installed in the circuit to prevent high currents from damaging the measurement system during breakdowns. Also, a blocking inductor was fitted in the circuit to present high impedance to the ripple control frequencies. The high frequency signals from the HV supply are prevented from entering the circuit and interfering with the measurements. The measurement of the current signal is done with the help of the high frequency current transformer which was fitted to the ground plate using copper bars as well as the shunt as shown in the figure 4.7(b).

During measurements using high voltage DC, the needle to ground distance was fixed at 5mm under negative polarity and 10mm under positive polarity. Small gaps were chosen because the HV source was capable of producing voltages up to 40 kV only and large gap distances would not breakdown below that voltage level. As a result, measurements were performed without the pressboard. A 8mm brass needle was used for the DC test set up.

a)   b)

Figure 4. 7 a): Test set up to detect streamers in air under DC b): Test set up to detect streamers in oil under DC

Figure 4.8 shows the current signals recorded by the HFCT during corona in air for positive and negative DC voltage. The signal recorded (in purple) has very few oscillations and provides a very accurate measurement of the magnitude of the signal. Since the polarity of the streamer cannot be observed using the light signal, the current signal can help identify this.

a)   b)
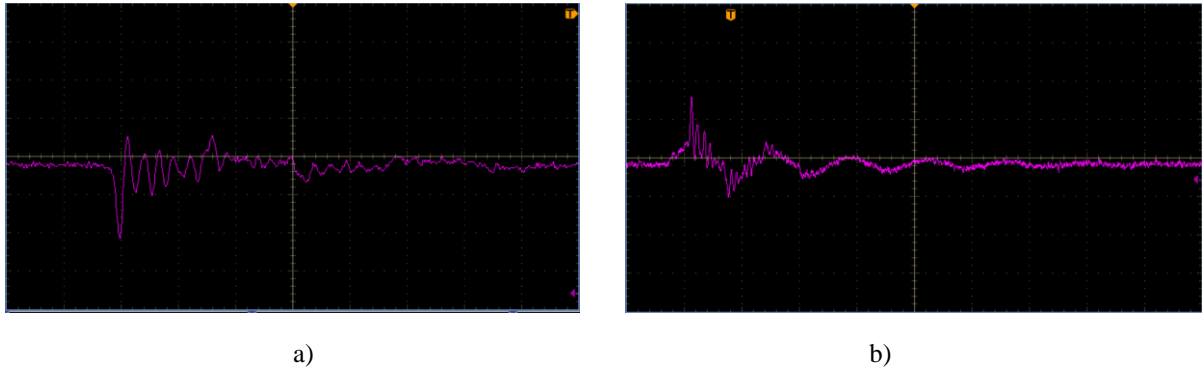
Figure 4. 8 a): negative streamer current signal in air under DC(5mV/div; 40ns/div) b): positive streamer current signal in air under DC(5mV/div;100ns/div)

In order to increase the sensitivity of current measurement, a 10Ω shunt was used. Though the HFCT is capable of recording the current signal as previously seen, the magnitude of the signal recorded is very low without the use of an amplifier. Hence, the current measurement was simultaneously done with the help of a coaxial shunt. However, the increased sensitivity of the shunt also resulted in the detection of the electrical noise signals up to 60mV(6mA) in magnitude in the grid as shown in figure 4.9. It can be observed that the signal is detected only by the shunt (green) while the PMT(yellow) and the HFCT(purple) do not show any signal. The PMT is not influenced by the noise signals in the grid while the HFCT is not sensitive enough to pick up these signals. Although these signals disturb the measurements of the signal from the streamers, the magnitude of the streamer current signal recorded by the shunt is significantly higher. Moreover, the PMT signal as well as the signal from the HFCT can be used to distinguish the noise signal from the signal of the streamers. Appropriate shielding of shunt could have eliminated these disturbances.
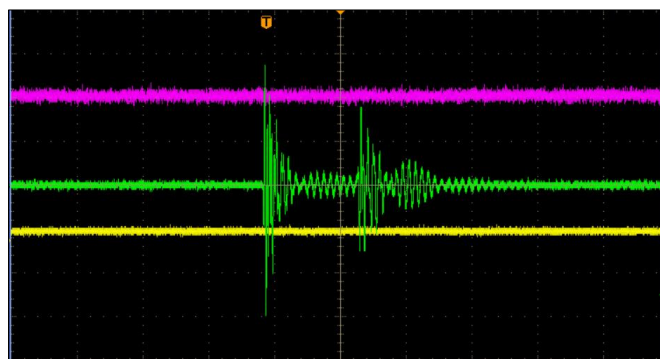
Figure 4. 9: Electrical disturbance recorded by the 10Ω shunt during DC testing (shunt signal: 20mV/div;2μs/div)

62

4.1.2.2 Diagnostics using ATP-EMTP for impulse testing

During the lightning impulse tests, it was seen that the charging and triggering process of the sphere gaps in the impulse generator induced noise signals at the wave front of the voltage. Before performing tests with the lightning impulse generator, the breakdown process was simulated in the ATP Software to better understand the capacitive currents that can be expected. This section analyzes the presence of coupling capacitor during the detection of streamers under impulse testing. Appendix A provides a brief introduction to this software.

Taking into account the LC oscillations in impulse voltages, the wave front time is specified as 1.67 times the time taken by the wave to reach 90% of its peak value starting from 30% of its peak value. The nominal wave tail time is measured till the point where the voltage is 50% of its peak value from the nominal starting time. The standard wave shape of the lightning impulse voltage according to IEC 60060-1 is 1.2/50 micro second(wave front of 1.2us and wave tail of 50us) with a tolerance of 60% on the wave front and 20% on the wave tail. Components of the impulse generator includes [63]:

Triggering system:

Triggered sphere gaps are used to determine the exact moment of firing. Trigger impulse of a smaller voltage magnitude breaks down this gap and results in UV radiations to be released in the gap. This process initiates the breakdown of the main gap.

Spark Gaps and capacitors:

Spark gaps are aligned and arranged vertically one over the other on such a way that the irradiation produced in one gap can initiate the breakdown process in the next one. If the radiations are blocked, the firing will not be consistent. Generator capacitors are designed for several charging and discharging operations.

Front and Tail resistance:

The front resistor determines the front time and the tail resistor determines the tail time to half the peak value. These resistors are usually either bifilar wound or non-inductive thin flat insulating sheets. The ratio of these resistors also affects the overall efficiency of the generator.

Charging resistor:

These are non-inductive resistors that are connected in parallel to the tail resistor. They are required to charge the generator and are selected such that they do not affect the discharging resistor.

Measuring System:

This comprises of a voltage divider connected to an effectively shielded digital recorder through coaxial cables. The divider used for investigation in this thesis is capacitive in nature. Current measurements for impulse voltages are generally done with the help of coaxial shunts.

Parasitic elements:

Testing at high frequencies can cause the stray inductance and capacitance in the circuit to play an important role. They cause significant distortion between the source and test sample. This can include the stray capacitance between the divider and ground, inductance of the leads etc. For the simulation performed in ATP in this thesis, these parasitic elements are ignored.

Overall, in order to maintain the wave shape of the impulse, the resistance and capacitance of the circuit should be maintained at 500Ω, 1000pF or vice versa. The ATP model for the lighting impulse generator along with the dividers, capacitors and resistors is created according to table 4.2 which introduces the different components used in the model. The model is presented in the appendix. The breakdown process was simulated with the help of a switch in the ATP software. The switch was triggered to close after 20us, which is expected to be the duration to breakdown during impulse testing. The ATP model used to simulate the breakdown process is also presented in the appendix. Figure 4.10 shows the positive impulse voltage waveform measured in the ATP software during the breakdown process and when the voltage levels are below breakdown.

Description	Value
Front resistor	130Ω
Tail resistor	140Ω
Capacitance of test object	5-10pF
Coupling capacitor	500pF
Divider capacitance ratio	920nF : 1nF
Divider resistance ratio	304Ω : 1Ω

Table 4. 2: Components and their values used for the ATP simulation of the test set up under LI voltage

On comparing the waveforms with and without the coupling capacitor(CC), no significant difference was observed. Figure 4.10(a) shows the voltage waveform for both cases. Tail chopped impulse breakdown waveform without the coupling capacitor is shown in figure 4.10(b).

a)   b)
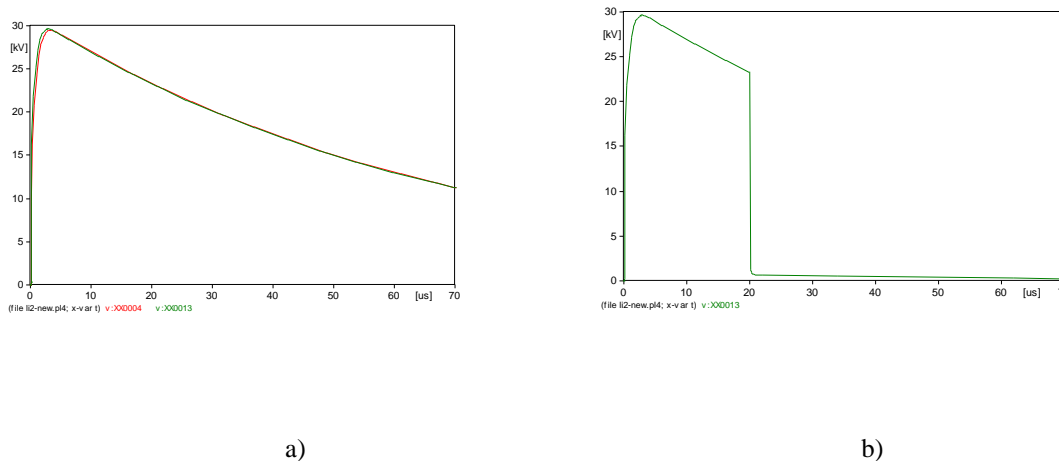
Figure 4. 10 a): ATP simulation of LI waveform(XX004-with CC;XX0013-without CC) b): ATP simulation of LI waveform after breakdown(without CC)

The voltage waveforms for both cases represent standard lightning impulse voltages. However, on closer examination of the current waveform measured at the shunt ,a capacitive dissipation of the current is observed during the presence of the coupling capacitor as seen in figure 4.11. For both cases, a high current is recorded at the instant of

sparking of the capacitors. The streamer current magnitudes which are to be measured are significantly lesser and hence, the capacitive dissipation of this initial current could affect the detection of streamers.

a)

b)
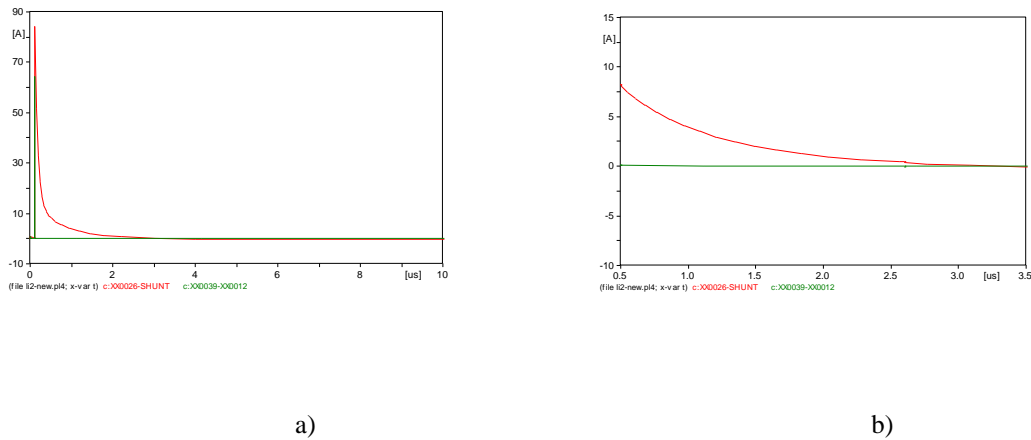
Figure 4. 11 a),b): ATP simulation of current through shunt during positive impulse voltage of 30 kV(XX0026-SHUNT :with CC; XX0039-XX0012: without CC)

A similar phenomenon was observed during breakdown with the coupling capacitor connected, where a capacitive discharge was observed in the current signal recorded by the shunt. High currents are recorded at the time of breakdown during which the protection system installed in the setup will trigger. The current signal recorded during actual testing would also be affected by the parasitic elements in the circuit resulting in LC oscillations of large amplitudes and time constants.

For the lightning impulse testing, signal from the streamer were recorded only with the shunt and PMT. Adequate protection was installed to ensure that the oscilloscope remains unaffected due to large currents during breakdown. Figure 4.12 shows the capacitive current recorded by the 10Ω shunt(green signal) when the coupling capacitor(500pF) was installed in parallel to the sample during negative impulse of 60 kV. The capacitive dissipation was much slower than expected with large oscillations recorded at the beginning. Unlike the testing with the DC voltage, coupling capacitor was not used while testing under impulse voltage as large capacitive currents were recorded during the first few μs which dissipated slowly, preventing the accurate detection of streamers.
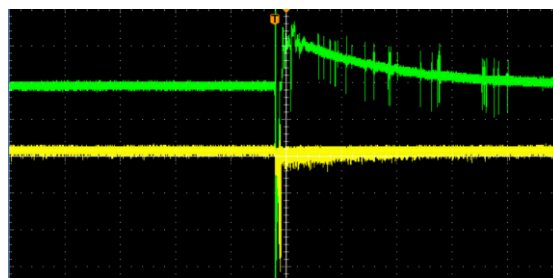
Figure 4. 12: Effect of coupling capacitor on the electrical signal under impulse voltage(shunt signal(green)- 200mA/div; time- 40μs/div)

Significant difference was observed between the current signal recorded by the 1Ω and 10Ω shunt. Similar to the scenario during the test set up with DC voltage, increasing the

resistance of the shunt causing the damping of the LC oscillations in the current (green signal) as shown in figure 4.13. The current signal recorded by the 10Ω shunt correlates with the light(yellow signal) from the streamers much more accurately as seen in figure 4.13(b). The attenuation in these oscillations provides accurate current signals during streamer activity from which the magnitude and energy of the streamers can be determined. The current signals recorded by the 1Ω shunt lasted for approximately 200ns, while the current signals from the 10Ω shunt where around 10ns.

a)   b)
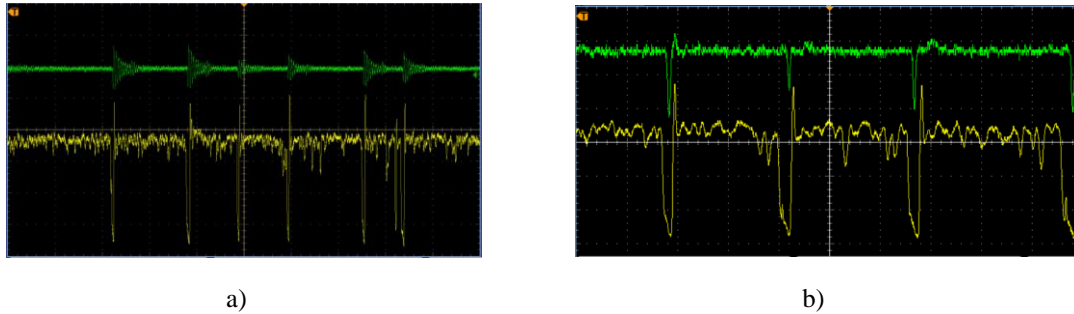
Figure 4. 13 a): Streamer current signal recorded by 1Ω shunt under impulse voltage(time- 400ns/div) b): Streamer current signal recorded by 10Ω shunt under impulse voltage(time- 200ns/div)

The final test set up fot the electrical detection of streamers in the needle-PB-pane geometry used a single stage of the impulse generator. An external resistor of 200Ω was used to generate the lighting impulse waveform according to the standards. Capacitve divider was used to measure the voltage as shown in the figure 4.14. The overall test set up was kept very compact ot reduce the inductance of the loop and the effect of the parasitic elements. Measurement of the current signal was performed with oscilloscope while the voltage waveform was recorded by the Haefely measurement system.
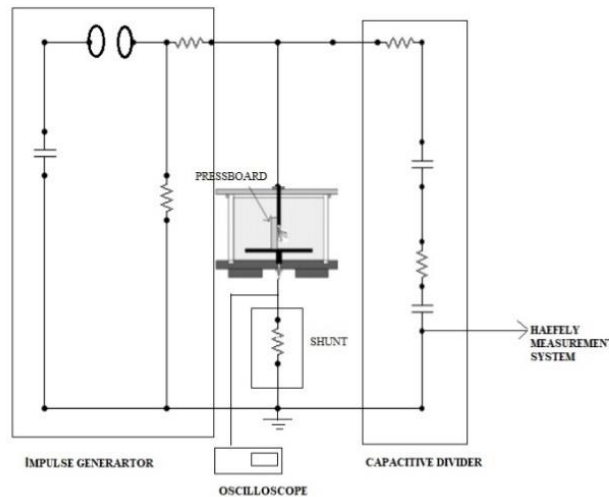
Figure 4. 14: Circuit diagram of the modified test set up for electrical detection of streamers under impulse voltages

Figure 4.15(b) depicts the test set sample used for lightning impulse testing. The shunt was mounted directly under the test cell eliminating the effect of stray inductance due to

66

unnecessary leads. The shunt was left unshielded as the initial disturbance during the charging of the impulse generator could not be eliminated. Tungsten needle, 30mm in length, was installed along the surface of a pressboard to simulate surface discharges as shown in figure 4.15(a). The needle-ground distance was adjusted to 25mm and the needle was inspected after breakdowns to ensure that the tip remains sharp.

a)   b)

Figure 4. 15 a): Simulating surface discharges in oil under impulse voltage b): test sample under impulse voltage

4.1.2.3 Measurement using oscilloscope

As seen previously, measurements with the Haefely impulse measurement system 744 records initial lightning impulse disturbances which are up to 10A in magnitude depending upon the voltage applied as shown in figure 4.16(a). For the study of streamers under lightning impulse, the current signal to be measured was expected in the range of few hundred mA. This necessitated the use of a measuring system that can focus only on the mA scale only without taking into consideration the initial disturbances from the impulse generator. It can be seen from figure 4.16(b) that the detection of streamers is unclear with the Haefely measuring system where the streamer magnitudes are significantly lesser than the initial disturbances.

a)   b)
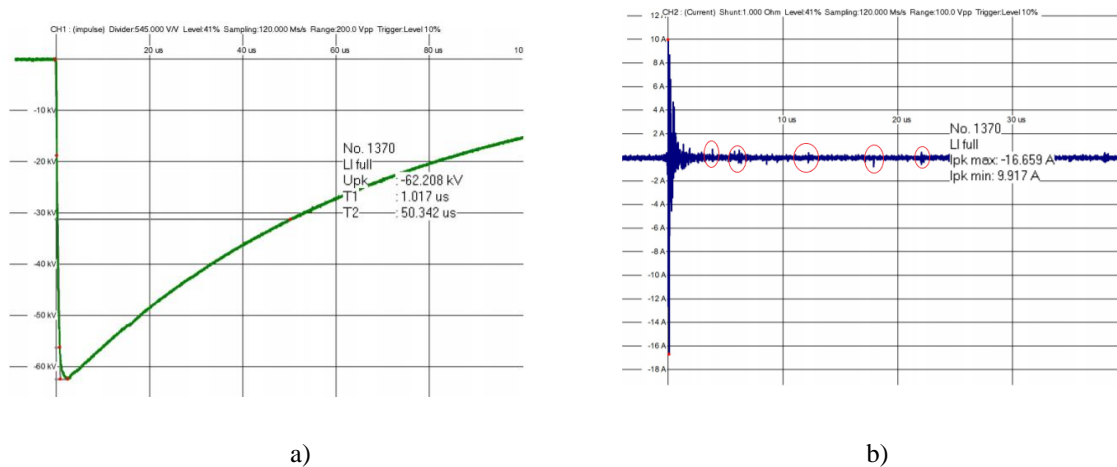
Figure 4. 16 a): Impulse voltage waveform recorded by the Haefely system b): Streamer current signal recorded by the Haefely system

For this purpose, the Tektronix DPO 3034B four channel digital storage oscilloscope was used. This DPO has a maximum sampling rate of 2.5GS/s and frequency range of up to 300MHz. The HTS-B-01 50Ω coaxial cable was used to connect the shunt to the oscilloscope. These types of cables are known for their high efficiency and low losses. Furthermore, before connecting the coaxial cable to the channel of the oscilloscope, it was terminated with an impedance equal to the characteristic impedance of the cable in order to ensure that no reflections can occur. Fast transients entering the cable can undergo multiple reflections if it is not correctly terminated, thereby affecting the performance. Figure 4.17(a) shows the response of the oscilloscope to an impulse voltage of 130 kV with the coaxial cable disconnected from the shunt and grounded. It was seen that severe disturbances up to 150mV was recorded by the scope. These disturbances from the impulse generated can affect the measurements of the current signals during streamer propagation.

a)   b)
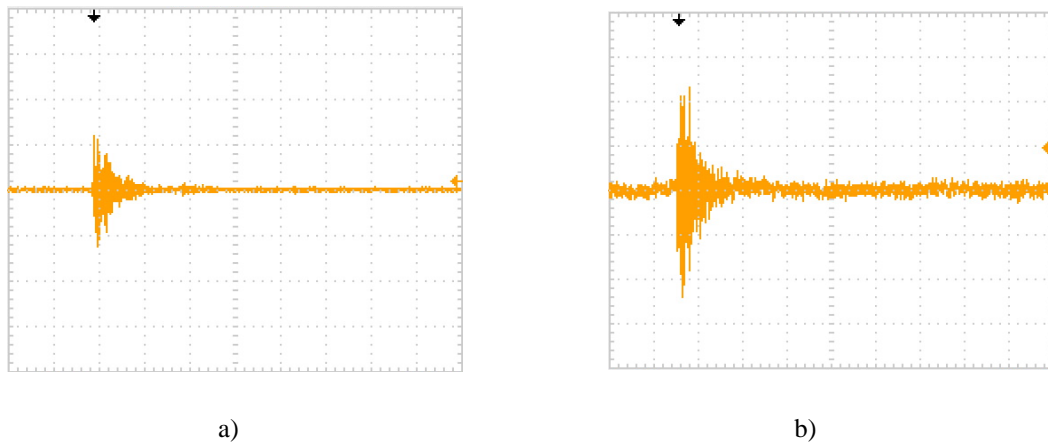
Figure 4. 17 a): Disturbance recorded by the scope(no EMC shielding) due to the charging of the impulse generator(100mV.div;2μs/div) b): Disturbance recorded by the scope(with EMC shielding) due to the charging of the impulse generator(5mV.div;2μs/div)

In order to reduce these disturbances recorded, the oscilloscope was shielded by an electromagnetic compatible(EMC) box shown in figure 4.18(a). This helped was done to prevent the oscilloscope from getting affected by unwanted effects such as electromagnetic interferences. The EMC cabinet or box comprises of r-f filters which significantly reduced the disturbances recorded by the oscilloscope as shown in figure 4.17(b). The voltage applied was 130 kV with the coaxial cable disconnected from the shunt and grounded. The maximum disturbance was recorded to be approximately 12mV. As mentioned previously, overvoltage protection was installed before testing as shown in figure 4.18(b).

a)   b)
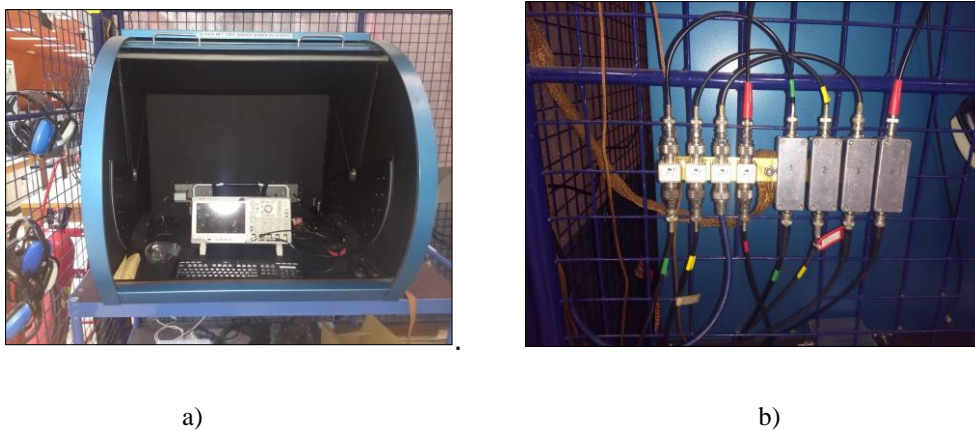
Figure 4. 18 a): EMC box for the DPO b):Overvoltage protection for the DPO

4.1.3 PART 3- Test set up with winding

Research on the detection of streamers through optical and electrical techniques initiated from winding samples has never been performed before and could be vital in fully understanding the streamer characteristics in ester. Though streamers could be initiated due to protrusions on conductors, particles due to contamination, these scenarios are avoided as far as possible during the transformer design. Streamers initiated due to windings represent a much more homogenous field which could alter its characteristics. Test set ups involving the Weidmann configuration could help in better validating the use of ester in power transformers. The large size of the windings makes it harder to determine the exact initiation site for the streamers. Studies done previously focus on the breakdown strength of ester and mineral oil under different electrode arrangements as shown in figure 4. 19. However, understanding the streamer characteristics could help better determine the extent of this.

Figure 4. 19: Weidmann test set up [46]

The winding arrangement shown in figure 1.5 was modified in order to localise the streamer phenomenon to a smaller area. Large winding configurations would mean that the streamer process and the following breakdown could occur at any place along the length of the winding, making it difficult for the electrical and optical detection of streamers. Though the optical fibre cables are very sensitive, the small diameter of the bundle prevents it from capturing all the light from the streamers that occur at greater distance from it. This could further mean that the signal detected by the electrical and optical sensor will not correlate during streamer activity. A similar arrangement to figure 1.5, created by using curved polygons was simulated in COMSOL 2D to get an idea about the electric field between the windings. The geometry of the arrangement used here resembles two conductors with rounded ends in ester separated by a fixed distance as shown in figure 4.20 (a). The distance between the windings was given as 10mm. The lower winding was set to ground potential and the other winding was given a potential of 100 kV.
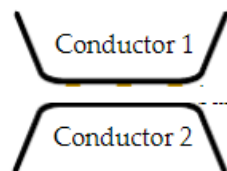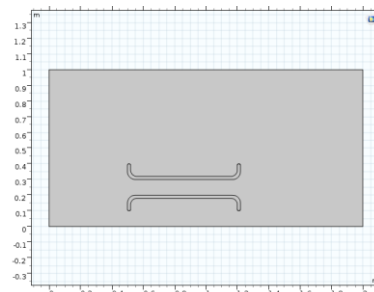
a)   b)

Figure 4. 20 a): Winding arrangement resembling figure 1.3 [87] b):Comsol geometry

69

On analysing the electric field, a uniform high stress was observed across the windings as shown in figure 4.21. The electric field at the edge of the windings were slightly larger, thereby increasing the probability of breakdown at these locations. This suggested that the detection of streamers in the existing configuration of windings will be problematic as the exact location of streamer initiation is hard to predict.

a)   b)
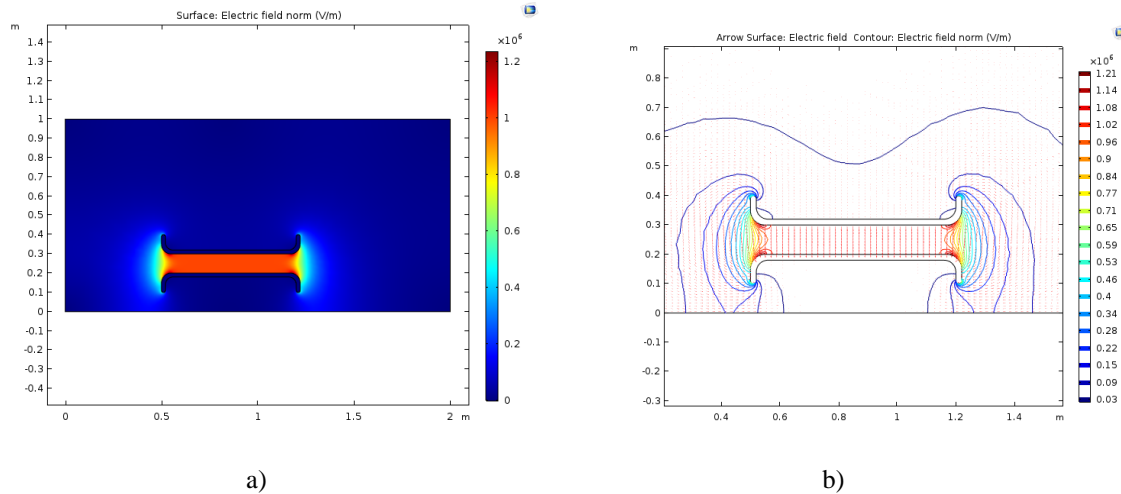
Figure 4. 21 a): Electric field between the windings b):Electric field lines between the windings

Hence, a single conductor with a ground electrode was used for streamer detection in this thesis. Placing a ground plate on the bottom of the tank was also not preferred as the electric field at the edges of the winding was much larger as seen in figure 4.22(b). This was not desired as larger electric stress at the edges of the winding distances could possibly result in flashovers from the back side of the electrodes to other parts of the tank.

a)   b)
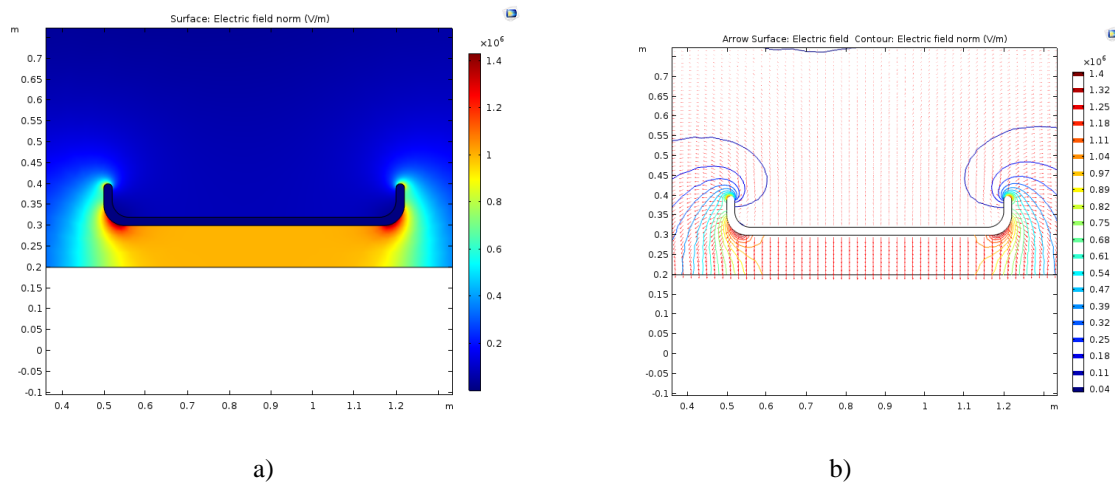
Figure 4. 22 a):Electric field between winding and ground plate b): Electric field lines between winding and ground plate

The winding electrode arrangement used in this thesis is shown in figure 4.23(a). Unlike arrangements used in previous studies, the ground electrode was semi-spherical in shape in order to prevent the breakdowns at the extreme ends of the windings. High voltage was applied to conductor(winding) 1.

70
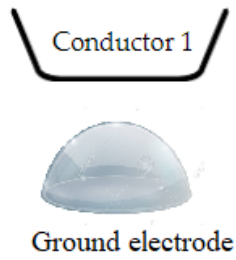
a)   b)

Figure 4. 23 a): Winding-ground configuration b):Semi-spherical ground electrode

This arrangement, when simulated in comsol, showed that the electric field was highest between the high voltage winding and the top of the semi-spherical ground electrode. As a result, flashover to other parts of the tank are prevented and the streamer inception site can be narrowed down for better detection with the optical and electrical sensors.
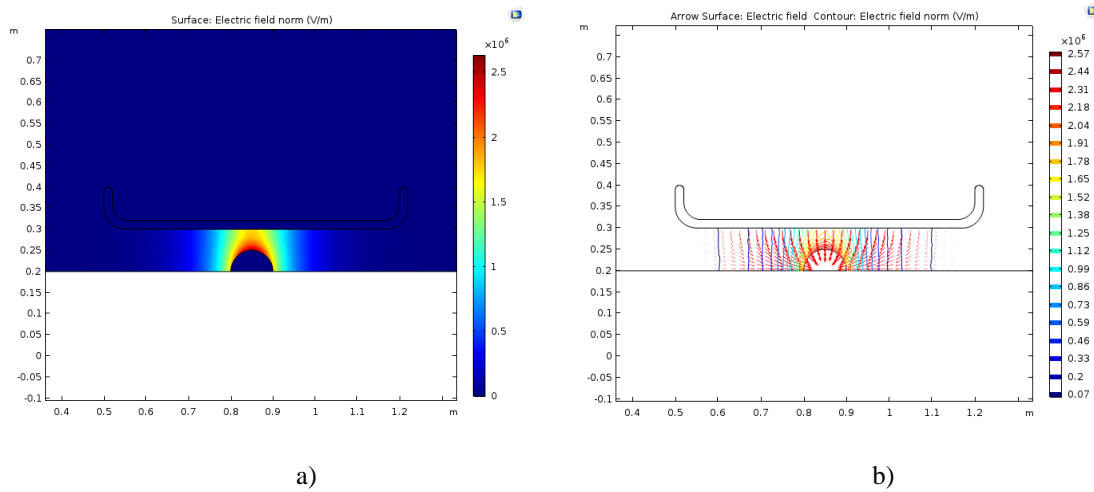
a)   b)

Figure 4. 24 a):Electric field plot- winding-semi-sphere configuration b):Electric field lines plot- winding-semi-sphere configuration

The test set up was immersed in a 2400 litre tank with the 10Ω shunt attached to the bottom of the tank, directly below the ground electrode and connected to ground. The distance between the winding and the ground plate was fixed at 1mm-5mm in order to limit the breakdown voltage to lower values which can be handled easily. However, after each breakdown, though a new winding was prepared similar to the previous one, small differences in the winding geometry existed. This caused slight variations in the gap distance between the winding and the ground electrode. Figure 4.25 is a 3D representation of the test configuration in the tank for electrical detection of the streamers. The winding was shaped as shown in figure 4.26. Wooden transformer blocks were present on either side of the semi spherical electrode initially to adjust the gap between the winding and the ground.

71
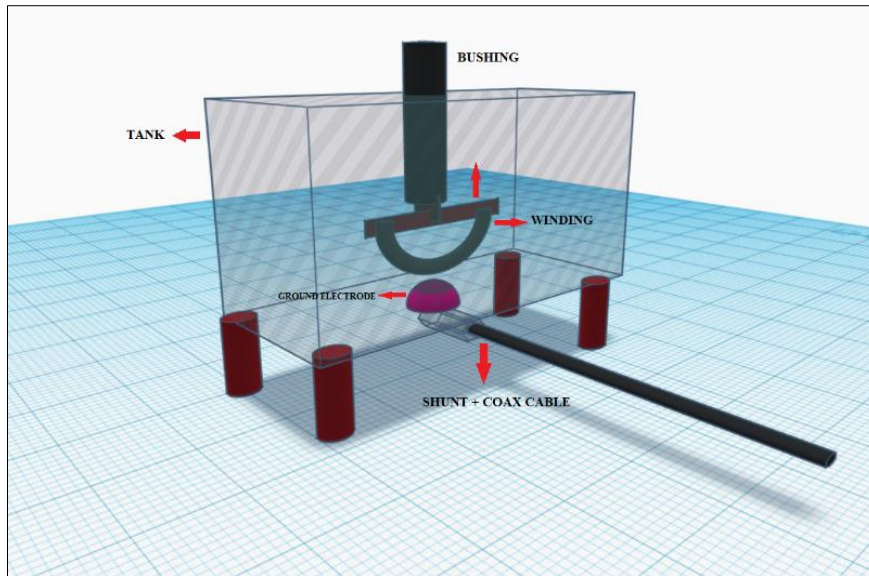
Figure 4. 25: 3D representation of electrical set up used to detect streamers from windings

Lightning impulse voltages were applied to windings through the bushing with the basic insulation level at 450 kV. The use of alligator clips/clamps was avoided in order to reduce the stress inside the tank to low levels and prevent flashover problems. Both the ends of the winding was attached to the bushing with the help of a steel rod as shown in figure 4.26. The presence of sharp points on the electrodes could result in a high local stress concentration thereby initiating unnecessary breakdown. The final circuit diagram along with the optical set up is discussed in chapter 5.
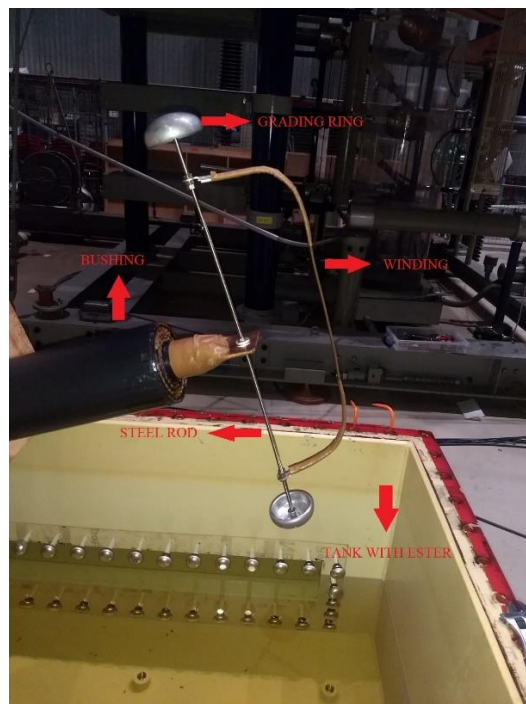
Figure 4. 26: Winding attached to bushing using steel rod

Impulse tests with the winding arrangement were performed at significantly high voltage levels of up to 300 kV. Also, the presence of the metallic tank can lead to EMC coupling with the shunt, thereby resulting in higher interference. As a result, the charging of the generator to higher voltage levels resulted in higher EMC disturbances to be recorded by the shunt. Due to the high sensitivity of the shunt, large number of noise signals were recorded as shown in figure 4.27. Here, the applied negative voltage level was 200 kV and the winding was not installed. These noise signals were of similar magnitude to the streamer signals observed during tests with the winding and prevented the accurate detection of streamer signals.

Figure 4. 27: Current noise signal without winding installed at 200 kV(current- 2V/div; time-40μs/div)

It can be observed from figure 4.27 that most of the noise signals were recorded after the first 35us whereas the streamer activities begin much earlier as discussed in chapter 6. However, on applying higher voltage levels, streamer activity can last up to 40us and during such cases, the noise signal interferes with the detection of streamers. On closer examination of the noise signals, it can be observed that these signals have large number of oscillations which last up to 600us. Current signal associated with the streamers originating from windings have a shorter time duration with lesser number of oscillations as seen in chapter 6. Moreover, the polarity of current signal can also be used to distinguish between the noise and streamer signal. The presence of light signals corresponding to the current signal plays a crucial role in indicating if streamer activity has occurred or not. Figure 4.28 shows the noise signal recorded by the shunt without any corresponding light signal. During certain measurements under LI voltage, current measurement was not recorded due to the disturbances of the noise signals from the impulse generator and the grid. Optical detection of streamers was preferred in such cases.
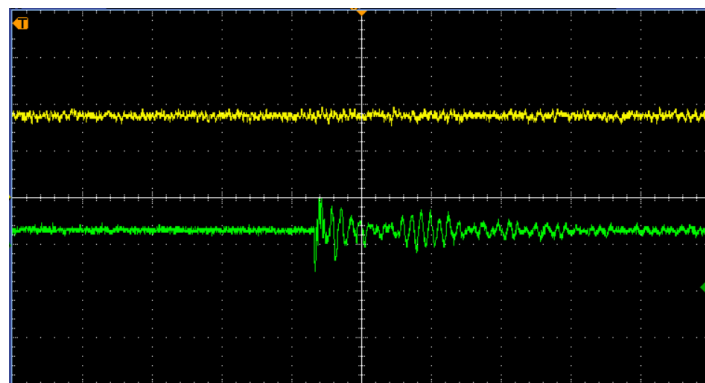
Figure 4. 28: Current noise signal without winding installed at 200 kV(current- 2V/div; time-200ns/div)

4.2 Summary

This chapter has discussed the various investigations and diagnosis performed in order to accurately measure the streamers in ester under DC and lightning impulse voltage. To obtain accurate data about the streamer activity, it is important to ensure that the signal detected is free from disturbances and oscillations. Various investigations were conducted to obtain electrical signals that could correlate with the light signals detected by the PMT. The chapter analyses the problems faced during the diagnosis of the test set up through experiments and software modelling. Solutions to these problems are discussed and the final test set up with the winding arrangement is explained. Investigations performed in this thesis can provide useful information for the possible test set up that will be used during the final full scale testing for different electrode configurations. Though electrical signals of streamers were detected successfully under different configurations, the high sensitivity of the shunt to the noise signals prevented the use of electrical detection during certain measurements.

5. Optical diagnosis of measurement set-up for streamer detection

This chapter provides the description of the optical measurement system used for detecting light signals during streamers in the transformer insulation under DC and lightning impulse. The chapter begins with the description of the optical sensor used and the research behind choosing the sensor. The positioning of the sensing system is explained and the problems faced during initial tests with the sensors is highlighted. The final experimental test set up for streamer detection during small scale testing is presented along with the challenges faced during optical detection. The following part of the chapter lists the different tests performed to ensure that only the streamer light is captured by the optical sensing system, along with their results and inferences. The chapter concludes by introducing the optical system used to detect streamers originating from transformer windings. The final test set up is presented and the limitations of the optical sensor are discussed.

5.1 Optical sensor for streamer detection

Though optical detection of streamers has been carried out in the past, the knowledge in choosing the right detector is still limited. Various parameters have to be considered before selecting the right optical sensor and this section briefly describes these parameters. On comparing these parameters and consulting different optical sensor manufactures as well as previous researchers, the choice for the optical sensor used in this thesis was made.

- **WAVELENGTH RANGE:** Light emitted during the streamer propagation has a distinct wavelength range. The initial development of streamers lies in the lower wavelength region (UV spectrum) and as the streamers propagate to result in the breakdown, the light reaches the visible spectrum.
- **QUANTUME EFFICIENCY**: Not all photons emitted by the light source are converted by the optical sensor into electron hole pairs. The quantum efficiency can be expressed as the ratio of the number of electrons produced to the number of incident photons. For photomultipliers, the quantum efficiency (QE) is calculated from the radiant sensitivity(RS) as

$$QE(\%) = \left(\frac{RS \left(in \ \frac{mA}{w} \right)}{\lambda (in \ m)} \right) * 124$$

- **RISE TIME**: The optical sensor used should have a proper time response for the registration of fast pulses with rise time of the order of 1-2ns [28].
- **GAIN:** The output of optical sensors is generally in terms of current. Light observed by the sensor needs to be amplifies several times in order to record the signal. This

current amplification plays a crucial role while selecting the optical sensor to be used. Optical sensors with high sensitivity should be chosen in order to ensure the detection of streamers.

- **SIGNAL TO NOISE RATIO:** Noise signal in optical sensors can be observed when the sensor is switched on in the dark without applying any control voltage or can also be generated during the input of signal light. These components are associated with the dark current rate or dark count emitted by the photo cathode in the sensor. The optical sensor to be used must have a high SNR to ensure accurate measurement of signals.

Based on these above parameters and in depth literature survey, the **photomultiplier tube** was selected as the appropriate sensor for the detection of streamers. The primary reason behind is this is the fact that the light emitted by the streamers is extremely weak and undergoes absorption and dispersion before reaching the sides of the test cell containing the dielectric liquid. Such weak lights cannot be captured by other optical sensors and only the PMT has a high enough sensitivity and gain to record the signals. Furthermore, PMTs have a fast rise time and allow the signal to be displayed on the oscilloscope. Photomultiplier tubes are preferred to detect faint optical signals emitted from weak sources. When compared to APD, they offer larger active area and thus making it possible to capture light signals that are scattered and diverged [64]. Moreover, the high internal gain of the PMT reduces the effective noise of the amplifier and improve the SNR of the overall detector amplifier system. Thus, in this thesis, optical detection of streamers has been performed with the use of PMT and optical fibers.

A major drawback of using the photomultiplier is its susceptibility to magnetic interference. Since PMT's function on accelerating electrons, the trajectory of these low energy electrons is easily manipulated by magnetic fields, thereby affecting the sensitivity of the anode. The sensitivity of the head on type PMT is reduced by 50% by a magnetic flux density of below few millitesla. By using a metal package PMT, the distance between the photocathode and the first dynode is reduced thereby reducing the effect of magnetic fields.

5.2 Photomultiplier tubes

Photomultiplier tube is essentially a vacuum phototube which is used for the extremely sensitive detection of light in the UV, visible and near infrared ranges of the EM spectrum [65]. It consists of a photocathode, focusing electrodes, an electron multiplier anode generally sealed into an evacuated glass tube as shown in the figure 5.1.
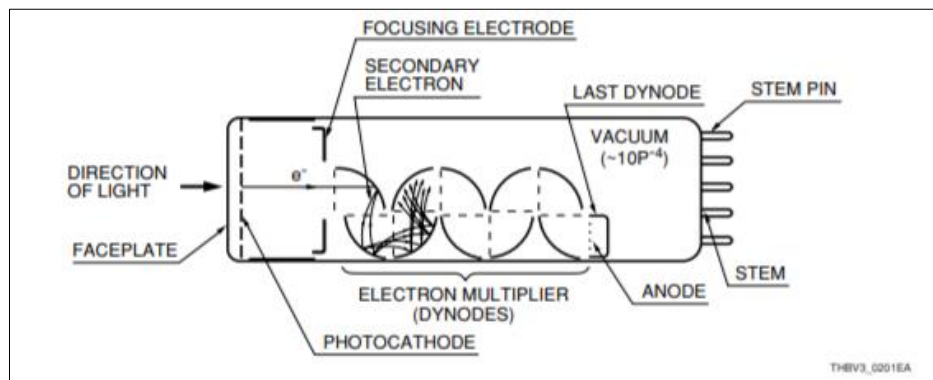
Figure 5. 1: Photomultiplier Tube [66]

Its ability to multiply the current produced by the detected light by around 100 million times(160dB) makes it suitable for ultra-high response and extremely sensitive applications. The advantages of these detectors over other photosensitive devices are its characteristics such as high internal gain, high response rate, low noise and choice of larger photosensitive area[67].

WORKING PRINCIPLE:

The working principle is based on the photoelectric effect and secondary emission. The process of converting the light entering the tube into an output signal takes place in the following way[66]:

1. Light enters the tube through the input window
2. Photoelectrons are emitted into vacuum as the light excites the electrons in the photocathode through external photoelectric effect
3. The accelerating photoelectrons are then focused onto the first dynode by the focusing electrode. The secondary electron emission results in the multiplication of these electrons, which is repeated at every successive dynode.
4. Finally, the anode captures the multiplied secondary electrons emitted from the last dynode

5.2.1 Thorlabs PMT 1001/M

After multiple discussions with Professor Pawel Rozga from the University of Lodz, Poland and Thorlabs (Germany), the photomultiplier 1001(/M) was chosen to be used for the optical sensing of streamers in this thesis. Selecting the right PMT for the investigations done in this thesis involved careful study and took up a lot of time. While different manufacturers provided solutions for the same, other parameters such as cost, delivery time and ease of communication had to be considered before making the final decision.
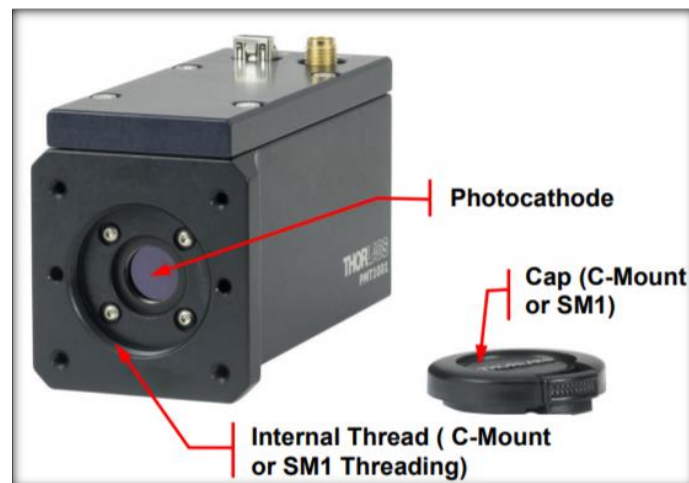
Figure 5. 2: PMT 1001/M [68]

The PMT 1001M is a non-cooled GaAsP PMT with SMI threaded aperture and metric mounting threads. It has a photocathode active area of 8mm. The photocurrent collected at the anode is sent to a built in transimpedance amplifier that converts the current signal into voltage after additional amplification. Table 5.1 provides the technical specifications of the PMT 1001M.

PARAMETERS	VALUES
Wavelength Range	230-920nm
Peak Wavelength	630nm
Gain	$>3*10^6$
Quantum efficiency at peak wavelength(anode)	>15%
Rise time	0.57ns
Photocathode type	Head on, Multialkali
Amplifier gain	11000+1000/-500V/A
Amplifier bandwidth	DC-80MHz(software configurable)
Dark Current	10nA(typical)

Table 5. 1: Technical specifications of PMT 1001/M

The light to voltage conversion is obtained for the below equation

$$V = TG * RS * G * P$$

where V represents the output voltage(In V), RS is the sensitivity(in A/W), G is the gain and P is the input optical power(in W) [68]. Figures 5.3(a) and 5.3(b) are used to estimate the radiant sensitivity and gain of the PMT respectively [67]. The maximum radiant sensitivity of the PMT is 78mA/W with a maximum output voltage of +/- 1.5V at 50Ω load.
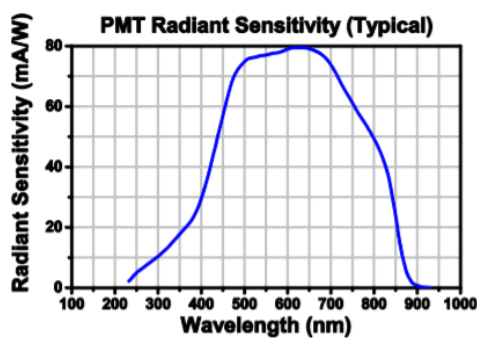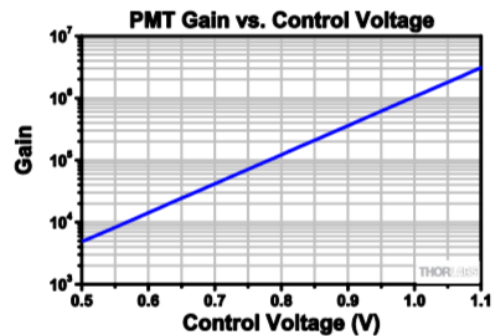
a)   b)

Figure 5. 3: a) PMT sensitivity as a function of wavelength b) PMT gain as a function of voltage

As previously mentioned, the PMT has an integrated amplifier that is designed to detect signals from DC-80MHz. It also comprises of a low pass filter that allows the amplifier to work at different ranges(250kHz, 2.5MHz, 80MHz). The impedance is driven up to 1.5V after buffering the output as shown in figure 5.4.
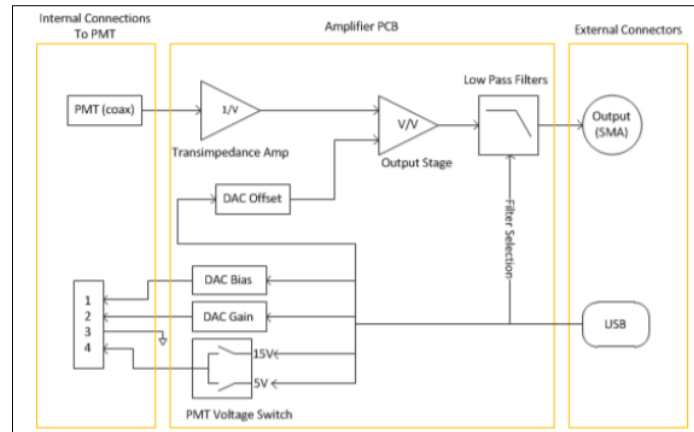
Figure 5. 4: PMT 1001/M-internal design [68]

5.3 Optical fiber bundle

Fiber optic sensing has been performed in various fields for several years such as science, healthcare, electrical appliances, defense and other related studies. Their small size and light weight make them an optimal solution for various applications. The use of fiber optic bundles in the optical sensing of discharges and streamers has witnessed a steady increase over the past few years due to their inertness to chemical substances, ability to withstand high temperatures and immunity to electromagnetic interferences [69].

Detection of streamers under lightning impulse voltage involves the measurement of light signals of a particular wavelength or frequency. Optical fiber bundles establish a connection between spectrometer, light source for measurement and evaluation of the signals [70]. The bundle is composed of several fibers which are bonded and arranged in a particular manner to suit the receiver.

Figure 5. 5: Fiber optic bundle[70]

Research by [71] was conducted to detect partial discharges using optical fiber cables and photomultiplier. The fiber optic bundle was used as a receiver unit to collect the light

radiations emitted during the partial discharge and to guide the signals to a photomultiplier. Several experiments have been performed in the past for the detection of streamers under lighting impulses using fiber optical sensing such as [72].

5.3.1 Choice of fiber optic bundle

The fiber optic bundle used for capturing the light from during the streamer was purchased from FiberCable Connect, Munich, Germany. Based on the dimensions of the PMT and its SM1SA connector, it was suggested that the diameter of the bundle should be 2.5mm for the best performance of the PMT. Larger fiber bundle could capture larger amounts of light, oversaturating the PMT. The beam divergence angle out from the fiber bundle is approximately 25°, and a larger fiber diameter could result in the PMT active area not being illuminated. In order to prevent any flashover to the fiber cables during the lightning impulse voltage, the cables are enclosed in a PVC tube. One end of the bundle is fitted with a SMA connector(male) which is compatible for the SM1SA adapter. The other end is fitted with a two part non-metallic polyetheretherketone(PEEK) ferrule as shown in the figure 5.6. PEEK fittings are chemically inert and bio- compatible, making it a convenient choice. The length of the fiber bundle used was 8m.
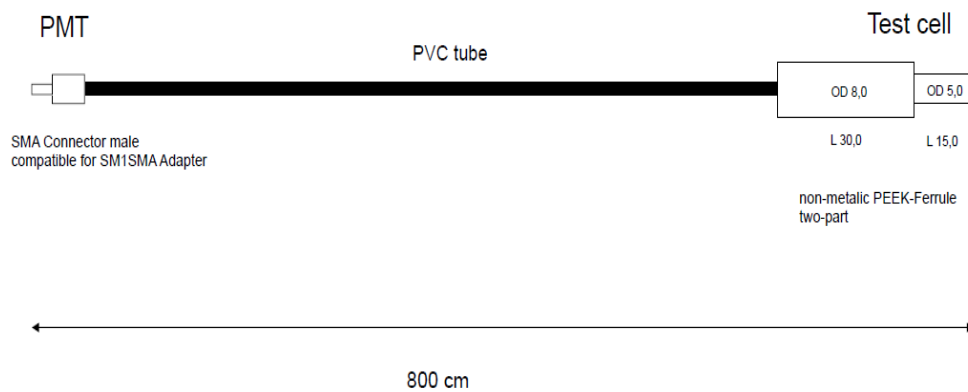
Figure 5. 6: Optical fiber bundle- FiberCable Connect, Germany

Table 5.2 provides details about the fibre specifications. The entire fibre bundle is composed of 85 fibre cables glued in SMA ferrule. The diameter of the bundle is 2.5mm as shown in figure 5.7.

Fibre cable component	Value
Core diameter	200 um +/- 2%
Cladding diameter	220um+/- 2%
Jacket diameter	245um +/- 5%
Jacket material	Polyamide

Table 5. 2: Technical specifications of optical fiber bundle- FiberCable Connect, Germany

85 single Fibers
glued in SMA-Ferrule

2.5mm
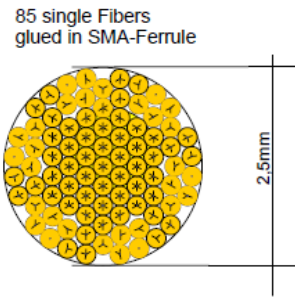
Figure 5. 7: Optical fiber bundle comprising of fiber cables- FiberCable Connect, Germany

Due to delivery time constraints and other issues, the initial tests were done with the fiber optic cable obtained from Thorlabs shown in figure 5.8. The fiber optic bundle is 2m in length and consists of 7 high grade optical fibers in a round configuration combined in an SMA 905 connector. The fiber bundles are primarily designed for coupling to light sources and are enclosed in a stainless steel tubing .
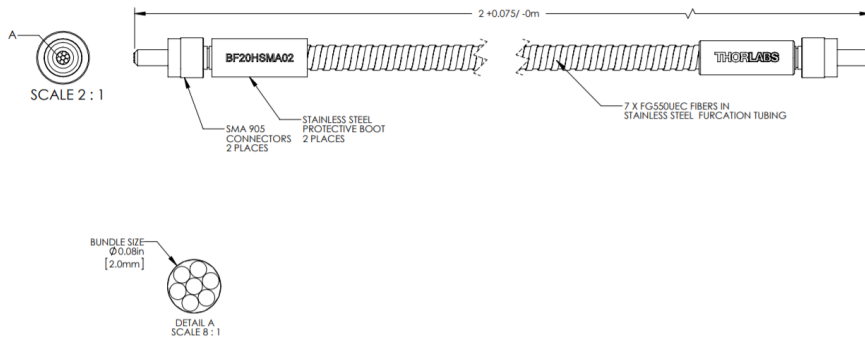
Figure 5. 8: Optical fiber bundle- Thorlabs, Germany

Table 5.3 provides the specification for the fiber bundle. The optical bundle chosen was preferred because of its larger diameter, allowing more light to flow through it. The higher bend radius makes it a more flexible option.

Property	Value
Aperture	2.0mm
Wavelength range	250-1200nm
Core diameter	550um
Bend Radius	20cm
Usable Area	56%
Number of fibers	7

Table 5. 3: Technical specifications of optical fiber bundle- Thorlabs, Germany

The position of the fiber bundle had to be adjusted in a way to view the streamer activity in the needle plane set up. As seen previously, the test cell was placed over a metal case containing the shunt for electrical measurement of streamers. A holder made of wood was designed to position the fiber cable firmly in a way so that it could see the streamer activity between the needle plane configuration. This was done to ensure that the cable does not move during the test and maximum amount of light can be recorded. Figure 5.9(a) shows the 2D model of the optical set up of the fiber cable viewing the test cell as well as the designed holder. The other end of the fiber cable was connected through the SMA connector to the PMT which was placed in a well shielded box to prevent any interference from the ambient light. The PMT was controlled by a laptop placed inside the box. The PMT software was used to alter the gain of the PMT and switch the frequency range of its amplifier.

a)   b)
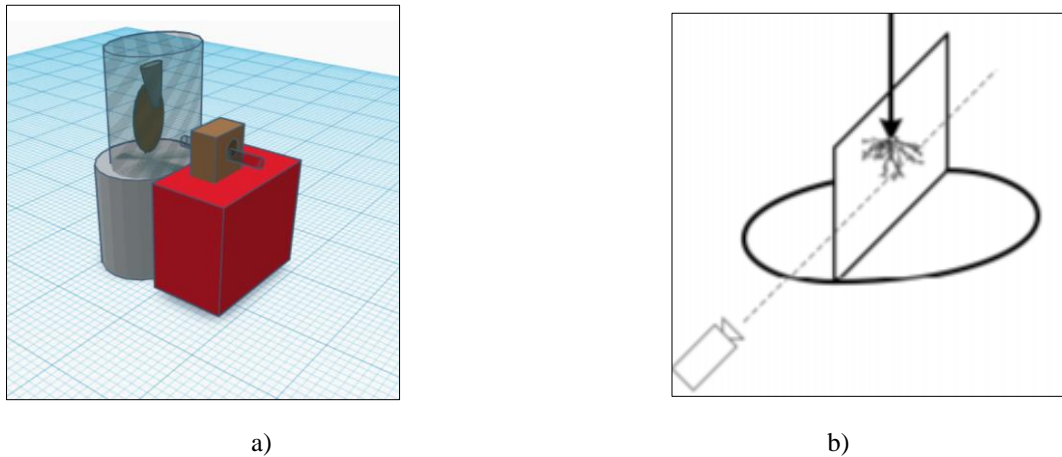
Figure 5. 9: a) 3D model of the test set up with fiber bundle b) Streamer light signal during surface discharge captured by the PMT

The initial tests, which were performed with the fiber bundle purchased from Thorlabs suggested that the presence of a metallic tubing around the fiber cables was significantly affecting the measurements while performing the impulse tests in dark. The fiber bundle was very susceptible to the interference caused by the impulse generator. Moreover, the metallic tube allowed other noise signals to enter into the PMT, causing various disturbances in the signal. Figure 5.10(a) shows the initial disturbance in the current(purple) and PMT signal (yellow) during the charging of the impulse generator when the bandwidth of the PMT amplifier was set to 2.5MHz with the test object disconnected. On increasing the amplifier bandwidth to 80MHz, higher noise signals were recorded which affected the streamer signal measurements. The fiber bundle from FiberCable Connect was used to make the final measurements and analysis.

a)   b)
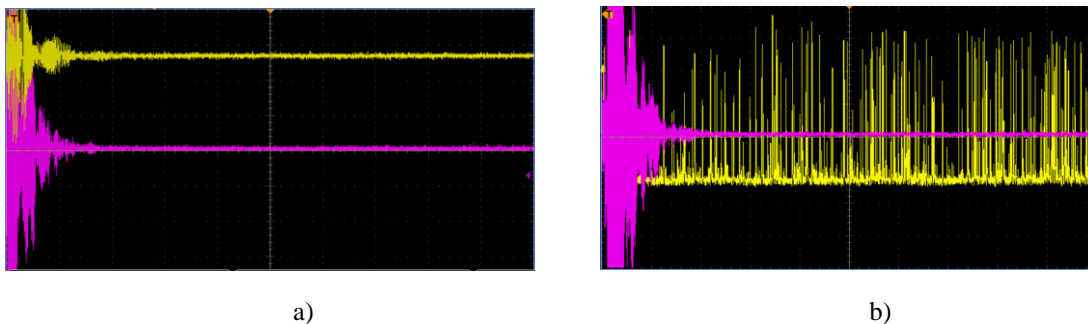
Figure 5. 10: a) Disturbance in optical signal due to LI generator, PMT amplifier bandwidth- 2.5MHz b) Disturbance in optical signal due to LI generator, PMT amplifier bandwidth- 80MHz

5.4 Experimental test set-up and diagnosis

 DC measurements for the needle-plane configuration were performed in the faraday cage in order to ensure complete darkness during measurements. A needle to plane set up was used without any pressboard immersed in ester. Two different DC high voltage source was used to provide both positive and negative voltage. Streamers were detected both electrically as well optically and compared to see the correlation between the two. The position of the optical bundle was adjusted to see the center of the needle plane set up in order to capture as much light as possible. Figure 5.11 shows the experimental set up used for DC test set up.

a)   b)
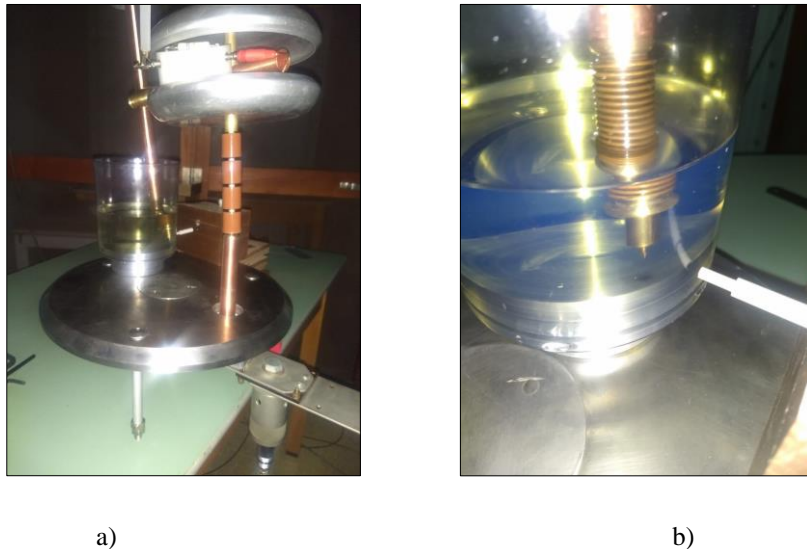
Figure 5. 11: a) Electrical and optical streamer detection- DC b) Optical fibre position for detecting streamer activity in ester-DC

Lightning impulse tests were performed with the Haefely 4MV , 20 stage lightning impulse generator. As mentioned previously, the PMT and the laptop were placed in metal box and shielded from the light outside as shown in figure 5.12(b). The experiments were performed in as little light as possible, though complete darkness could not be achieved. A wooden support was placed next to the test cell, between the impulse generator and fiber bundle to ensure that the light from the sparking of the sphere gaps did not affect the PMT recordings. Coaxial cables were used for recording the PMT and shunt data, which were connected to the Tektronix DPO 3054 and terminated by 50Ω shunt. The voltage was recorded by the Haefely Lightning impulse measuring system to ensure a standard 1.2/50 us lightning impulse waveform. The needle to ground configuration was used with the pressboard placed along the tip of the needle. The distance from the needle to ground was 2.5cm. Investigation with the lightning impulse was performed with both mineral oil and ester insulation. The test cell was covered with tap to prevent additional light from affecting the streamer signal captured by the fiber bundle as shown in 5.12(a).

a)   b)

Figure 5. 12: a) Electrical and optical streamer detection test set up- LI testing b) Metal cage in which the PMT was situated

After reviweing different electrial and optial sensors, a finalized circuit diagram for lighting impulse testing is presented in figure 5.13. All the connections to the measurement systems are done through coaxial cables which pass through the coax protector/overvolatge protetor(spark gaps and TVS diode). Sharp points are avoided and round plates are installed to ensure that the electric field at the vicinity of the test set up is never high.
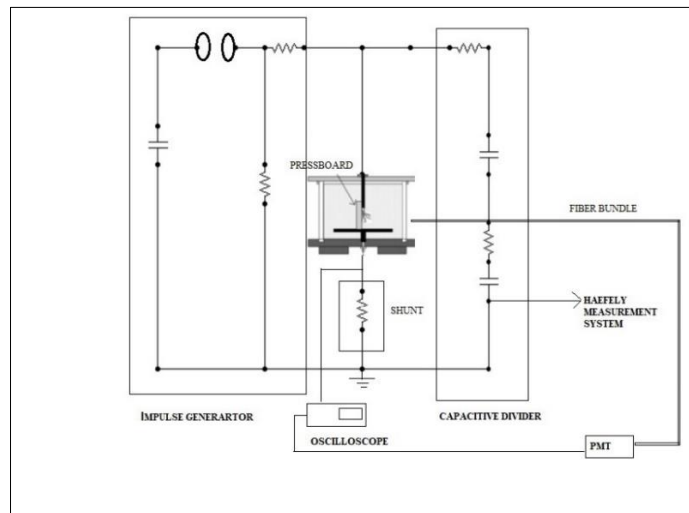
Figure 5. 13: Circuit diagram for the finalized test set up- electrical and optical streamer detection

Figure 5.14 shows the experimental test set up performed in the TU Delft, high voltage lab.
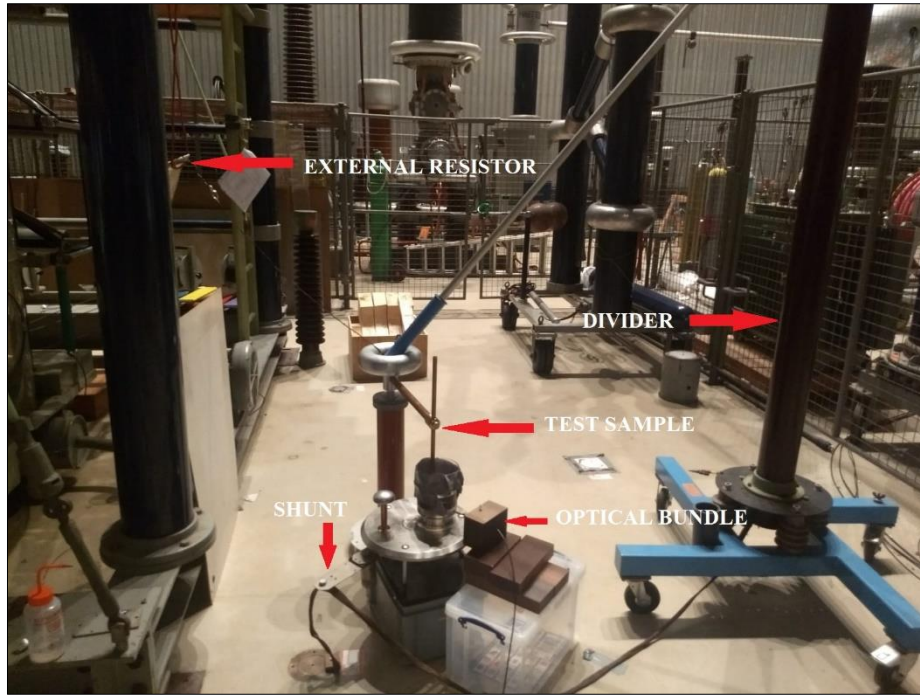
Figure 5. 14: Final test set up- electrical and optical streamer detection under LI voltage in needle-plane configuration

During the measurements, the gain of the PMT was set to 1(control voltage = 0.6V) in order to limit the high frequency noise signals which are shown in figure 5.15. Due to the high sensitivity of the PMT, setting higher gain to the PMT resulted in the saturation of the PMT during the detection of streamers. These noise signals were recorded in a dark room after disconnecting the fiber bundle and covering the PMT to prevent any light from entering. The signals showed in the figure 5.15 were observed when the amplifier frequency bandwidth was set to DC-80MHz. Measurements were done with different frequency ranges of the amplifier, but the noise signals did not create a significant disturbance during the measurement of the streamers as the light from the streamers were of a much higher magnitude. As seen in figure(yellow signal), the amplitude of the noise signal was around 60mV with the gain of the PMT set to 1 during DC testing in the Faraday cage. The light from streamer signals recorded were around 500mV-3V, which ensured that the signal to noise ratio was very low. From the figure, it can also be seen that each pulse had a time duration of approximately 15ns with a rise time of around 7ns.
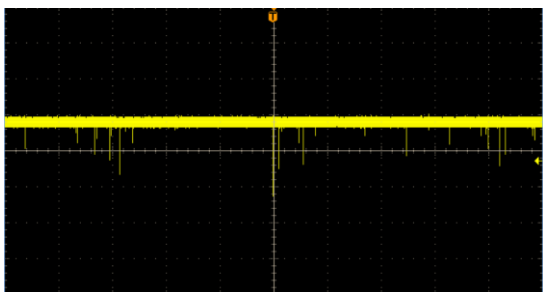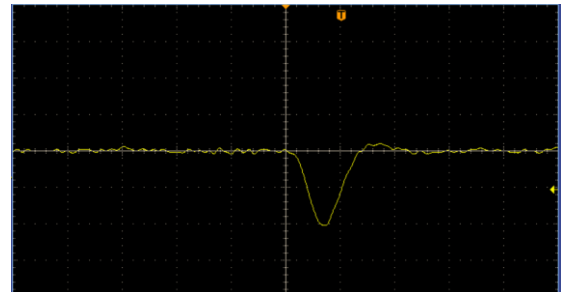
a)   b)

Figure 5. 15: PMT noise signals (20mV/div; 20μs/div)- DC testing b) PMT noise signal (20mV/div; 20ns/div)- DC testing

Optical analysis during lighting impulses provided significantly more disturbances from the PMT as complete darkness could not be achieved during these tests. As the tests were performed in a large hall, the PMT was always exposed to a small amount of outside light recording larger signals before the start of the test. As seen in figure 5.16, the PMT recorded signals of magnitude around 200mV when the room was kept as dark as possible. Though the PMT was placed inside a metal box, a small opening was made for allowing the fiber optic cables to enter. But these noise disturbances did not influence the readings during the streamer activity under the needle-plane set up as the light pulses of the streamers were in the range of 1.5V- 3V.

a)   b)
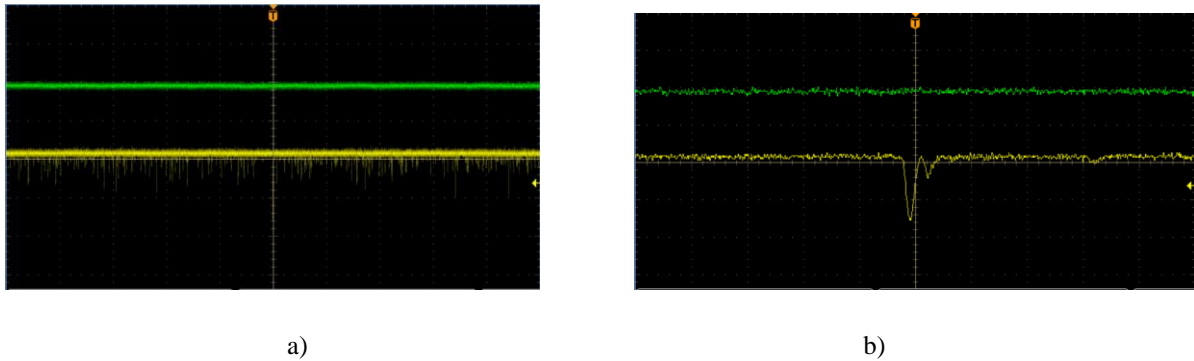
Figure 5. 16: a) PMT noise signals (200mV/div; 1μs/div)- LI testing b) PMT noise signal (200mV/div; 40ns/div) DC testing

These noise signals could have been present due to any of the following reasons:

- Not keeping the PMT in dark, even when not in use, can increase the dark count which could take several hours to dissipate. Though PMTs are designed to produce current because of the light incident on the photocathode, they will produce currents regardless of whether light is present. This signal that results in the absence of light is known as dark current and can interfere with the measurements by degrading the signal to noise ratio. This is mainly due to the thermionic emission of electrons from the photocathode and first few dynodes but with far smaller contributions from cosmic rays and radioactive decay [68].
- Insufficient warm up time for the PMT before testing.
- Temperature of the room is not cold enough to reduce the dark count rate.

Though no such disturbances were observed on setting the amplifier bandwidth to 2.5MHz with the gain as 1 for DC tests, measurements were performed with the full bandwidth of the amplifier to record as many light pulses as possible. Moreover, each of the light pulses recorded with the 2.5MHz bandwidth had a significantly higher time duration as compared to the pulses recorded when the bandwidth was full. As a result, it could be possible that in some cases the PMT may not effectively record all the streamer activities occurring in short durations as seen later during the lighting impulse tests. Figure 5.17 shows the light signal recorded by the PMT with different bandwidths of the amplifier during corona in air with negative DC voltage of 24 kV. The time duration of the pulse with the 2.5MHz bandwidth is 250ns while that with the 80MHz bandwidth is 30ns. Also, it can be seen from figure 5.17 that the light pulse is of higher magnitude when the bandwidth of the amplifier is set to 80MHz. In this case, the current signal recorded by the HFCT were of equal magnitude. Figure 5.17 (b) shows the clipping of the light signal during the saturation of the PMT.

a)   b)
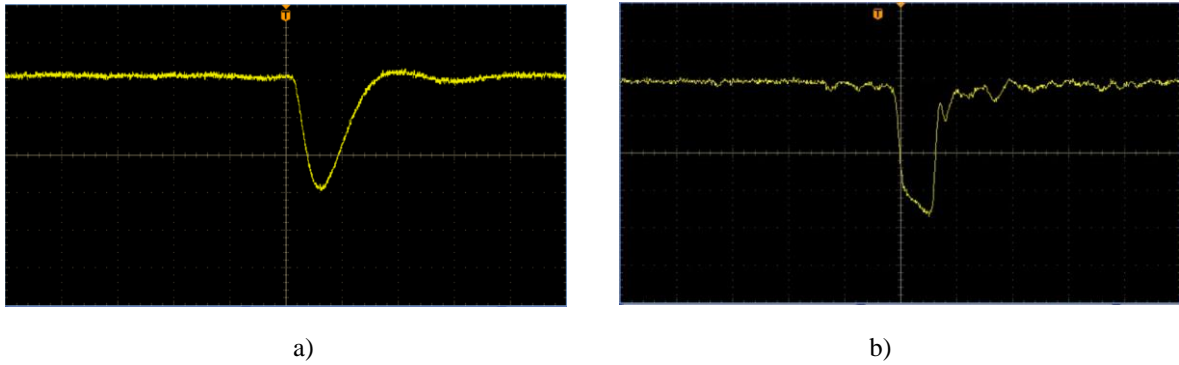
Figure 5. 17: a) Light signal during streamers in air- PMT amplifier bandwidth set to 2.5MHz (100mV/div;200ns/div) b)
Light signal during streamers in air- PMT amplifier bandwidth set to 80MHz (500mV/div;200ns/div)

To attempt to overcome the problem of saturation of the PMT, a cap of diameter 3.5mm was placed over the fiber bundle to lmit the amount of light captured by the fibers during the streamer activity as shown in figure 5.18(b). On aplying a lightning impulse voltage of 50 kV, no streamer signal was recorded by the PMT though current signal was recorded by the 10Ω shunt as shown in figure 5.18(a). As a result, the fiber bunlde was placed without the cap during testing and measurements. This however led to the saturation of the PMT signal during significant streamer activity and hence the magnitude of the streamers was also compared using the current signal for analysis. The PMT light signal however provided information about the intensity of streamer activity in the dielectrics.

a)   b)
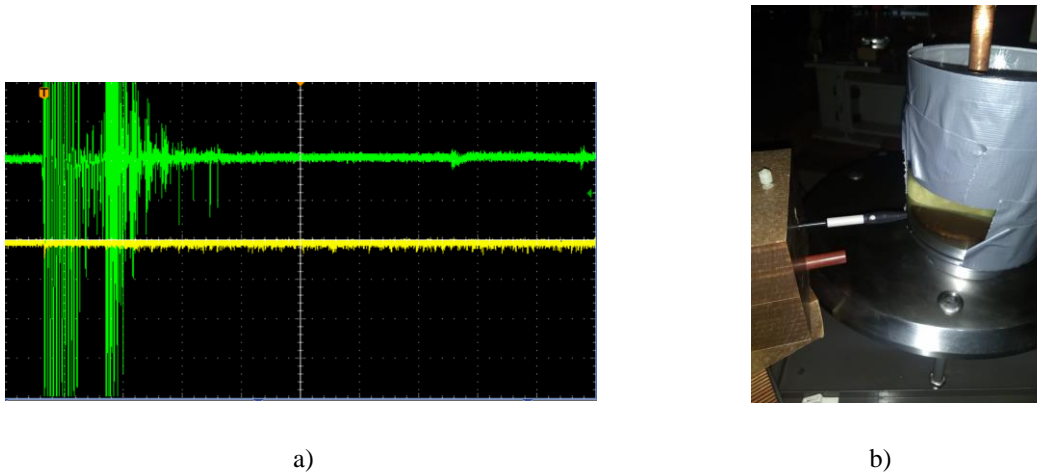
Figure 5. 18: a) Electrical and optical signal during LI testing with cap to prevent the PMT saturation(500mV/div; 2μs/div)
b) Fibre bundle with cap to prevent saturation of PMT

During the diagnosis for the lightning impulse tests as well as DC tesin, different test set ups were investigated to ensure that the signal captured by the fiber optic bundle was due to the streamers created by the needle-PB arrangement. These tests were repeated a number of times at various voltage levels to confirm that the PMT was recording only the streamer signas and also enabled us to select the appropriate PMT control settings. The high sensitivity of the PMT made it necessary to use it at the lowest possible gain with the amplifier setting at 80MHz. Table 5.4 provides the description of the various tests performed , along with the observations and inferences obtained from them during LI testing. For each of the tests, the set up was arranged according to the circuit diagram depicted in figure. The signal depcted by the shunt(1Ω) is represented by the signal in green, while the yellow signal represents the light.

Description of Test performed	Observation	Infererence
Without the needle and holder to observe the influence of possible cornoa from the other test objects(70 kV applied voltage)	500mV/division-light signal; 500mA/division-current signal, 1µs/division- time	The PMT was unaffected by possible discharges due to other test objects in the set up
Without the needle to observe the effect of possible surface discharges from the holder(70 kV applied voltage)	500mV/division-light signal; 500mA/division-current signal, 4µs/division- time	The PMT was unaffected by possible surface discharges due to the holder on the PB and oil.
Blocking the fiber sensor to ensure no magnetic coupling is affecting the PMT recordings(55 kV applied voltage)	500mV/division-light signal; 500mA/division-current signal, 2µs/division- time	The shunt recorded streamers while no signal was captured by the PMT eliminating the possibility of magnetic coupling between the shunt and PMT.
Removing the wodden barracade between the test cell and spark gaps(45 kV applied voltage)		The PMT signal is saturated by the light from the sparking of the sphere gaps and takes a significant time to reach steady state.
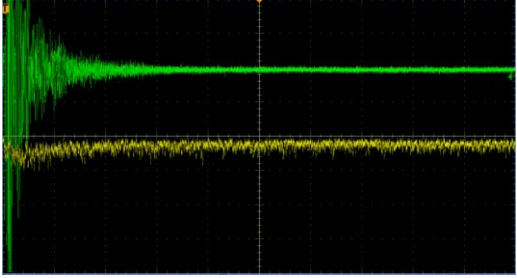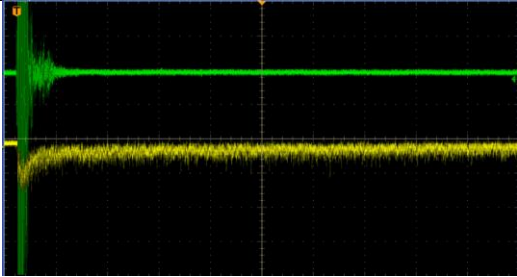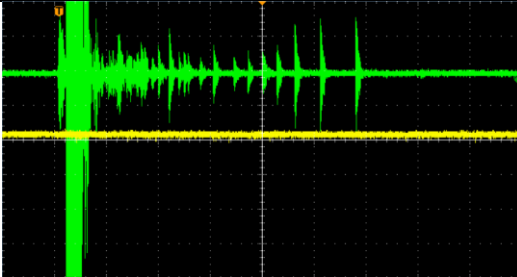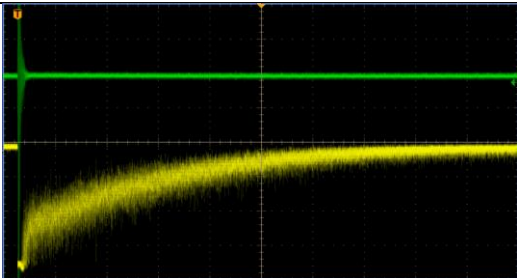
	500mV/division-light signal; 500mA/division-current signal, 20µs/division- time	The presence of the wodden block is important for the measurements.
PMT amplifier set to 2.5MHz, gain=1(50 kV applied voltage)	500mV/division-light signal; 500mA/division-current signal, 2µs/division- time	The streamers are recorded only by the shunt, the PMT is unable to capture the signals from the streamers.
PMT amplifier set to 2.5MHz, gain=20(50 kV applied voltage)	500mV/division-light signal; 500mA/division-current signal, 2µs/division- time	The PMT signal is saturated immediately and is unable to record the streamer activity.
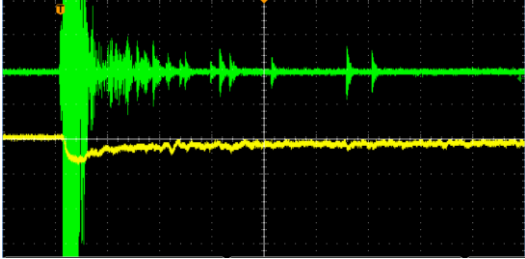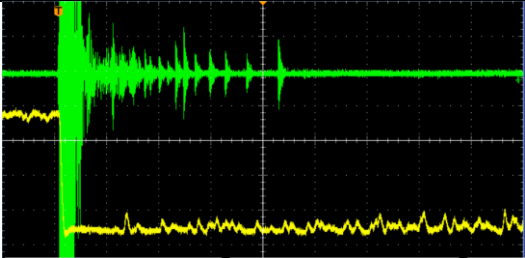
Table 5. 4: Optical diagnosis during LI testing under needle-PB-plane set-up

Optical detection of streamers with the winding arrangement was performed by immersing the fiber bundle inside the tank filled with the ester insulation. The fiber optic bundle was positioned in such a way that it could capture as much as light as possible due to the streamers originating from the winding. The windings were made to rest on wooden blocks on opposite sides of the ground electrode to ensure appropriate gap between the ground electrode and the winding. Before the test set up was prepared, the fiber bundle manufacturers were contacted to ensure that the cable does not get damaged on placing inside ester. Figure 5.19 represents a 3D model of the final test set up for the streamer detection in ester with the winding arrangement.
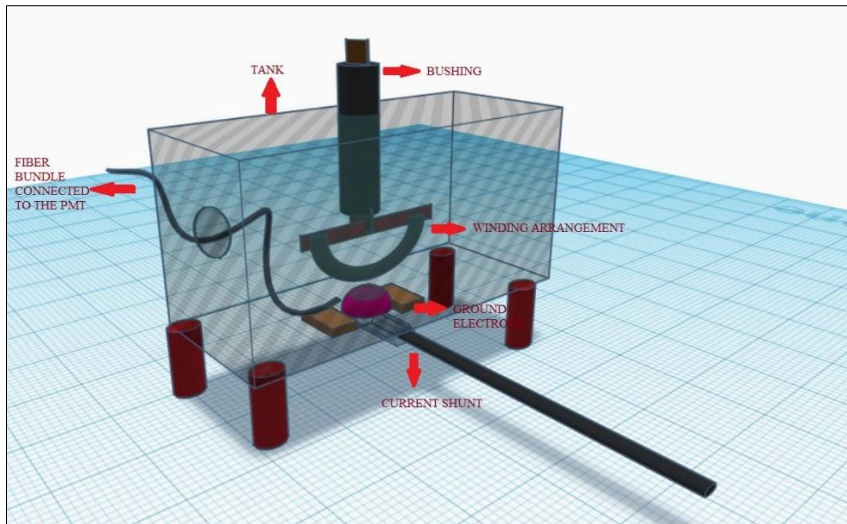
Figure 5. 19: 3D representation for streamer detection from windings in ester

Since the gap between the winding and the bottom electrode was extremely small, the positioning of the fiber bundle proved to be crucial. As seen in figure 5.20(b), the fiber bundle was carefully placed close to the top of the ground electrode in order to capture as much light as possible. The tank was covered from top using wooden structures to ensure no external light interferes with the optical detection of streamers as shown in figure 5.20(a).
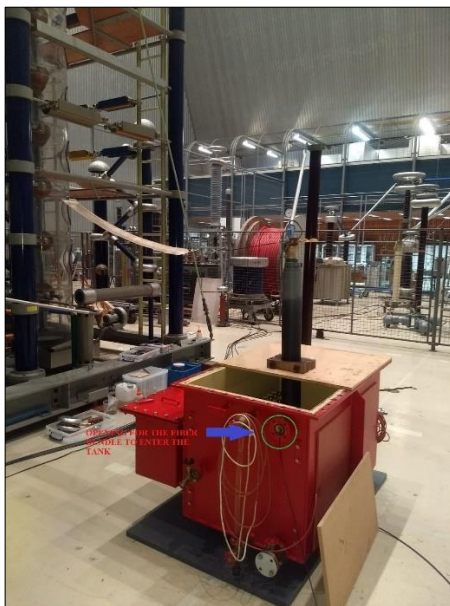
a)

b)

Figure 5. 20 a):Optical bundle entering the tank   b):Positioning the fibre bundle for the optical detection of streamers

The final test set up for detecting streamers under impulse voltages from windings was prepared according to the circuit diagram shown in figure 5.13. The test set up included a 100Ω external resistor to ensure appropriate waveshape and a capacitive divider to measure the impulses. Voltage measurement was performed by the Haefely measurement system

while the streamers were detected by the DPO 3054 oscilloscope. Figure 5.21 shows the final test set up used in this thesis for streamer detection originating from transformer windings in ester .
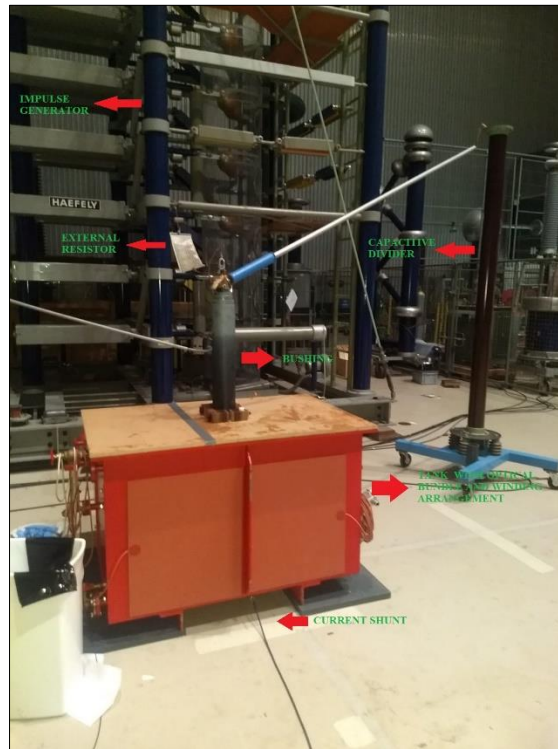
Figure 5. 21: Test set up used in this thesis for streamer detection from transformer windings in ester

Though the tank was completely covered to prevent any light from entering, the PMT generated noise signals which interfered with the detection of streamers originating from the winding. Unlike streamers generated in a divergent field with the needle and pressboard, streamers from the paper insulated winding were expected to be much smaller in magnitude as seen in chapter 6. The noise signal generated from the PMT (yellow) is shown in figure 5.22(a). On examining a single noise signal, it was seen that the magnitude of these signals could reach up to 100mV with a time duration of 16ns.
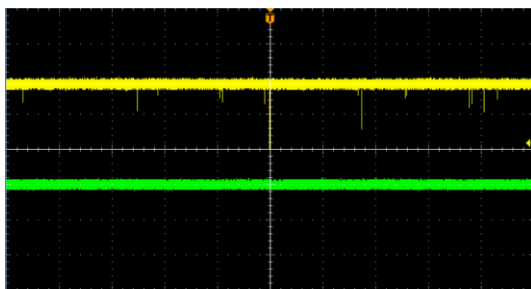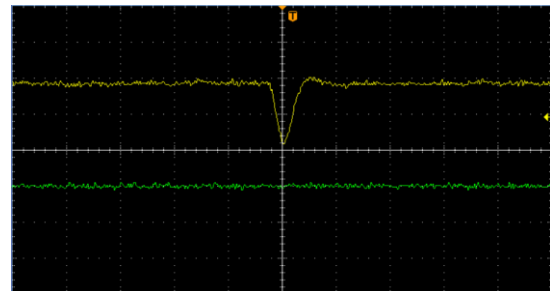
a)   b)

Figure 5. 22 a): Noise signals generated by the PMT (light- 50mV/div; time-800μs/div) b): Noise signal generated by the PMT (light- 50mV/div; time-20ns/div)

Figure 5.22(a) further provides an indication about the frequency of the noise signal generated by the PMT. Investigation under lightning impulse without the winding was performed to ensure that the fiber bundle does not capture light due to discharges from the steel rod or the bushing. It can be seen from figure 5.23(a), during an impulse of 200 kV, that similar to the disturbance of current signal (green) recorded by the shunt, the light signal is also affected due to the charging of the impulse generator for the first few us. The pulse recorded by the PMT does not indicate a streamer or any other discharge, but represents the noise pulse of generated by the PMT itself. This is because during streamer activity, significantly larger number of pulses will be observed continuously and this will be discussed in detail in chapter 6. This is further confirmed by figure 5.23(b), which shows the noise signal generated by the PMT throughout the time duration of 1ms. Though the noise signal generated by the PMT hinders the accurate detection of streamers optically, significant difference in the frequency of pulses during the streamer activity enabled the successful detection of streamers originating from the windings.

a)   b)
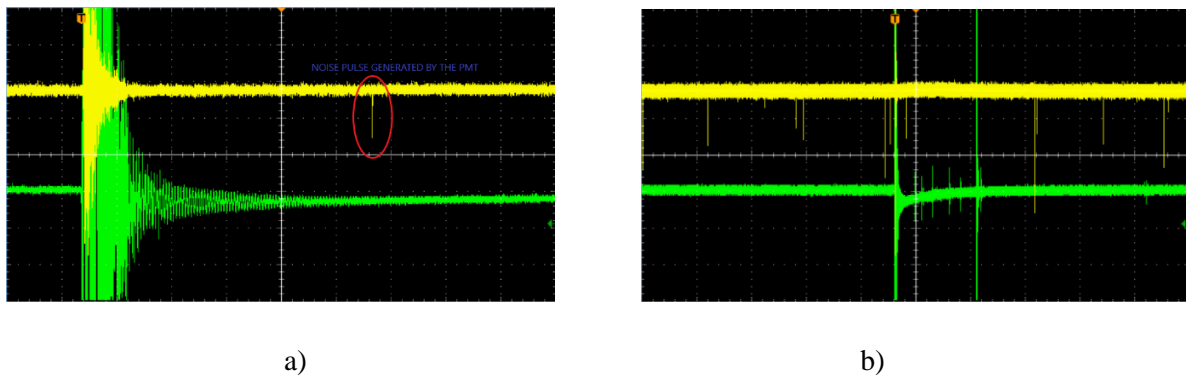
Figure 5. 23 a): Noise signal generated by the PMT during impulse testing without winding (light- 20mV/div; current- 2V/div; time-4μs/div) b): Noise signals generated by the PMT during impulse testing without winding (light- 20mV/div; current- 2V/div; time-200μs/div)

5.5 Summary

This chapter discusses the steps involved in choosing the equipments for the optical detection of the streamers. Various factors such as delivery time, cost, ease of contact with supplier had to be taken into consideration before selecting the products. Furthermore, different specifications had to be analyzed to make a conclusive decision on the photomultiplier model and fiber bundle purchased. Testing performed in Lodz University of Technology provided useful information on the test set up and choice of the optical detectors. Furthermore, positioning of the fiber bundle plays a crucial role in obtaining accurate results. The fiber bundle was then placed inside a specially designed holder in order to precisely position it for best results. The chapter provides the readers with the description of the test set up used for the optical and electrical detection in DC and lightning impulse investigations under divergent fields using needle and PB. Various diagnostic tests were performed to ensure that the fiber bundle was not sensing unwanted discharges that may occur in the test set up. Finally, the chapter introduces the optical detection set up used recording streamer light signals originating from transformer windings in ester. It concludes with a discussion about the noise signals recorded during impulse testing generated by the PMT. Though the noise signals are of similar magnitudes to the streamers recorded, the streamers could be clearly distinguished as seen in the next chapter. However, analysis of light signal recorded when the streamer activity was not prominent was considerable affected due to the presence of this noise.

6. Measurements and analysis

This chapter is dedicated to streamer detection using the optical sensing system comprising of PMT 1001/M and the fiber bundle as well as electrical techniques using HFCT and coaxial shunts. Primary tests were performed using DC voltage as the PMT 1001/M has been introduced for the first time in streamer detection. The analysis and interpretation of the results for DC testing are presented simultaneously to help the readers understand the measurements recorded. The chapter also presents the results recorded during the streamer detection under impulse voltages for different configurations mentioned in the previous chapters, followed by some statistical analyses.

6.1 Theory

As discussed in chapter 2, streamers are composed of two parts: the propagating ionizing front called streamer head and the streamer channel which is filled with plasma constituting the streamer tail. These rapidly extending ionized channels can be observed in solids, liquids as well as gaseous mediums. They are generated by high electric fields and the voltage at which streamers initiate is called the streamer inception voltage. Figure 6.1 depicts the propagation of streamers in transformer oil under different gaps and voltages.
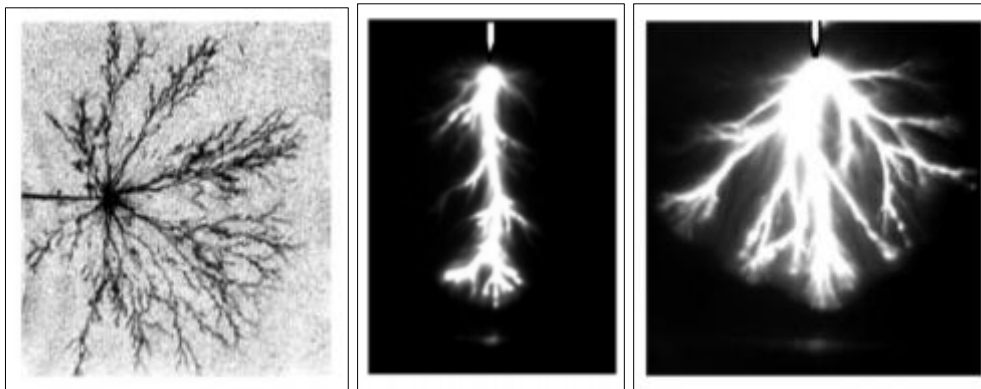
Figure 6. 1: Different types of streamer propagation in transformer insulation [29]

Breakdown process in insulating mediums is preceded by streamer initiation and propagation. Breakdown voltage can be regarded as the critical voltage which is needed to cause the streamers to completely bridge the gap between two electrodes and thereby leading to a breakdown. When the applied voltage exceeds the inception voltage but falls short of the breakdown voltage, the streamers propagate through the medium for a certain distance before getting extinguished. As the streamer propagates, the voltage drop along the channel and its branches causes the electric field at the streamer head to drop below the ionization strength. Research done previously show us that positive streamers have a lower breakdown strength and are considered more dangerous to the electrical equipment.

Most researchers have recorded voltage, current and light emitted during the occurrence of streamers. The shape of streamers have been captured by high speed cameras and various properties such as speed, stopping length, transient current have been studied. Streamer

propagation can be classified based on the velocity into different modes [73]. First mode streamers are generally unlikely to cause a breakdown and will traverse small distances before getting extinguished. They travel with a velocity of 0.1mm/µs and are characterized by bus like channels. On further increasing the voltage, the second mode of streamers can be initiated. These streamers propagate with supersonic velocity 10 times higher than the 1st mode and are characterized by some light emission and re illumination. This mode of propagation is generally very close to breakdown and is an important factor in determining the breakdown process. The appear as filaments with a change from the cylindrical to spherical form and the number of branches increases with increase in the voltage.

Acceleration voltage(Va) is the voltage which causes the transition of the 3rd mode streamers into 4th mode streamers. On increasing the voltage higher to a level below the Va, the second mode streamers switch to the third mode. These streamers generally travel with velocities of 10-20km/s for a particular distance before switching back to the second mode streamers. If the voltage is higher than Va, fourth mode streamers with speeds of up to 100mm/us can be observed in the form of few luminous branches before breakdown is reached[2]. The relationship between modes of propagation, velocity of propagation and applied voltage are graphically depicted in figure 6.2.
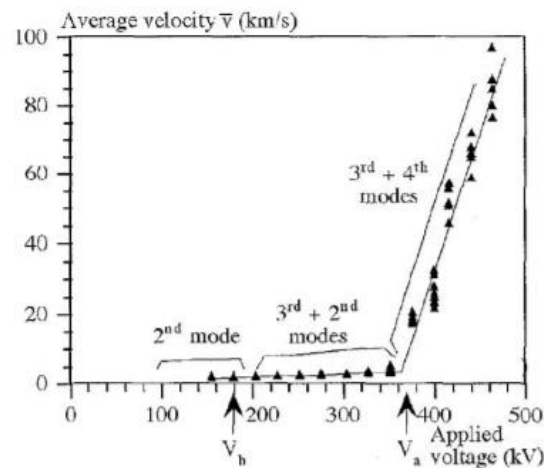
Figure 6. 2: Streamer Propagation modes at different voltages for 10cm gap in transformer oil [74]

Time to breakdown has been investigated with respect to the applied voltage in many previous investigations under uniform and nonuniform fields. Research by [79] confirms that the time to breakdown reduces with increase in applied voltage. On increasing the voltage beyond the acceleration voltage, the time to breakdown has a significant drop due to the drastic increase in velocity of the 4th mode propagation of streamers. Moreover, the length of streamers increases with increase in applied voltage until breakdown occurs. Streamers become more conductive on reaching the acceleration voltage [78]. For negative streamers, the transition from the bush like structure to a filamentary one happens at a much higher voltage as compared to the positive streamers. Since the filamentary streamers propagate much more easily, the positive streamers have a longer stopping length as compared to the negative ones.
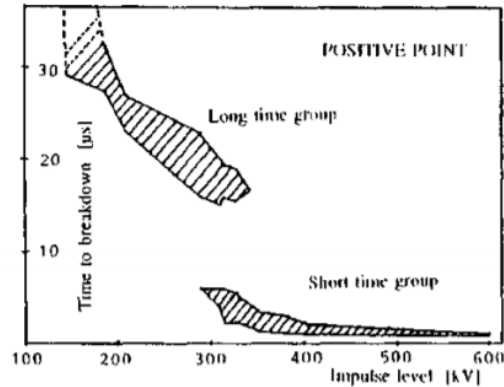
Figure 6. 3: Time to breakdown at different voltage levels [79]

Previous investigations by [75] discussed the effect of shielding on the accelerating and breakdown voltage. Shielding is a phenomenon by which the streamer channels distort and reduce the electric field of each other. Research done by [75] suggests that a pressboard placed in parallel to the electric field would enhance the propagation of streamers. On placing the electrode along an insulating surface as shown in figure, the streamer branches are constrained and thus reduced, causing the effect of shielding to also reduce.

Figure 6. 4: Effect of shielding during surface discharges [76]

As the streamers approach the 4th mode of propagation, the number of branches are significantly reduced. Thus, on reaching the acceleration voltage, [75] suggested that the shielding effect is reduced. Thus, the streamer propagation between the breakdown and acceleration voltage along the surface is slow with a rapid change in velocity when the voltage reaches Va. By placing an insulating surface in parallel to the electrode, the shielding effect is reduced, and Va should thus be lesser.

Furthermore, the electric field is distorted due to the presence of the dielectric surface. While the component of E parallel to the interface is continuous across the boundary, the discontinuity in the perpendicular component will alter the electric field depending upon the properties of the surface. Photons emitted by the streamer channel could be absorbed by the surface, exciting a molecule to reach a higher energy state. Generally, these molecules undergo de excitation through non radiative process which tend to dominate the radiative process. Hence, most molecules which absorb the photons are not likely to re-emit them [77].

95

6.2 Measurement and analysis- DC testing

There is a significant difference between the streamer characteristics in ester and mineral oil for both polarities. This section describes the streamers in terms of their current and emitted light magnitude for different voltage levels up to breakdown performed in the TU Delft High voltage lab. The experimental test set up is described in section 4.1.2.1 as well as 5.4. Oscillograms used in the following sections depict the typical current and light signal emitted during the voltage application. The response from the photomultiplier is represented by the yellow signal ,the purple signal corresponds to the current pulse from the HFCT and the green signal is the current pulse recorded by the 10Ω shunt .

6.2.1 Negative polarity

The negative streamers were recorded with the needle to ground distance of 5mm. This section investigates the properties of negative streamers as shown in figure 6.5, during its inception, where the voltage applied was 19 kV. Under negative polarity, generally a single pulse is detected in both light and current signal separated by some time duration. The negative current signals have a shorter time duration of around 150-200ns when compared to the positive streamers. From figure 6.5 it can be seen that the signal is first recorded by the shunt, followed by the HFCT and then the PMT. Moreover, the sensitivity of the shunt is much higher than that of the HFCT as expected.

a)   b)

Figure 6. 5: a) Streamer signals in ester-19 kV(HFCT signal(purple)-2mV/division, light signal(yellow)- 200mV/division, shunt signal(green)- 50mV/division, time-100ns/division) b) Streamer signals in ester-19 kV(HFCT signal(purple)- 2mV/division, light signal(yellow)- 200mV/division, shunt signal(green)- 50mV/division, time-200ns/division)

On increasing the voltage to 22 kV, the frequency of pulses increased, with the intensity of the light and current signals also increasing in magnitude for ester as seen in figure 6.6(b). The light signal recorded corresponds to the current signal for most pulses. From these figures, it is evident that there is a significant difference in the associated current and light signals for the negative streamers in ester and mineral oil. The current signal in mineral oil is mainly a single pulse with a time duration of 250ns while the time duration for the streamer signals in ester was higher(1μs) with a greater number of pulses. Also, the magnitude of the current and light signal were much higher in ester as compared to mineral oil for the same voltage level.

a)   b)

Figure 6. 6: a) Streamer signals in mineral oil-22 kV(HFCT signal(purple)-2mV/division, light signal(yellow)-200mV/division, shunt signal(green)- 50mV/division, time-1μs/division) b) Streamer signals in ester-22 kV(HFCT signal(purple)-2mV/division, light signal(yellow)- 200mV/division, shunt signal(green)- 50mV/division, time-1μs/division)

Figure 6.7 shows the light and current signals recorded at a voltage level of 25 kV for ester and mineral oil. The light and current signals are characterized by a train of pulses growing in amplitude. Sometimes, the light signal does not correspond to any current signal as shown in figure 6.7(b) for mineral oil. This could be associated with some light signals that appear after the end of a single large pulse and the absence of current signal could be due to re illumination [81].

a)   b)

Figure 6. 7: a) Streamer signals in mineral oil-25 kV(HFCT signal(purple)-2mV/division, light signal(yellow)-200mV/division, shunt signal(green)- 50mV/division, time-1μs/division) b) Streamer signals in ester-25 kV(HFCT signal(purple)-10mV/division, light signal(yellow)- 500mV/division, shunt signal(green)- 200mV/division, time-400ns/division)

Further increasing the voltage close to the breakdown level causes the streamer activity to grow more significantly in case of the ester. This could suggest that the negative streamers in mineral oil do not show as much change in shape and size as compared to the streamers in ester which elongate and branch more easily. Larger amplitudes of current signals in case of ester could suggest that the negative streamers propagate further as the voltage increases as compared to mineral oil. Figure 6.8 shows the streamer signals obtained for 27 kV for ester and mineral oil. The frequency of the current pulses not being associated with the light signals also increases with the increase in voltage. The total duration of the light signal is generally longer than that of the corresponding currents, especially in case of mineral oil.

a)   b)

Figure 6. 8: a) Streamer signals in mineral oil-27 kV(HFCT signal(purple)-10mV/division, light signal(yellow)- 1V/division, shunt signal(green)- 500mV/division, time-1μs/division) b) Streamer signals in ester-27 kV(HFCT signal(purple)- 5mV/division, light signal(yellow)- 500mV/division, shunt signal(green)- 200mV/division, time-400ns/division)

Unlike the positive streamers, negative streamers don't result in breakdown immediately for both liquids. The breakdown voltage observed for the negative polarity was higher than the positive voltage. This is because under the positive polarity, the positive charges are concentrated at the streamer head, enhancing the boundary field. This further promotes the streamer propagation and thereby lowers the breakdown voltage. On the contrary, the boundary field is weakened in case of the negative polarity as the negative space charges shield the tip. Thus, the streamer propagation is hindered, and the breakdown voltage is higher. The breakdown voltage observed for both liquids were approximately the same value as the gap distance between the needle and ground was very small. However, significant difference is observed in the streamer activity leading to breakdown between ester and mineral oil. Figure 6.9 shows the streamer signals recorded during breakdown at 30 kV for mineral oil and ester. In both oscillograms, a long current train with discrete pulses is observed before the final breakdown. The duration of the streamer signals is significantly higher in ester and also presents much higher magnitudes of the current signals. This further confirms that the streamer propagation in ester is less hindered when compared to mineral oil. This could also suggest that the streamers in ester propagate longer distances as compared to mineral oil and thereby resulting in lower breakdown voltages with larger gaps between the needle and ground. This difference in negative streamer propagation between the two liquids could be because of the difference in electronegativity caused by electron scavengers. Highly electronegative oxygen atoms existing in the ester molecular structure could be a reason for higher streamer activity in ester.

a)   b)

Figure 6. 9: a) Streamer signals in mineral oil-30 kV(HFCT signal(purple)-10mV/division, light signal(yellow)- 1V/division, shunt signal(green)- 100mV/division, time-1μs/division) b) Streamer signals in ester-30 kV(HFCT signal(purple)- 20mV/division, light signal(yellow)- 1V/division, shunt signal(green)- 500mV/division, time-400ns/division)

Table 6.1 and 6.2 provide the details of the magnitude and duration of the current and light signals recorded during negative polarity for both the liquids.

MINERAL OIL					
Voltage (kV)	Peak Light Signal	Peak Current Signal(mA)	Time duration of current signal	Time duration of light signal	Number of current pulses
19	200mV	5	250ns	250ns	1
22	200mV	10	300ns	900ns	1-2
25	600mV	25	2µs-3µs	6µs	3-6
27	2V	50	4µs-5µs	9µs	7-10
30 (breakdown)	>2V	100	4µs-6µs	6µs	10-13

Table 6. 1: Streamer signal analysis under DC field- mineral oil

ESTER					
Voltage (kV)	Peak Light Signal	Peak Current Signal(mA)	Time duration of current signals	Time duration of light signals	Number of current pulses
19	1.2-1.5V	7.5	300ns	250ns	1-2
22	1.5V	15	800ns	800ns	2-4
25	2V	50	2µs-3µs	2µs-3µs	10-15
27	2V	75	3µs-4µs	3µs-4µs	15-20
30 (breakdown)	>2V	>400	5µs-6µs	6µs	>20

Table 6. 2: Streamer signal analysis under DC field- ester

From the above tables, it is clear that the streamers grow in frequency and magnitude with the increase in voltage for both the liquids. The growth of the streamer activity is much more prominent in ester as compared to mineral oil. More significant differences can be obtained by increasing the needle to ground plate distance.

6.2.2 Positive polarity

Positive streamers have a different current waveform when compared to the negative streamers. As previously mentioned, breakdown in the positive polarity is significantly lower than the negative polarity. Hence, the needle to ground distance was increased to 1cm in order to observe the streamer characteristics before breakdown. Figure 6.10 represents the current signal from the HFCT and light signal of the streamers in ester when the applied voltage is 24 kV. Unlike the negative streamers, the streamer inception voltage is much

higher and very close to the breakdown voltage for small distances. The emitted light signal corresponds to the current signal which is significantly different from the negative pulses. The current associated with both the liquids are similar as seen in figure 6.10 .They consist of continuous discrete pulses superimposed by a number of fast pulses [80].When compared to the negative streamers, the intensity and frequency of the light signal observed during the positive polarity is higher. This suggests that the streamers under positive polarity are brighter than the negative ones. However, the current signals from the shunt are significantly lower in amplitude for the positive streamers for both liquids. Similar to the negative streamers, the streamer activity is more prominent and for a longer duration of time in ester when compared to mineral oil.

a)   b)
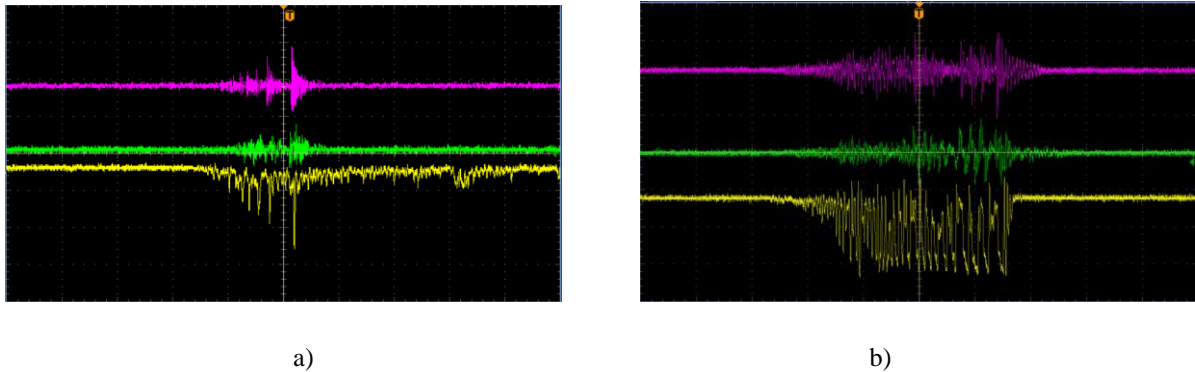
Figure 6. 10: a) Streamer signals in mineral oil+24 kV(HFCT signal(purple)-10mV/division, light signal(yellow)-500mV/division, shunt signal(green)- 100mV/division, time-400ns/division) b) Streamer signals in ester+24 kV(HFCT signal(purple)-20mV/division, light signal(yellow)- 2V/division, shunt signal(green)- 100mV/division, time-400ns/division)

On increasing the voltage further to 26 kV, the light signal emitted was more intense with larger current signals for both liquids. The magnitude of the current signal was higher in ester when compared to mineral oil. It is clearer that the current signal is composed of a continuous component superimposed by a train of high frequency pulses for both liquids. The high frequency current pulses are of much higher magnitude in case of ester as compared to mineral oil. This provides an indication that the streamers are growing in magnitude as the voltage is increased.

a)   b)
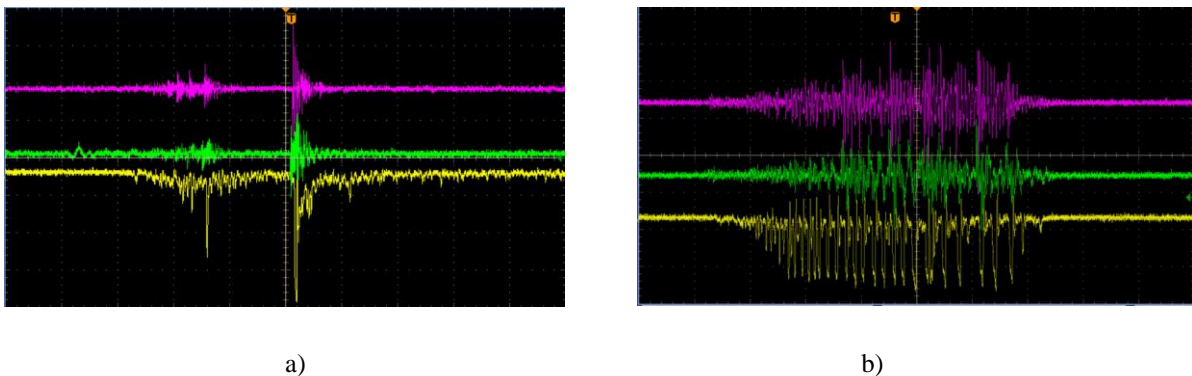
Figure 6. 11: a) Streamer signals in mineral oil+26 kV(HFCT signal(purple)-10mV/division, light signal(yellow)-500mV/division, shunt signal(green)- 100mV/division, time-400ns/division) b) Streamer signals in ester+26 kV(HFCT signal(purple)-20mV/division, light signal(yellow)- 1V/division, shunt signal(green)- 100mV/division, time-400ns/division)

Figure 6.12 shows the oscillogram of the light and current signal for voltage of 28 kV, very close to the breakdown voltage. At higher voltages, it can be observed that the current signals are mainly composed of the high frequency component. These types of current signals are previously associated with hybrid streamers where in the filamentary streamers initially propagate up to a certain length before transforming into slower streamers with periodic illuminations similar to the negative pulses which are then represented by discrete pulses [84]. The time duration as well as intensity of streamer signals are much higher in ester just like the measurements under negative polarity.

a)   b)
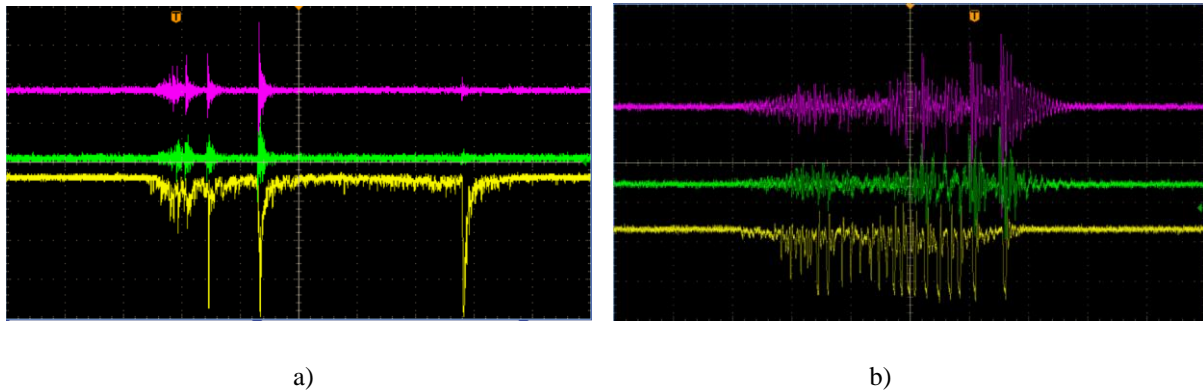
Figure 6. 12: a) Streamer signals in mineral oil+28 kV(HFCT signal(purple)-10mV/division, light signal(yellow)-500mV/division, shunt signal(green)- 100mV/division, time-1μs/division) b) Streamer signals in ester+28 kV(HFCT signal(purple)-20mV/division, light signal(yellow)- 1V/division, shunt signal(green)- 100mV/division, time-400ns/division)

Breakdown for both liquids was observed at approximately same voltage. The fact that the breakdown voltage in case of positive streamers is much closer to the inception voltage suggests that the stopping length of the positive streamers increases more drastically with the increase in voltage. As a result, the streamers attain higher modes of propagation at lower voltages eventually leading to breakdown faster. On comparing the current signal with the pre-breakdown signals, there was a gradual increase in amplitude of the current signal during breakdown for both liquids. The current signal becomes stronger and after a few us, the streamer propagates to the ground plate indicating the breakdown event. As seen in figure 6.13, streamer signals are more severe in ester when compared to mineral oil. During streamer propagation, the streamer splits from the main channel which originates from the needle tip and new side branches are produced. Increased streamer current signal observed for ester suggests that positive streamers in ester have a better ability to branch out when compared to mineral oil. The duration of breakdown in ester at 30 kV was 9-11μs while in mineral oil was 5-6μs for the same voltage level.

a)   b)
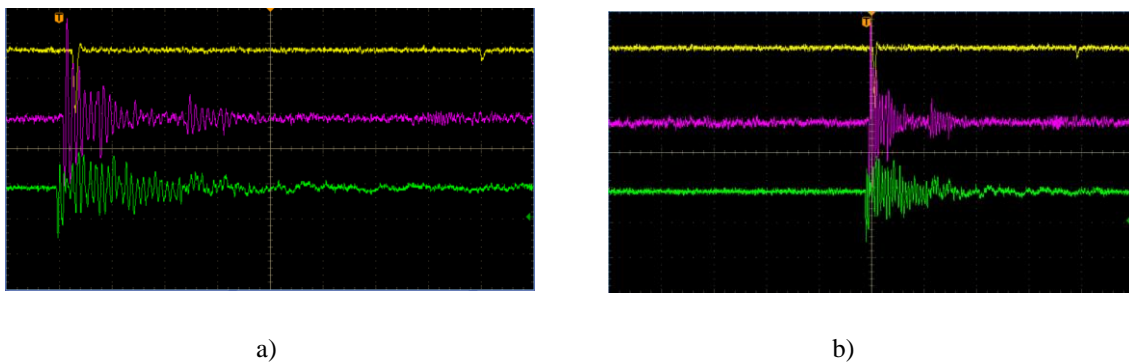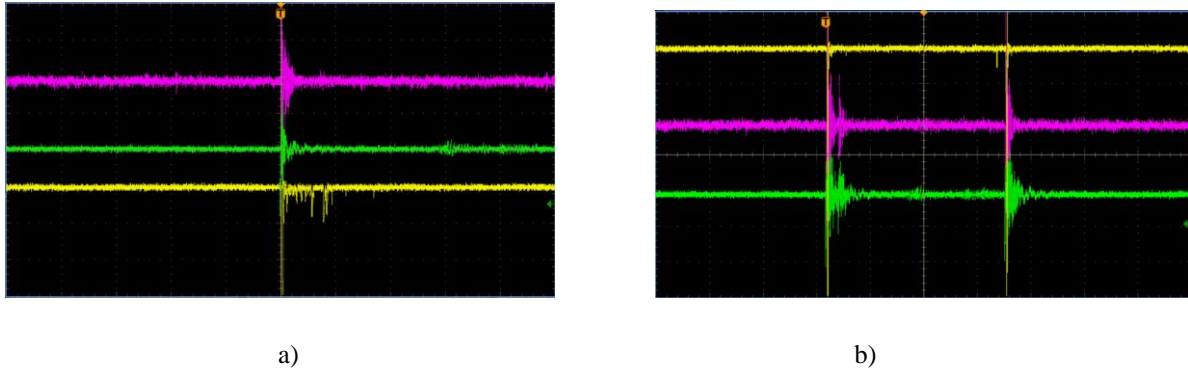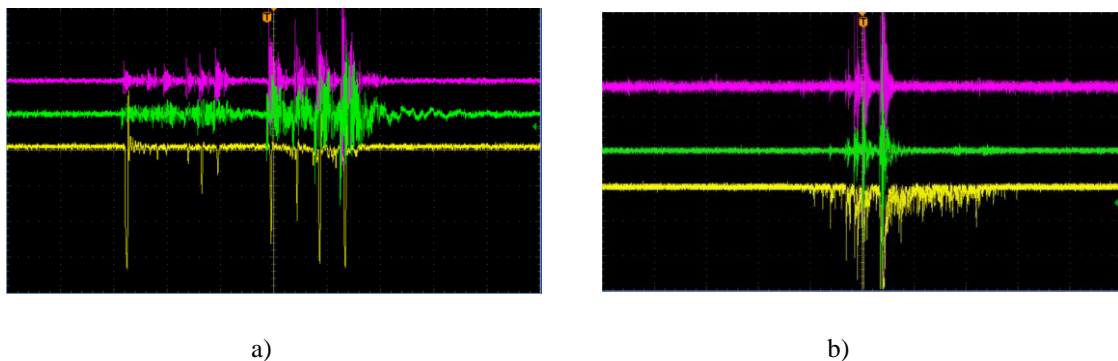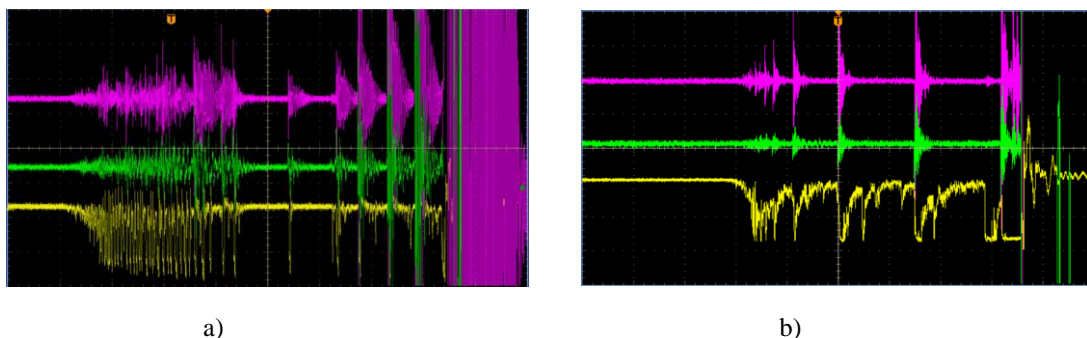
Figure 6. 13: a) Streamer signals in ester +30 kV(HFCT signal(purple)-20mV/division, light signal(yellow)- 1V/division, shunt signal(green)- 500mV/division, time-1μs/division) b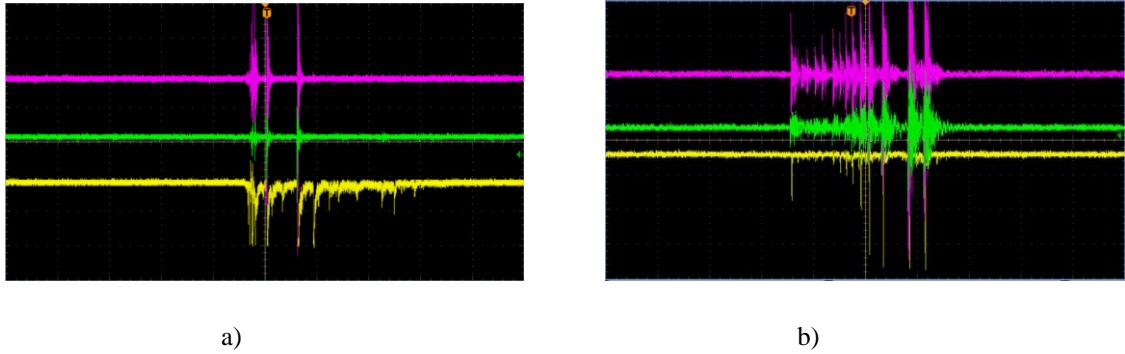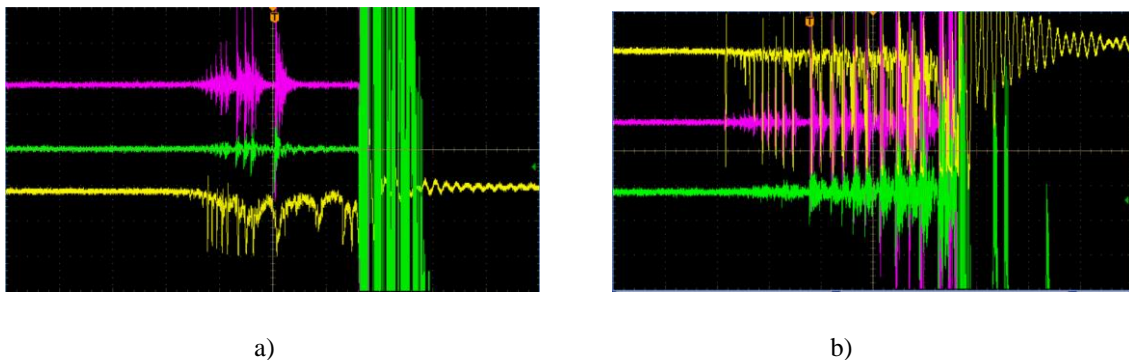) Streamer signals in mineral oil+30 kV(HFCT signal(purple)-20mV/division, light signal(yellow)- 1V/division, shunt signal(green)- 100mV/division, time-400ns/division)

On analyzing the different waveforms, it can be observed that the positive streamers are characterized by current signals comprising of high frequency oscillations superimposed on low frequency positive pulse for both liquids. On increasing to higher voltage levels, there is an increased light signal, current signal as well as duration of the pulse which can be observed. This suggests that the charge transfer is higher as the electric field rises. The signal observed for the negative streamers are much more different than the positive streamers. The pulses recorded have a much shorter duration and appear as a train of signals with increasing distance. These train of pulses indicate a series of injection of electrons from the surface of the cathode, triggering the electron avalanche process for these streamers. In both liquids, the streamers emitted light in the form of discrete pulses with the frequency dependent on the applied voltage level. On increasing the voltage, these pulses tend to exhibit continuous components on which are superimposed other pulses with less regular and weaker frequencies than the one before. Though this continuous component is of weaker magnitude, it grows with the increase in applied voltage [83]. Negative streamers displayed higher number of current pulses during various voltage levels as well as breakdown, especially for ester. This could be due to the previously explained fact that negative streamers propagate with more number of branches and offshoots when compared to the positive streamers. Overall, the streamer phenomenon is more prominent and less hindered in ester, probably owing to its more favorable molecular structure.

6.3 Streamer detection in Lodz University of Technology

This section of the chapter discusses the experimental test set up and measurements performed in Lodz university of Technology under the supervision of Professor Rozga and his team. The experimental test set up consisted of 6 stage(up to 500 kV) lightning impulse Marx generator with a storage energy of 2.2kJ, resistive divider, point-sphere electrode system and photomultiplier as shown in the figure 6.14(b). Along with the resistive divider, a peak value meter was installed to measure the lightning impulse voltage. The test cell was made of Perspex with a volume of 5L. The distance between the needle tip(50um radius of curvature) and grounded sphere was 20mm. The tests were carried out with synthetic ester (Midel 7131) as well as mineral oil (Shell Diala B) in order to understand the difference in streamer propagation in both the dielectric liquids. Detection of streamers was done with the help of photomultiplier- Hamamatsu R1925A with a wavelength range from 300-850nm. The light signal was captured by the fiber optic cable with 37 individual fibers with an active surface of 5mm. The cables were placed at the walls of the test cell at a distance of 10cm from the needle-sphere configuration placed in a specially designed holder as seen in figure 6.14(a). The aluminum end of the fiber optic cable was fitted to the hole of the PMT housing placed inside a faraday cage. The length of fiber bundle was 4 meters. The PMT recorded the light between the needle and the grounded sphere. The PMT was supplied with a voltage of 800V, connected to an amplifier and waveforms were recorded on the Tektronix DPO 3054.

a)   b)

Figure 6. 14: a) Test cell along with fiber bundle holder- Lodz University of Technology b) Test set up-Lodz University of Technology

Measurements were conducted from 80 kV(negative polarity) up to breakdown voltage with steps of approximately 5 kV. 1 minute of waiting time was given betweeen each step. Experiments were performed in a dark room to ensure outside light does not interfere with the PMT reocordings. Figure 6.15 shows the oscillogram recording for a lightning impulse voltage of 85 kV in mineral oil.
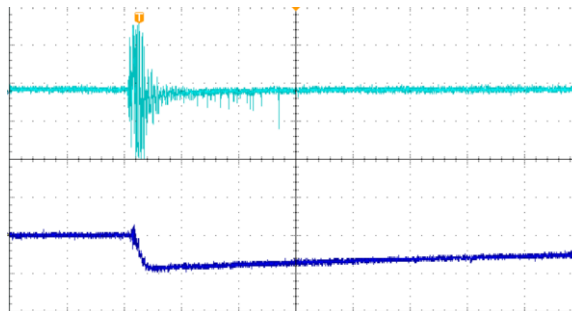
Figure 6. 15: Streamer signals in mineral oil- 85 kV (voltage-100V/division, light signal- 2V/division, time-4µs/division)

The oscillogram shows a sequence of discrete pulse rising with time. The first few µs of the data is ignored as they are disturbances from the impulse generator. The streamers are recorded for up to 10µs before they extinguish. The streamers develop step by step with each one being linked to the streamer extension. Similar recordings were observed for the synthetic ester with a voltage of 80 kV as shown in figure 6.16.
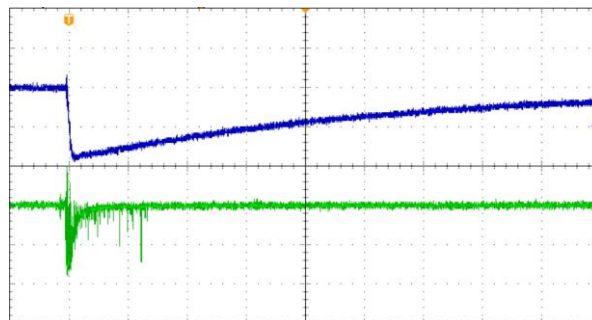
Figure 6. 16: Ester- 80 kV (voltage-50V/division, light signal- 2V/division, time-10µs/division)

On increasing the voltage to higher levels, significant differences were noticed for the development of streamers. Figure 6.17 shows the oscillogram for 90 kV voltage for mineral oil and ester insulation.

<table>
<tr><td align="center">a)</td><td align="center">b)</td></tr>
</table>
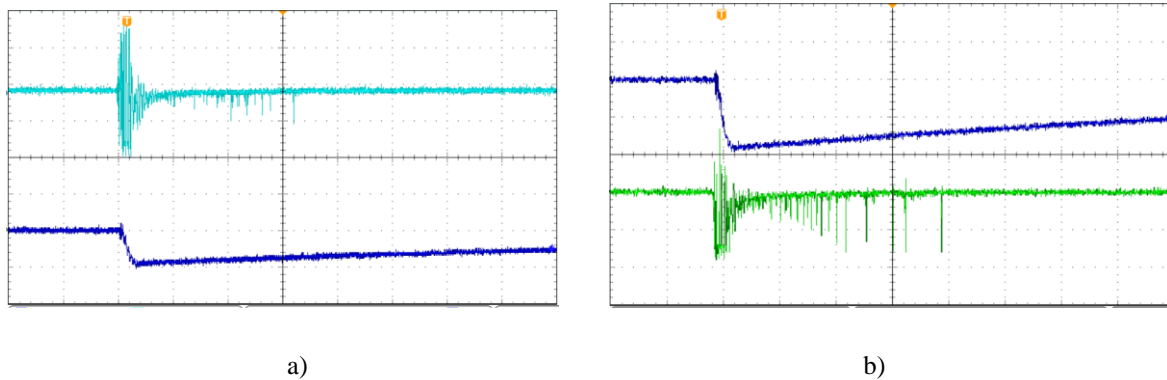
Figure 6. 17: a) Streamer signals in mineral oil- 90 kV voltage-100V/division, light signal- 2V/division, time-4µs/division b)Streamer signals in ester- 90 kV voltage-50V/division, light signal- 2V/division, time-4µs/division

It can be seen that both the amplitude and frequency corresponding to the light pulses is higher for the ester insulation. While streamers in ester are recorded up to 16µs, the streamers in mineral oil extinguish after 13µs. This could suggest that the streamers have propagated further in ester insulation as compared to mineral oil for the same applied voltage. This could also be an indication of the more branched propagation of streamers in ester under negative polarity.

Figure 6.18 shows the streamer data recorded at voltage levels close to breakdown. From the recordings, it is clear that streamers in mineral oil extinguish after 18µs when the applied voltage is 97 kV. But the intensity and frequency of the light signals is higher than the ones observed previously. In case of ester, with an applied voltage of 96 kV, the streamers completely bridge the gap, leading to a breakdown after 25µs. This suggests that the accelerating voltage is lower in case of ester insulation as compared to the mineral oil. The inception voltage of the fast propagating streamers is thus lower in ester insulation as compared to mineral oil. This also provides a further clarification to the previous statement that the streamers in ester propagate further when compared to mineral oil for the same applied voltage.

<table>
<tr><td align="center">a)</td><td align="center">b)</td></tr>
</table>
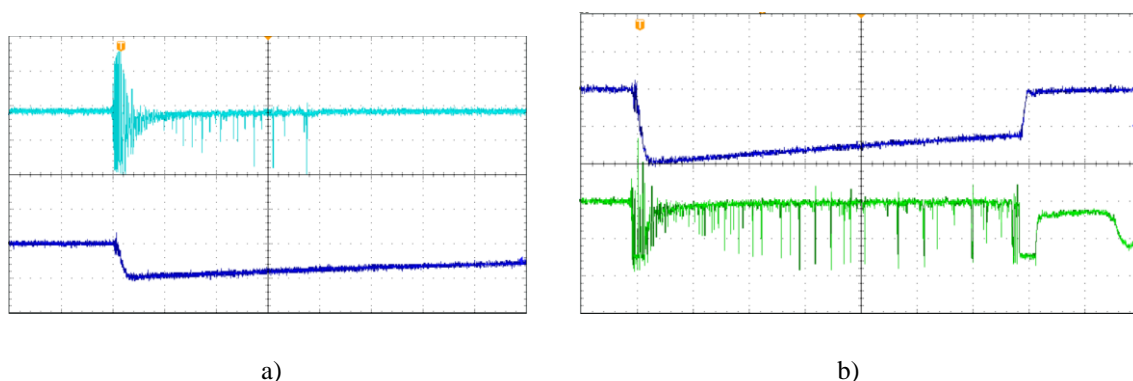
Figure 6. 18: a) Streamer signals in mineral oil- 97 kV voltage-100V/division, light signal- 2V/division, time-4µs/division b) Streamer signal in ester- 96 kV voltage-50V/division, light signal- 2V/division, time-4µs/division

Figure 6.19 shows the oscillogram during breakdown in mineral oil at 110 kV. The breakdown takes place after approximately 20μs. For both cases, the breakdown took place in the tail of the lightning impulse. The shorter breakdown time could be due to the fact that a higher voltage was needed to breakdown the mineral oil configuration. Thus, streamer propagation was easier and enabling them to reach longer distances eventually leading to breakdown. Breakdown in ester was associated with streamers of higher light intensity and frequency suggesting that streamers propagate more easily in ester.
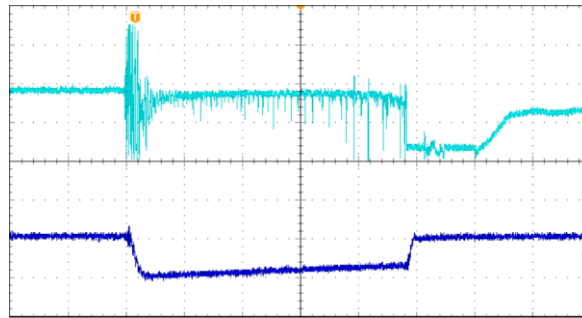
Figure 6. 19: Streamer signals in mineral oil- 110 kV voltage-100V/division, light signal- 2V/division, time-4μs/division

6.4 Measurement and analysis- Impulse testing for needle-plane configuration

The propagation of streamers in synthetic ester and mineral oil can be studied by recording oscilloscope traces of the current pulses and light emitted as seen in the previous sections. In the following section, the characteristics of streamers are analyzed along the pressboard surface in dielectric insulation under positive and negative voltages. The test set up for the same has been discussed in section 4.1.2 and 5.4 Furthermore, breakdown of ester and mineral oil is also investigated under divergent fields using a needle plane configuration in the absence of press board. Charging of the impulse generator induces noises and interference in the measurements for the first few μs and this is ignored during the analysis. The response from the photomultiplier is represented by the yellow signal and the green signal corresponds to the current pulse recorded by the 10Ω shunt.

6.4.1 Ester

Figure 6.20 shows the cluster of light and current signal recorded during low voltage levels, just higher than the streamer inception level. The positive streamer inception voltage for the given distance was significantly lower for both liquids as the breakdown process occurs at lower voltages. The frequency range of the amplifier of the photomultiplier was adjusted to 0-80MHz. A train of discrete pulses with increasing amplitude is recorded for both the light signal as well as the current signal. Due to the saturation of the PMT signal, the magnitude of the light signal cannot be accurately determined. Compared to the negative streamers, positive streamers have a higher repetition rate with lower amplitude. The high intensity in the positive streamer signals tend to show a weak DC component. Most of the light pulses correlate with the current signal with respect to the time of occurrence. This is can be associated with the full reillumination from the tip of the needle to the streamer head. In some cases, the light pulses cannot be attributed to the current pulse. This is due to the

105

partial re illumination that may exist very close to the streamer head[82]. Light signal measured by the PMT are unidirectional (positive), but the polarity of the streamers can be determined with the current signal.

a)

b)

Figure 6. 20: a) Streamer signals in ester -50 kV(light signal(yellow- 1V/division, shunt signal(green)- 2V/division, time-4μs/division) b) Streamer signals in ester +42 kV (light signal(yellow)- 1V/division, shunt signal(green)- 1V/division, time-1μs/division)

With the increase in applied voltage, the amplitude and intensity of the current and light signal becomes stronger for both polarities. A continuous DC component can be observed for the positive streamers as shown in figure 6.21. This could be due to the continuous movement of large amounts of electrons in the backward direction generated due to the discharge at the streamer head. It can also be observed that the continuous component is more intense in the early phase of the streamer propagation which represents the short lived initial 3rd mode streamer propagation. Negative streamers increase in repetition rate as well as sustaining time as shown in figure 6.21(a). The streamer signals observed during the negative polarity have a significantly higher current amplitude.

a)

b)

Figure 6. 21: a) Streamer signals in ester -65 kV(light signal(yellow)- 1V/division, shunt signal(green)- 2V/division, time-4μs/division) b) Streamer signals in ester +50 kV (light signal(yellow)- 1V/division, shunt signal(green)- 1V/division, time-2μs/division)

On approaching the breakdown voltage, series of pulses with similar magnitude were observed at the start for the current and light signals during negative impulse voltages. Studies from other researchers using high speed cameras suggest that this could be similar to the 3rd+2nd propagation mode in open gaps. The current signal during breakdown under negative voltage shows different phases of streamer propagation. After the initial large pulses, a normal train of discrete pulses representing the 2nd mode propagation is recorded before again increasing in amplitude. These pulses constitute the 3rd mode streamers. The streamer signals of 2nd mode propagation is again recorded before breakdown occurs due to the 3rd and 4th mode streamer propagation. A similar phenomenon is observed by the

106

positive streamers, though the current pulses are significantly smaller than the negative streamer signals. Faster breakdown under positive voltage further indicates that the stopping length of positive streamers are higher than the negative streamers.

a)   b)

Figure 6. 22: a) Streamer signals in ester -70 kV(light signal(yellow)- 1V/division, shunt signal(green)- 2V/division, time-4μs/division) b) Streamer signals in ester +55V (light signal(yellow)- 1V/division, shunt signal(green)- 1V/division, time-4μs/division)

The breakdown voltage waveform for both polarities is shown in figure 6.23. It can be seen that the time taken to breakdown is much lower when the applied voltage is positive suggesting that the positive streamers are thinner with lesser branches and offshoots.
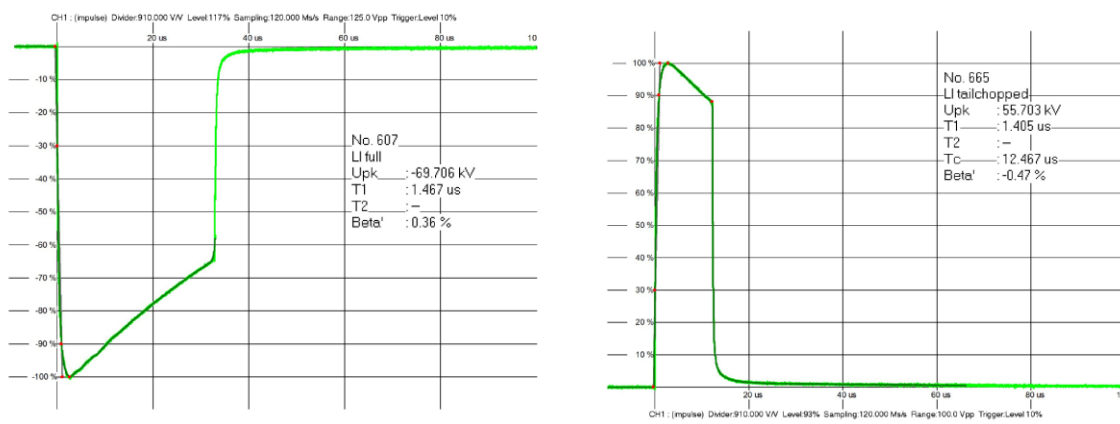
a)   b)

Figure 6. 23: a) Negative impulse waveform during breakdown in ester- 70 kV b) Positive impulse waveform during breakdown in ester +55 kV

As seen in some cases, the current pulses are not always accompanied by the light pulses. This would indicate the electro-hydrodynamic phenomenon(EHD) occur during the propagation of streamers. During the streamer expansion, there are regions of weak density which progress without any discharge occurrence. The fluorescent impurities present in the liquid under test could also be factor leading to the light pulses not being associated with the current signals.

6.4.1.1 Secondary reverse streamers in ester

During surface discharges under divergent fields, backward discharges having opposite polarity to the applied voltage were observed under both polarities, During the tail phase of

the impulse voltage, the needle electrode exhibits opposite polarity to the previously charged surface, inducing electric field in the reverse direction. In some cases, this electric field can be strong enough to produce back discharges. The presence of the PB on the needle tip helps in trapping the residual space charges and enable the back discharges through the charge memory effect. These discharges are often observed 100µs after the main streamer discharges.

Under the negative impulse, two different types of SRS can be observed [82]. Figure 6.24 shows the phenomenon of SRS when a negative voltage of 70 kV is applied. Here, the primary streamers as well as the secondary reverse streamers are shown. While the primary streamers show negative polarity for the current signal, the opposite polarity is depicted by the secondary reverse streamers. The SRS is observed after approximately 105µs and constitutes a long DC component imposed by discrete pulses in the light signal. These kind of streamer signals are found to be more branched and represent the 2nd mode streamers.

a)   b)

Figure 6. 24: a) SRS+PS signals in ester -70 kV(light signal(yellow)- 1V/division, shunt signal(green)- 2V/division, time-20µs/division) b) SRS in ester -70 kV (light signal(yellow)- 1V/division, shunt signal(green)- 2V/division, time-2µs/division)

Another type of SRS was observed when the applied negative voltage was 60 kV. Here, the primary streamers begin with large amplitude streamer signals which then switch to a train of pulses with lower amplitudes. This represents the 3rd + 2nd mode of streamer propagation. The SRS is observed after approximately 130µs, with polarity opposite to that of the primary streamers. This type of SRS is observed as discrete pulses and is associated with the 3rd mode streamers [82].

a)   b)
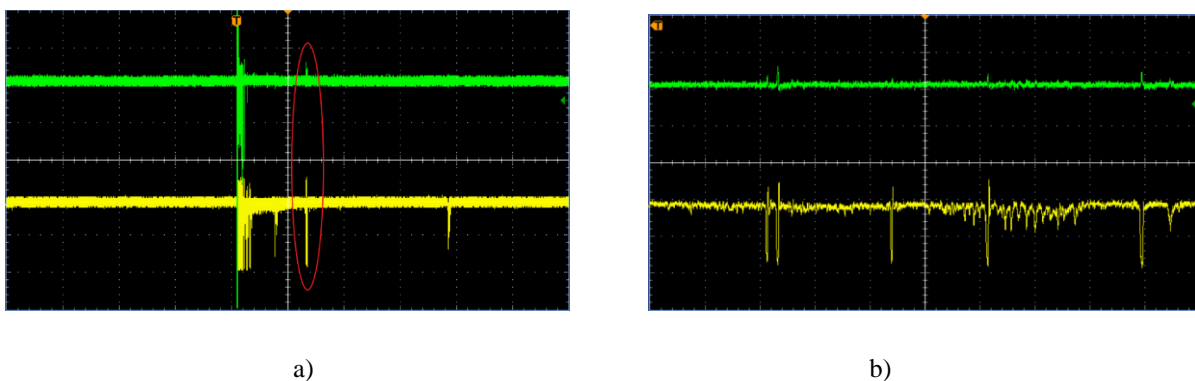
Figure 6. 25: a) SRS+PS signals in ester -60 kV(light signal(yellow)- 1V/division, shunt signal(green)- 2V/division, time-100µs/division) b) SRS in ester -60 kV (light signal(yellow)- 1V/division, shunt signal(green)- 2V/division, time-400ns/division)

SRS under positive polarity was observed at significantly faster with lesser intensity due to the low value of the applied voltage. Figure 6.26 shows the SRS phenomenon when the applied voltage is 40 kV under positive polarity. The SRS is observed after 16µs, when the voltage has fallen to approximately 33 kV. These secondary reverse streamers are observed as a train of discrete pulses, growing in amplitude. The SRS are clearly seen with current signals of negative polarity while the primary streamers are observed with positive current signals.

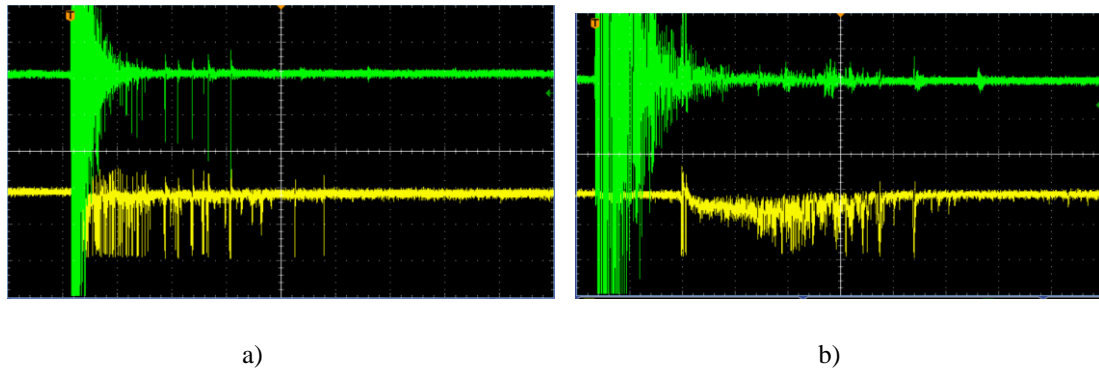a)   b)
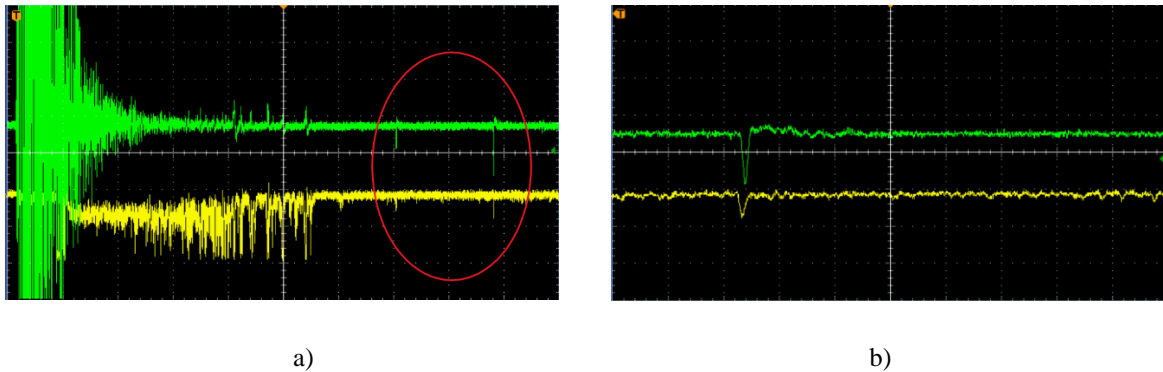
Figure 6. 26: a) SRS+PS signals in ester +40 kV(light signal(yellow)- 1V/division, shunt signal(green)- 1V/division, time-2µs/division) b) SRS in ester +40 kV (light signal(yellow)- 1V/division, shunt signal(green)- 1V/division, time-100ns/division)

The process of streamer initiation and propagation is a gaseous and electronic in nature constituting charge injection, ionization and thermal vaporization. As a result, a gaseous channel filled with charged particles is formed once the primary streamers are extinguished. When negative voltage is applied, the positive charges present in the streamer channel moves from the streamer head towards the needle tip while the electrons attach themselves to the liquid molecules as the they make their way to the ground plate. As previously mentioned, the electronegative oxygen atoms in ester trap free electrons which are therefore accumulated at the gas/liquid interface during the streamer propagation. The external electric field which pushes the positive ions to the needle electrode and negative ions to the ground slowly decays after the primary streamers. Thus, this results in the channel to shrink and cause a difference in ion concentration as shown in the figure 6.27(a). Thus, due to charge diffusion, the negative electrons move to the needle electrode. Thus, this builds up a space charge induced electric field with reverse polarity.

During the positive impulse, the electrons accumulated in the streamer channel move towards the needle tip while the positive charges slowly surround the streamer head as shown. The positive ions attract the negative charges in the surrounding medium and results is local recombination during the primary streamer propagation. When the primary streamer propagation stops, fewer residual charges are expected. Moreover, the positive streamer channel is much thinner, thereby leaving lesser charges. The SRS occurs close to the needle in a similar manner to the negative streamers involving charge diffusion but has a lesser amplitude [85].
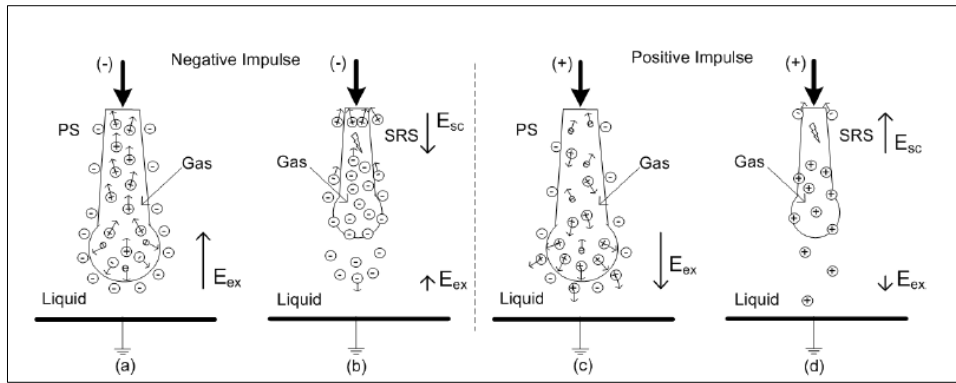
a)   b)

Figure 6. 27: a) SRS phenomenon under negative polarity b) SRS phenomenon under positive polarity [85]

6.4.2 Mineral oil

Figure 6.28 represents the streamer activity observed in mineral oil when the voltage applied was 50 kV. A number of signals are observed for the current and light components with most of the them correlating with each other. Similar to the signals observed for the ester insulation, the current consists of short pulses separated by a very small interval suggesting that the streamers propagate in steps at high velocities. In most cases, small number of weak light signals can be observed even after that current has been extinguished. This can be due to the weakly luminous zone at the streamer head which can also promote streamer propagation. While the streamer activity exists for about 12us, the light intensity of the recorded pulses and the magnitude of the current signals are lesser than the ones observed for the streamer propagation in ester. This could suggest that the ability for the streamers to propagate under lightning impulse is easier in ester when compared to mineral oil. The streamer. Under negative voltage, the streamer signal comprises of higher amplitude signals at the beginning, representing higher modes of propagation before exhibiting a train of pulses with lower amplitude. Positive streamers were recorded at lower voltages when compared to negative streamers, with much lesser streamer activity and light intensity. As seen in esters, positive streamers are less luminous and more filamentary when compared to the negative streamers.
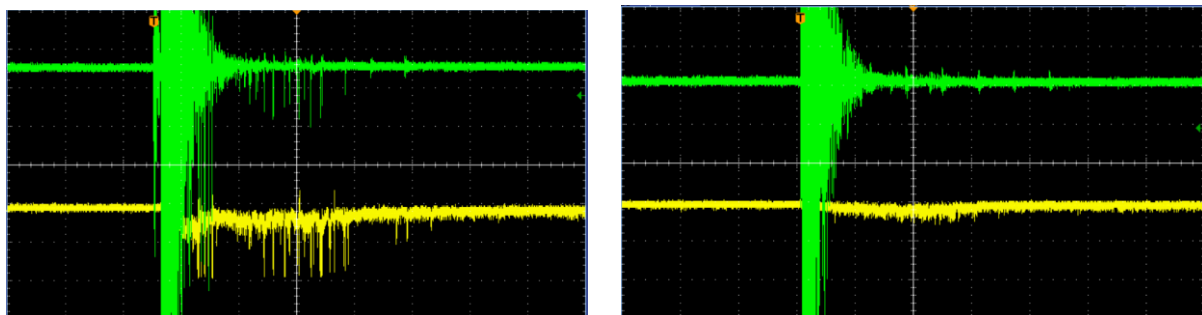
a)   b)
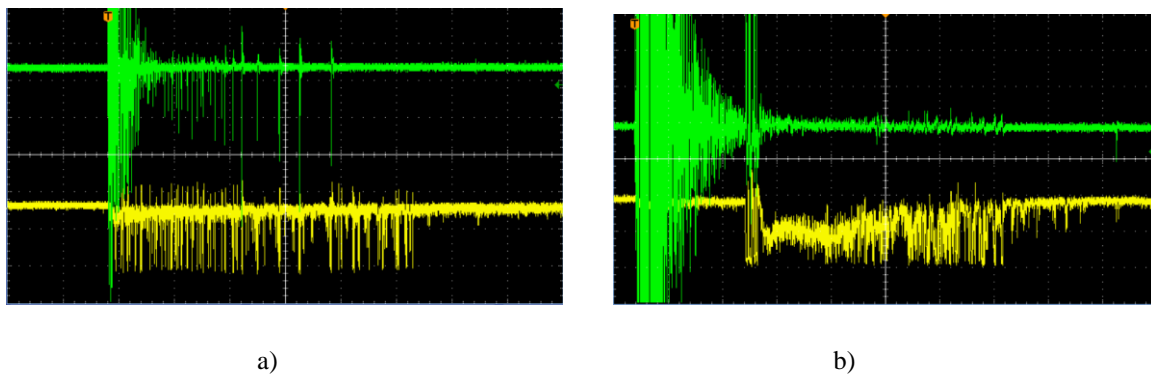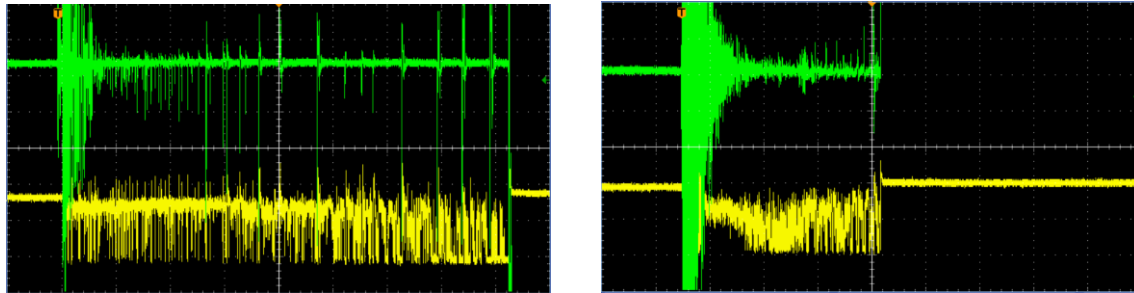
Figure 6. 28: a) Streamer signals in mineral oil -50 kV (light signal(yellow)- 1V/division, shunt signal(green)- 1V/division, time-4μs/division) b) Streamer signals in mineral oil +42 kV (light signal(yellow)- 1V/division, shunt signal(green)- 1V/division, time-4μs/division)

110

On increasing the applied voltage , it can be seen that the streamer activity grows in magnitude under both polarities, while the frequency of the streamer pulses remains similar to before. The signal recorded by the negative streamers are significantly lesser in number and intensity when compared to the pulses observed in ester. A higher amount of time is recorded in between the streamer pulses under negative polarity when compared to ester suggesting that the once the streamers are initiated, there is a higher resistance to their propagation in mineral oil. The higher frequency of pulses observed in case of ester suggests that the next step of propagation is easier in esters. These steps represent the extension of streamer channels due to the electric field and space charge of the previous discharge in the streamer channel. For the streamers to reignite, the electric field stress at each step should reach a level that can ionize the liquid to the extent of exciting the electrons. This re ignition process occurs more easily in ester where the streamers are more branched with larger number of offshoots.

a)   b)

Figure 6. 29: a) Streamer signals in mineral oil -65 kV (light signal(yellow)- 1V/division, shunt signal(green)- 1V/division, time-4μs/division) b) Streamer signals in mineral oil +46 kV (light signal(yellow)- 1V/division, shunt signal(green)-1V/division, time-2μs/division)

On reaching the breakdown voltage, significant difference in streamer signals is recorded between the two liquids under negative polarity. The breakdown level in case of mineral oil was similar to that of the ester liquid under both polarities, although streamer activity observed was much lesser. The number of light pulses and magnitude of current signal recorded by the oscilloscope for the streamer propagation is much higher in ester suggesting that the streamers are much more energetic when formed in ester as compared to mineral oil. The ability to form fast streamers which lead to breakdown is higher in case of ester which could result in a lower acceleration voltage when compared to mineral oil. Positive breakdown voltage is very close to the streamer inception voltage for both liquids indicating that once initiated, positive streamers propagate further and with higher velocity leading to faster breakdowns.

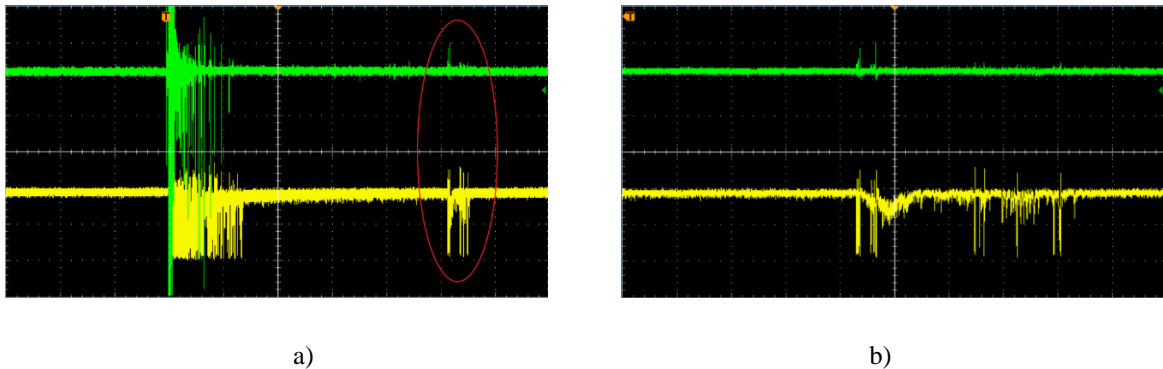a)   b)
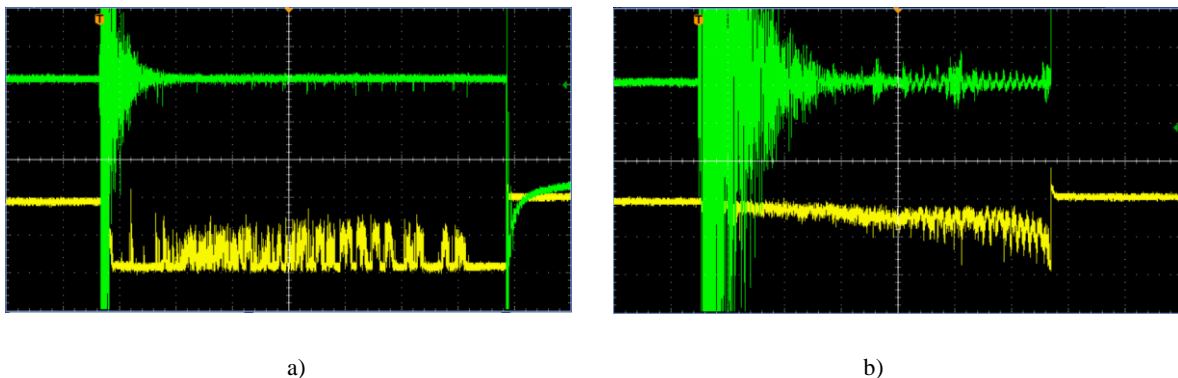
Figure 6. 30: a) Streamer signals in mineral oil -70 kV (light signal(yellow)- 1V/division, shunt signal(green)- 5V/division, time-4μs/division) b) Streamer signals in mineral oil +50 kV (light signal(yellow)- 1V/division, shunt signal(green)- 1V/division, time-2μs/division)

The tail chopped lightning impulse voltages are shown in figure 6.31 from which it is evident that the positive breakdown occurs much faster for mineral oil as well.

a)   b)
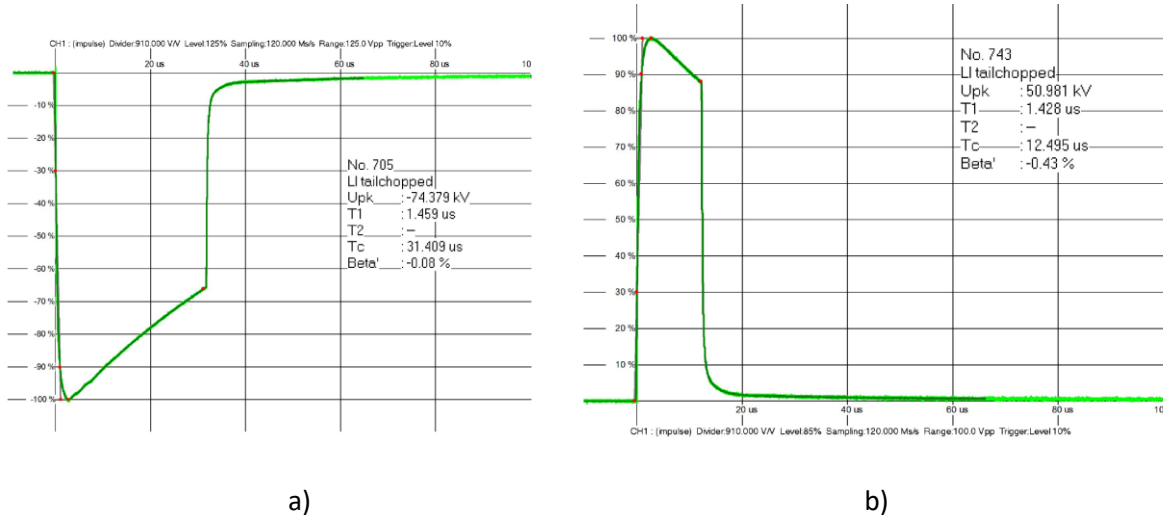
Figure 6. 31: a) Negative impulse waveform during breakdown in mineral oil- 75 kV b) Positive impulse waveform during breakdown in mineral oil +50 kV

Though the breakdown level under negative polarity is similar in this case, for tests in the absence of PB, the breakdown voltage is found to be lower for ester. Figure 6.32 shows the difference in streamer activity recorded during breakdown due to negative streamers during the absence of the PB by a 1Ω shunt and a less favorable fiber bundle. The breakdown voltage level was lower for ester with significantly higher streamer signals recorded. The streamer signal was recorded for a longer duration suggesting that the stopping length of streamers is higher in case of ester under negative polarity.

a)   b)
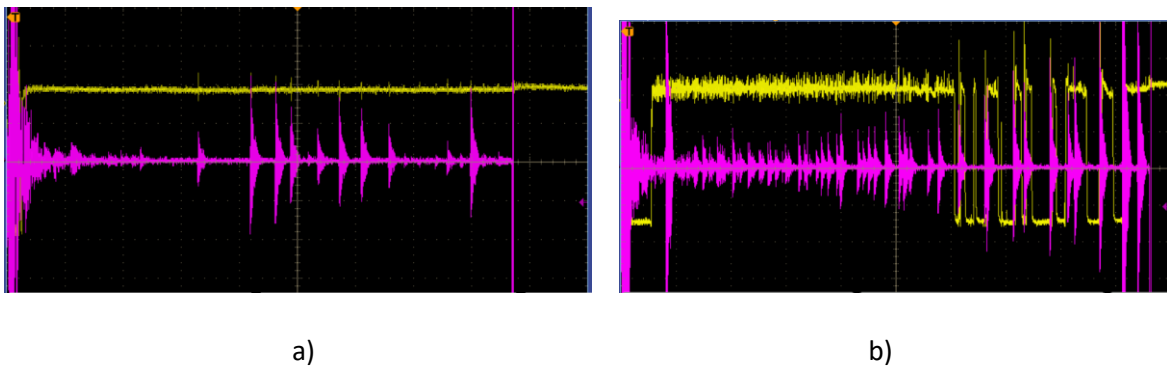
Figure 6. 32: a) Mineral oil- 90 kV current signal -500mV/division, light signal- 500mV/division, time-2μs/division b) - Ester- 80 kV current signal-1V/division, light signal- 500mV/division, time-2μs/division

112

6.5 Measurement and analysis- impulse testing for winding arrangement

Unlike measurement in highly non uniform fields seen in the previous sections, streamer detection with the winding set up used in this thesis was much more uncertain. As a result, impulse testing was performed from a particular voltage level up to breakdown in steps of 5 kV, with 5 impulses at each voltage level during the initial tests. This provided a higher chance of streamer detection under both polarities. For higher gap distances, single impulse was applied at each voltage level. The testing was carried out for different windings in order to confirm repeatability of results and obtain data for statistical analysis. The test set-up has been presented in sections 4.1.3 as well as 5.4. Streamer detection originating from transformer winding has never been performed before and very few investigations have been conducted to measure streamer properties in uniform fields[88].

6.5.1 Ester

Streamer inception voltage under negative polarity was different for each winding. This could be due to the slight change in geometry of the winding while preparing the test set up or due to the difference in the insulating properties of the windings itself. Figure 6.33 shows the streamer signal recorded by the PMT and shunt during streamer phenomenon under impulse voltage of 160 kV. Though the light signal is of the same level as that of the inherent PMT noise, the large frequency of the pulses and the corresponding current signals are a clear indication of the streamer activity. Figure 6.33(b) indicates that majority of the light pulses coincide with the current pulses. The current signals are distinguished by the noise signals based on their polarity and time duration. Unlike the noise signals, the current pulses have significantly lesser number of oscillations with a time duration of 200ns. It can also be observed that the streamer signals are recorded for approximately 30µs, which is a long period of time for gaps of 1mm when compared to the results obtained under the needle-plane configuration. One of the possible reasons for this is that multiple streamers can originate from different parts of the winding, thereby resulting in the sensors to detect streamers for a longer period of time. In the winding set up used, multiple defects can exist in different sites, promoting streamer activity at different places. Moreover, streamer signals observed in this configuration have a significantly lower light and current amplitude. The winding insulated by paper severely inhibits the streamer inception and the streamers originating are weaker. The presence of the wooden blocks on either side of the ground electrode plays a crucial role in promoting streamer activity. This is analyzed in the next sections.
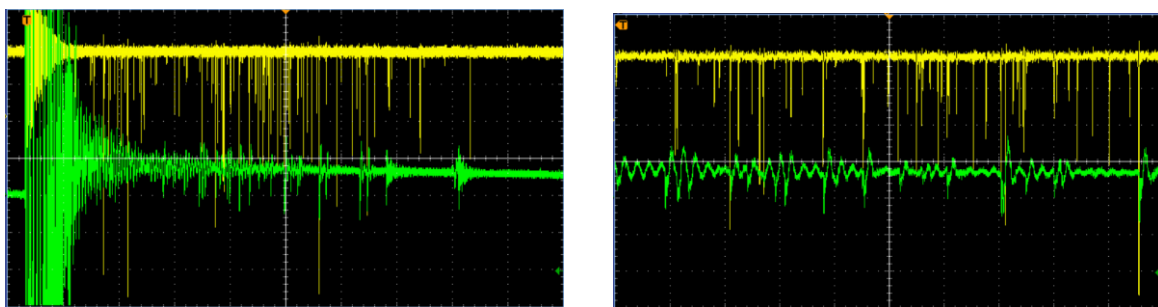
a)   b)

Figure 6. 33: a) Streamer signals -160 kV (light signal(yellow)- 20mV/division, shunt signal(green)- 2V/division, time- 4µs/division) b) Streamer signals- 160 kV (light signal(yellow)- 20mV/division, shunt signal(green)- 2V/division, time- 1µs/division)

On increasing the voltage level, the probability of the occurrence of streamer activity was found to be higher. Figure 6.34 depicts the streamer activity at 200 kV under negative polarity. As expected, the streamer signals are growing in amplitude with respect to the light and current pulses. Moreover, the streamer signals are found to last for a higher duration of time suggesting that the streamers originating under the negative polarity are more branched, similar to the phenomenon under the previous configurations. It can further be observed that most of the light and current signal correspond with each other.

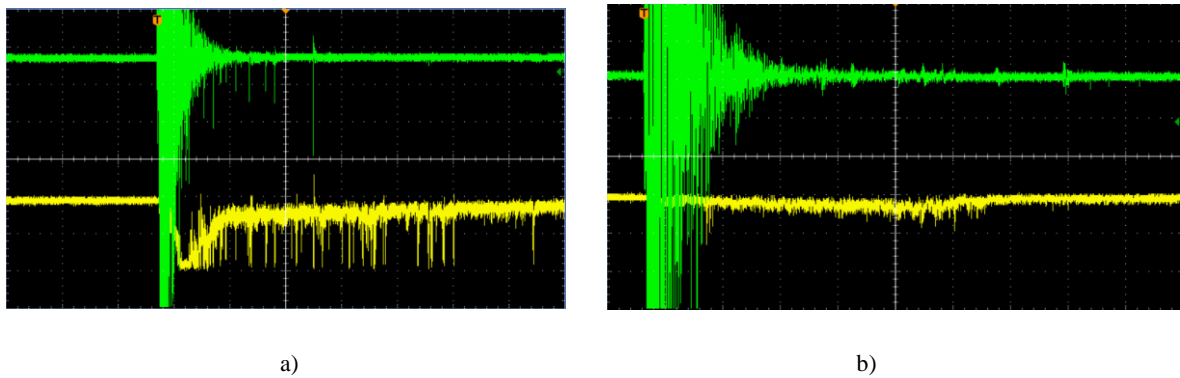a)   b)
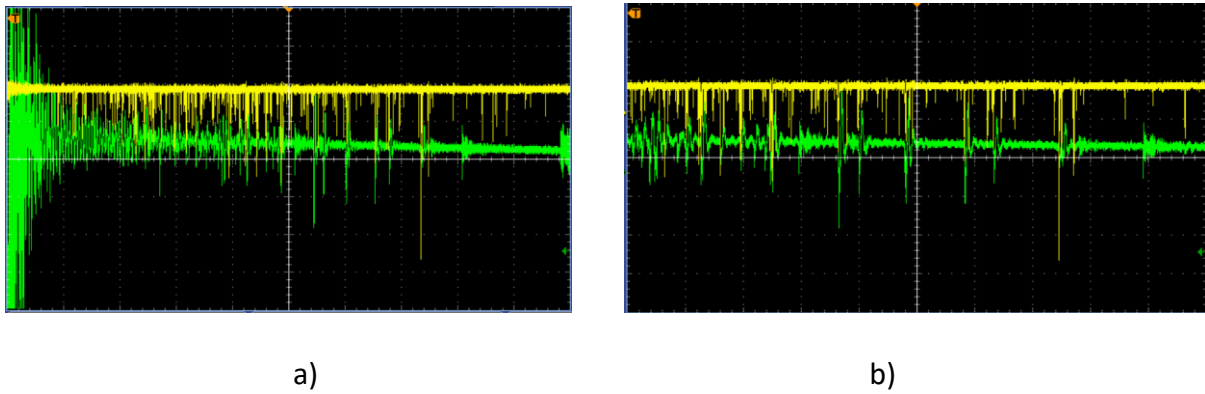
Figure 6. 34: a) Streamer signals -200 kV (light signal(yellow- 50mV/division, shunt signal(green)- 2V/division, time-4μs/division) b) Streamer signals- 200 kV (light signal(yellow)- 50mV/division, shunt signal(green)- 2V/division, time-1μs/division)

On increasing the voltage level to 240 kV, a similar trend was observed in the streamer activity recorded at the start. The intensity of the current and light signals increased and the streamer signals were recorded for a longer duration of time. However, at such high voltages, the phenomenon of secondary reverse streamers were also observed as shown in figure 6.35. While the current signal is severely disturbed by the charging of the impulse generator, the light signal proves to be crucial in the accurate detection of streamers. As previously mentioned, secondary reverse streamers during negative polarity are a result of the charge separation between the positive and negative ions when the positive ions accumulate at the cathode and the negative ions propagate to the ground electrode. Though the channel between the winding and ground electrode is smaller in length, the larger surface of the cathode results in a wider channel with larger number of positive ions. At such high voltage levels, the number of negative ions trapped by the electronegative oxygen molecules are significantly higher. As a result, there is a significant charge separation which leads to the diffusion of ions. This reverse movement of electrons is seen as secondary reverse streamers approximately after 160us. From figure 6.35(b), it can be observed that the streamers are represented by light and current pulses having continuous components lasting for approximately 8μs. The light intensity of these pulses are less than half that of the primary streamer signals. These streamers are similar to the type 1 SRS observed in the previous section with the needle-plane configuration.

a)   b)
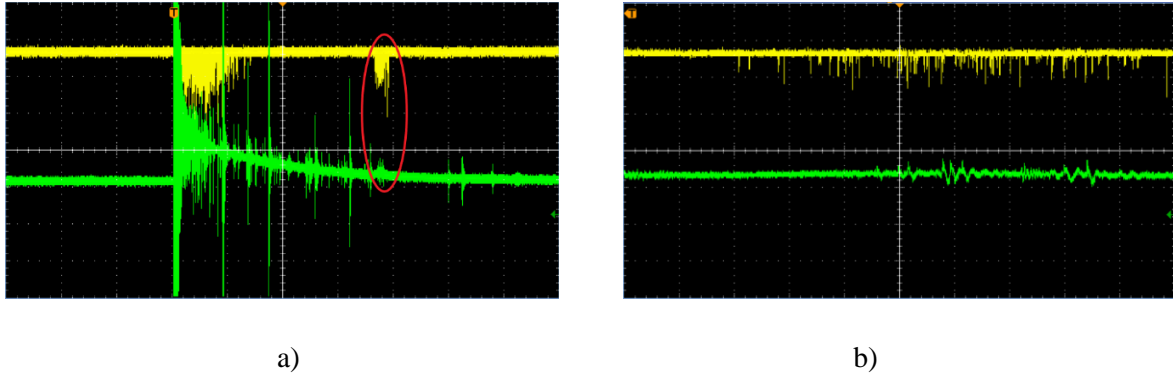
Figure 6. 35: a) SRS+PS signals in ester -220 kV(light signal(yellow)- 100mV/division, shunt signal(green)- 2V/division, time-40µs/division) b) SRS in ester -220 kV (light signal(yellow)- 100mV/division, shunt signal(green)- 2V/division, time-1µs/division)

A different type of SRS is observed for higher voltage levels of 240 kV. Here, the secondary reverse streamers are recorded in two separate time intervals as the voltage is decaying shown in figure 6.36. One of the possible explanations involves the structure of the bottom electrode. It is clear that the electric field between the winding and the bottom electrode is not uniform. The region between the winding and the top most point of the semi-spherical electrode has a higher electric field. As a result, the decay of the electric field is slower in these regions. This means that the electrons in this region continue to move to the anode for a slightly longer period of time when compared to those in the other parts. This could suggest that initially, the secondary reverse streamers involves the movement of electrons to the cathode from the other parts where the electric field has already decayed, followed by the movement of electrons in the region at the top of the anode where the field decay was slower. Moreover, the region between the winding and the top of the semi-sphere has a higher probability of streamers to originate and therefore, is accumulated with more number of ions. As a result, the secondary streamers observed due to the movement of electrons from this region is of significantly higher light and current amplitude. Here, the first set of SRS is observed after 110µs, while the second set with higher magnitude is seen after 135µs. The second set of SRS(type 2) have a much higher light magnitude as compared to the primary streamers and have a shorter duration than the SRS type 1. They are discrete signals similar to the pulses observed under the needle plane configuration.

a)   b)
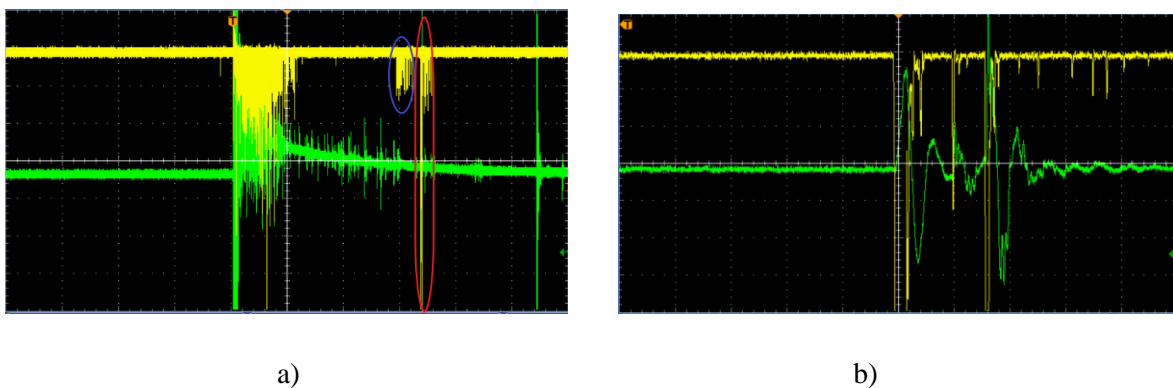
Figure 6. 36: a) SRS+PS signals in ester -240 kV(light signal(yellow)- 50mV/division, shunt signal(green)- 2V/division, time-40µs/division) b) 2nd SRS in ester -240 kV (light signal(yellow)- 50mV/division, shunt signal(green)- 2V/division, time-400ns/division)

On further increasing the voltage, it was observed that the time interval between the two sets of secondary reverse streamer also increased. At 260 kV, the first set of SRS(type 1) is observed after 140µs, while the second set of SRS is seen after 260µs(type 2) as shown in figure 6.37(a). At these voltage levels, the current shunt was disconnected to ensure safety to the measuring system. The reason for the delay in the second set of SRS can be associated to the considerable increase in electric field at the region between the winding and the top of the semi-spherical electrode which takes a longer time to decay. As a result the movement of the electrons to the cathode is slightly more delayed. When electric field reaches very high magnitudes, both sets of secondary reverse streamers show large magnitudes of light signal. This causes the electric field in these regions decay slower and the SRS phenomenon is observed after a longer time. This is seen in figure 6.37(b), when the voltage level is 270 kV. The first set of SRS is observed after 280µs while the second set of SRS is seen after 420µs. Though both these sets of secondary reverse streamers resemble type 2 streamers, SRS type 1 signals are also observed after approximately 100µs. Thus, under the winding configuration with wooden blocks, the secondary reverse streamer phenomenon are slightly different. The winding and the blocks provide a larger streamer channel, resulting in a different set of SRS.

a)   b)
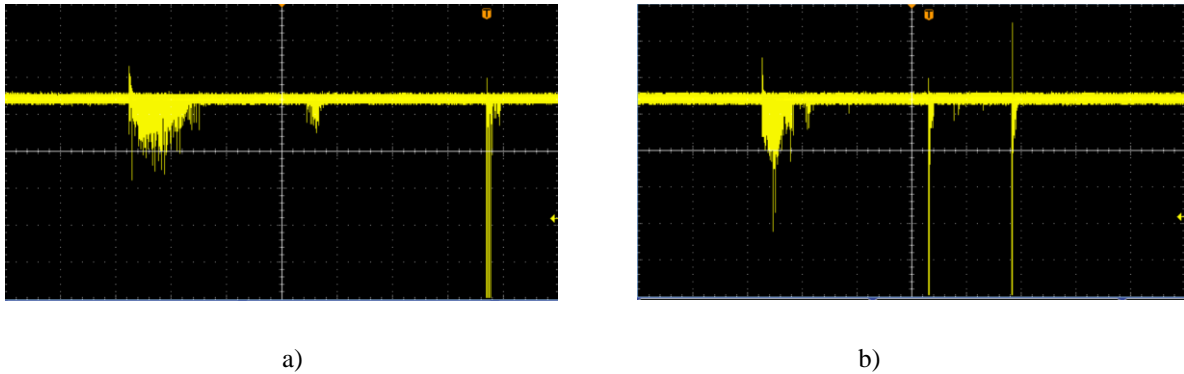
Figure 6. 37: a) SRS+PS signals in ester -260 kV(light signal- 100mV/division, time-40µs/division) b) SRS+PS in ester -270 kV (light signal- 100mV/division, time-100µs/division)

Breakdown was observed at 270 kV under negative impulse for one of the windings. After the breakdown, a black mark was observed on the winding indicating the point at which the breakdown channel was initiated. Also, the region near the breakdown was visibly filled with a black trace as shown in figure 6.38(a).

Figure 6. 38: a) Black trace observed after breakdown b) Black mark on the transformer winding after breakdown

Time duration for breakdown at this voltage level was extremely low as seen in figure 6.39(a). The breakdown channel was formed in approximately 800ns, resulting in a front chopped lighting impulse voltage waveform as shown in figure 6.39(b). Though multiple streamers are initiated near the cathode region, only one of them propagate to the ground electrode to cause breakdown. The streamer signals recorded right before breakdown have very high magnitudes of light signals carrying sufficient energy to cause breakdown.
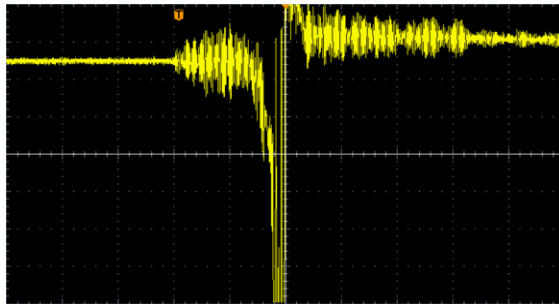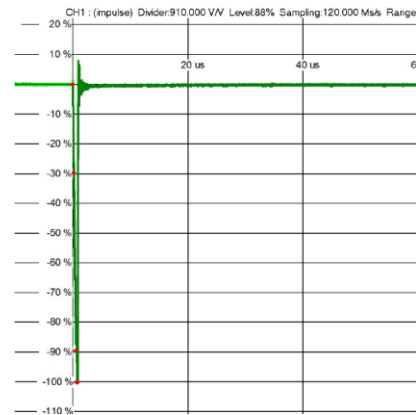
Figure 6. 39: a) Breakdown of transformer winding set up in ester -270 kV (light signal- 200mV/division, time- 400ns/division) b) Front chopped LI waveform during breakdown

However, the streamers observed during all the previous cases from the winding were found to be aided by the presence of the wooden blocks on either side of the ground electrode as previously mentioned. The wooden blocks resulted in a triple point between the winding, insulation and itself, enabling the streamers to propagate easily. This was verified by increasing the gap to 2mm and repeating the test with and without the block. There was significant difference in the streamer activity observed. Figure 6.40(a) depicts the streamer light and current signal observed during streamer inception at 230 kV with the presence of

117

the wooden blocks. As seen previously, discrete signals are captured, with the high amplitudes of light and current signals. Figure 6.40(b) represents the streamer light signal observed at 290 kV when the blocks are removed. Contrast to the streamer signal observed with the blocks, a single light pulse is detected of magnitude 100mV. However, this pulse may also be the noise signal generated by the PMT.

<div align="center">a)   b)</div>
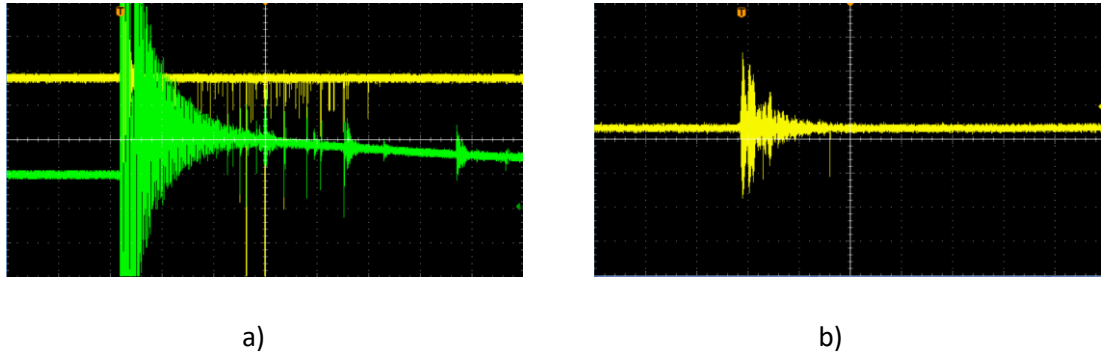
Figure 6. 40: a) Streamer signals in ester with wooden blocks -230 kV(light signal(yellow)- 50mV/division, shunt signal(green)- 2V/division, time-10µs/division) b)Streamer signals in ester without wooden blocks -290 kV (light signal-100mV/division, time-2µs/division)

On further increasing the voltage, the streamer signal continues to grow in frequency and amplitude when the wooden blocks are present. This can be seen in figure 6.41(a) when the applied voltage is 270 kV. However, with the wooden blocks removed, a single light pulse is recorded at 305 kV as seen in figure 6.41(b). The appearance of these light pulses at higher voltage levels suggest that they could be streamers originating from the winding and not the noise signal generated by the PMT. On further analysing the signal, it was seen that the duration of the pulse was approximately 8ns, which is significantly lower than the PMT noise signal and corresponds to the streamer signals. The significant contrast in streamer signals confirm that the streamer signals are more easily generated due to high tangential electric field on the surface of an insulation. This is similar to the previously explained use of the needle-PB-ground set up.

<div align="center">a)   b)</div>
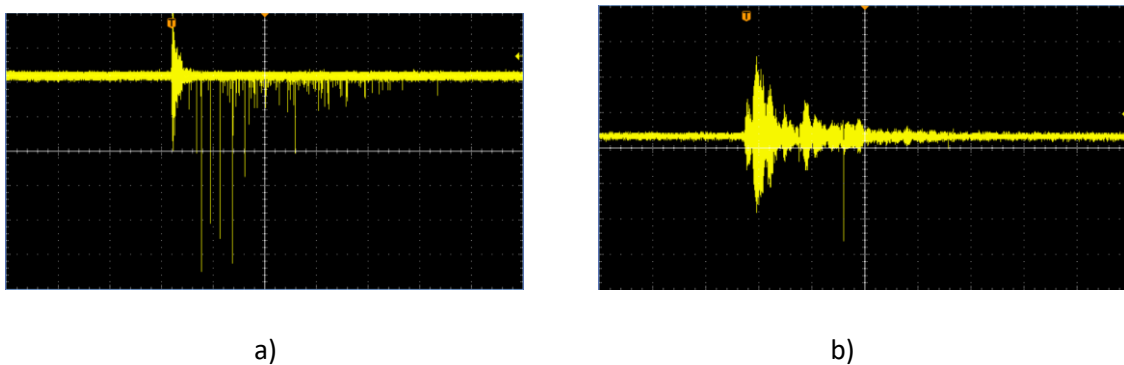
Figure 6. 41: a) Streamer signals in ester with wooden blocks -270 kV(light signal- 100mV/division, time-10µs/division) b)Streamer signals in ester without wooden blocks -305 kV (light signal- 100mV/division, time-1µs/division)

The breakdown voltage was observed at lower values when the breakdown process occurred on surface of the wooden blocks. The black traces and the breakdown mark on the edge of the winding confirmed the point of breakdown. Moreover, breakdown on the surface of the wooden block resulted in a much severe mark on the winding as compared to the breakdown process which took place without the wooden blocks. During surface breakdowns, the breakdown voltage was found to be 290 kV as shown in figure 6.42(a).

During breakdown without the wooden blocks, higher number streamer light signals are observed as shown in figure 6.42b). The longer duration of breakdown on the surface of the wooden blocks may also indicate that the breakdown was to the bottom of the tank, resulting in a longer gap to breakdown, as compared to the shorter distance between the winding and the ground electrode.

<table>
<tr><td>a)</td><td>b)</td></tr>
</table>
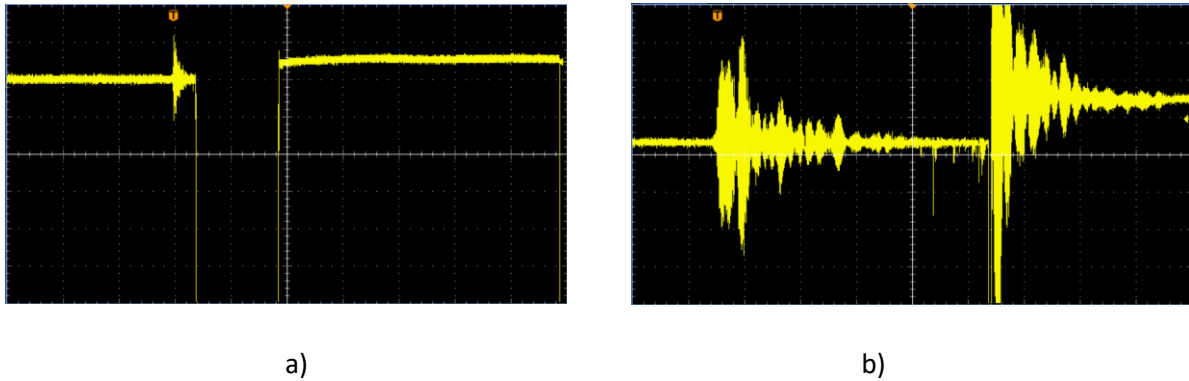
Figure 6. 42: a)Surface breakdown of transformer winding set up in ester along wooden block -290 kV (light signal-200mV/division, time-10μs/division) b) Breakdown of transformer winding set up without wooden block- 305 kV((light signal- 100mV/division, time-1μs/division)

The effect of triple point on the streamer activity generated by the winding was further analysed by inserting a spacer between the winding and ground electrode. The wooden blocks were removed to ensure that the streamers are recorded as a result of the spacer as shown in figure 6.43. Though the wooden blocks were helping the streamers to develop, in reality, such large surfaces are not present between the transformer windings. As a result, the use of spacers to simulate streamers on the surface can provide a better understanding during real life arrangements of the samples.
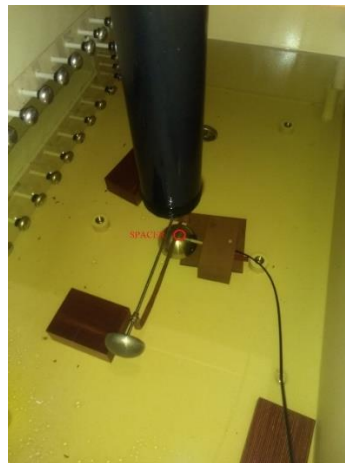
Figure 6. 43: Spacer inserted between the winding and ground electrode

With the presence of the spacer, streamer signals were more prominent when compared to the case without the wooden blocks, but less frequent than the streamer signals observed with the wooden blocks present. Moreover, the breakdown voltage was considerably lower, thereby reducing the streamer activity as the applied voltage was lesser when compared to the tests with the wooden blocks. Depending upon the positioning of the spacer and the exact distance between the winding and the ground electrode, streamer activity can vary as the electric field differs each time. Under negative polarity, streamer light signals were

119

recorded at 100 kV as shown in figure 6.44. Discrete light pulses are recorded suggesting that the growth of the streamers is through offshoots and branches. The time duration of the signal is approximately 13μs owing to the low applied voltage.

a)   b)
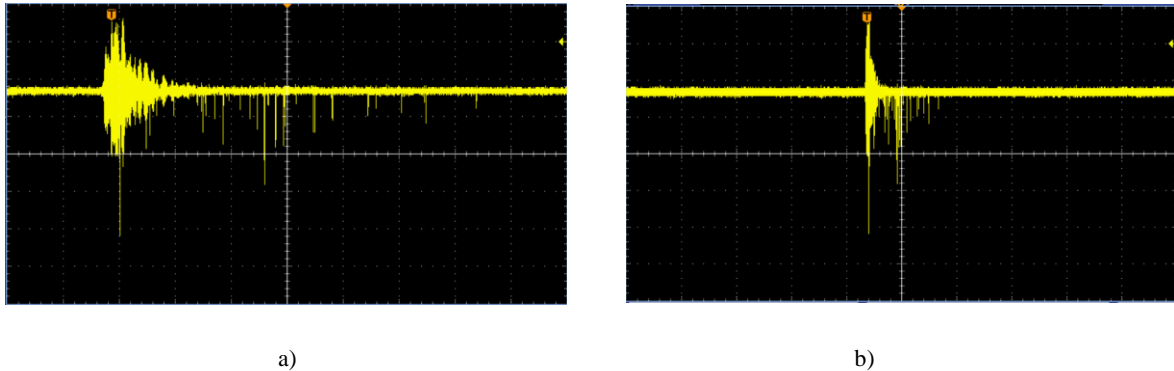
Figure 6. 44: a) Streamer light signals with spacer -100 kV (light signal- 50mV/division, time-2μs/division) b) Streamer light signals with spacer -100 kV (light signal- 50mV/division, time-10μs/division)

On increasing the voltage to 110 kV, the frequency and amplitude of the light signals increase. A train of pulses of increasing amplitude similar to the negative streamers observed during the needle-PB-ground set up are shown in figure 6.45.

a)   b)
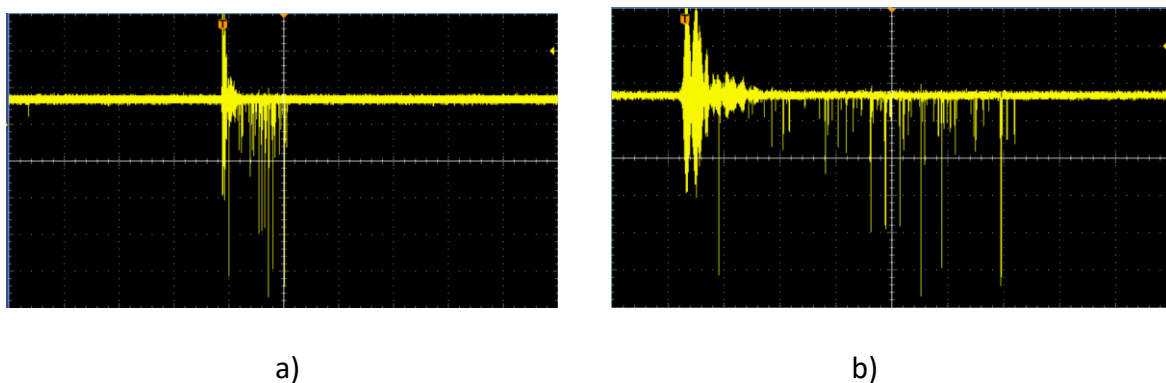
Figure 6. 45: a) Streamer light signals with spacer -110 kV (light signal- 50mV/division, time-10μs/division) b) Streamer light signals with spacer -110 kV (light signal- 50mV/division, time-2μs/division)

During breakdown, large pulses of similar magnitude are recorded at the beginning. These pulses represent streamers of the 3rd mode propagation as discussed previously. These streamer signals are followed by a train of pulses of lower magnitude before reaching breakdown. During breakdown, the higher modes of streamers propagation is observed for small distances at the start, before the streamers branch out and produce the final breakdown. Streamer signal during breakdown at 120 kV is shown in figure 6.46. The time duration of the breakdown was approximately 9μs.

a)   b)

Figure 6. 46: a) Streamer light signals with spacer -120 kV (light signal- 50mV/division, time-10μs/division) b) Streamer
light signals with spacer -120 kV (light signal- 50mV/division, time-1μs/division)

Streamers under positive polarity were not observed with the 1mm gap distance between the
winding and the ground electrode even during the presence of the wooden blocks. Figure
6.47(a) shows the light and current signal recorded during breakdown under positive polarity
at 120kV. The breakdown voltage was much lower when compared to the negative polarity
similar to the scenario with the needle-PB-ground plate configuration. This suggests the
positive streamers are more filamentary and lead to the breakdown much sooner after their
inception when compared to the negative streamers. The breakdown at lower voltages leads
to a longer duration of the process, resulting in a tail chopped impulse voltage as seen in
figure 6.47(b).

a)   b)
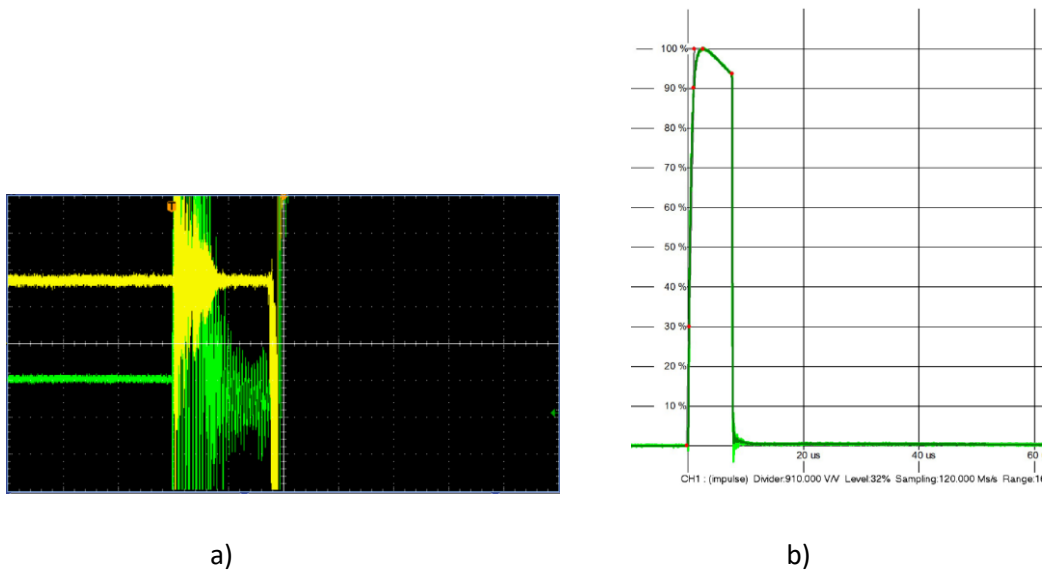
Figure 6. 47: a) Breakdown of transformer winding set up in ester +120 kV (light signal(yellow)- 20mV/division, shunt
signal(green)- 2V/div, time-4μs/division) b) Tail chopped LI waveform during breakdown

To increase the possibility of the streamer detection under positive polarity, the gap distance
between the winding and ground electrode was increased to 2mm. Unlike the negative
streamers, probability of detection of the positive streamers was extremely low. However, at
voltage level of 175 kV, streamer signals were observed as seen in figure 6.48. There is
significant difference in the streamer signals between the positive and negative streamers.
Under the positive polarity, streamer signals are observed in two sets. The first 10us depicts
light signals with much higher intensity and frequency. The following streamer signal are

121

represented by discrete light pulses with small time steps between each pulse. This suggests that the positive streamers initially propagate a particular length in a filamentary nature, before branching out to form streamers similar to those under negative polarity. The total duration of streamer signal is approximately 100us, suggesting that the streamers under positive polarity propagate further distances at a particular voltage level. The high intensity of light signals at the beginning also suggest that the streamers achieve higher modes of propagation much earlier under positive polarity.

a)   b)
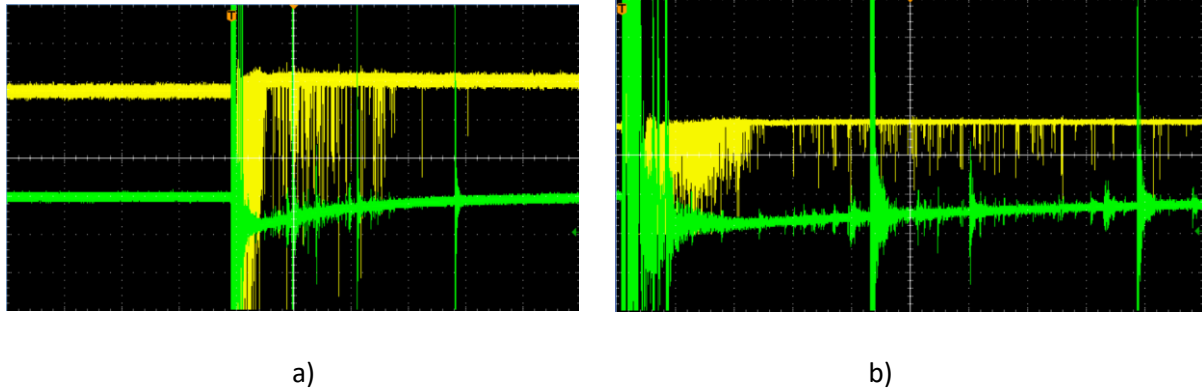
Figure 6. 48: a) Streamer signals +175 kV (light signal(yellow)- 20mV/division, shunt signal(green)- 2V/division, time-40μs/division) b) Streamer signals +175 kV (light signal(yellow)- 50mV/division, shunt signal(green)- 2V/division, time-10μs/division)

On increasing the voltage to 180 kV, similar positive streamer signals are observed as shown in figure 6.49. The overall duration of the streamer signal is seen to be approximately 120us. Moreover, the initial filamentary positive streamers are recorded for 25us, suggesting that the positive streamers are propagating further to the ground, possibly on the surface of the wooden blocks. The intensity and magnitude of the light pulses recorded are higher, indicating the streamers are growing in magnitude.

a)   b)
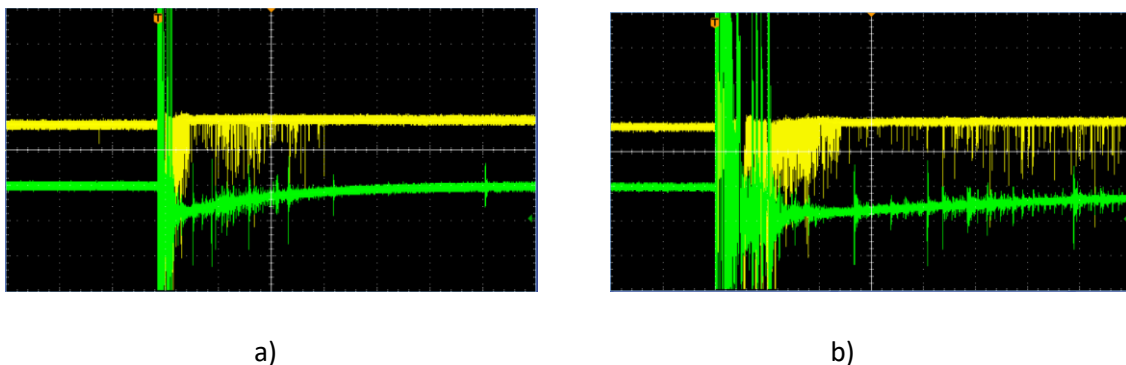
Figure 6. 49: a) Streamer signals +180 kV (light signal(yellow)- 50mV/division, shunt signal(green)- 2V/division, time-40μs/division) b) Streamer signals +180 kV (light signal(yellow)- 50mV/division, shunt signal(green)- 2V/division, time-10μs/division)

On repeating the experiment with the same voltage level, breakdown was observed. This clearly indicates the streamer inception voltage is very close to the breakdown voltage under positive polarity. Similar to the point-plane scenario, once incepted, streamers propagate with higher velocity and further distance under positive polarity resulting in lower breakdown voltages.
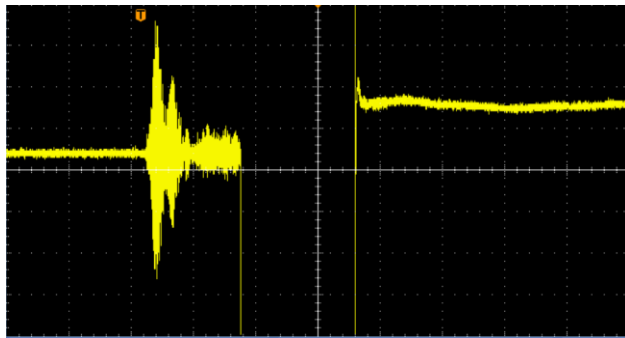
a)
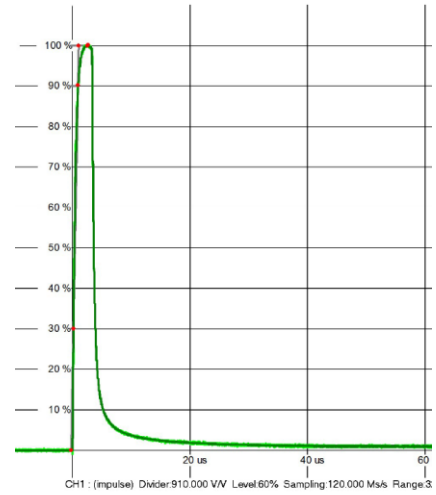
b)

Figure 6. 50: a) Breakdown of transformer winding set up in ester +190 kV (light signal- 100mV/division, time-1μs/division)
b) Tail chopped LI waveform during breakdown

On increasing the gap between the winding and ground electrode to 5mm, streamer activity during positive impulse voltage was significantly higher in magnitude. However, the frequency of streamer occurrence was very low, further suggesting that streamers under positive polarity lead to breakdown much faster. Grading rings were installed in the set up to prevent breakdowns at other parts of the tank. Due to the high value of breakdown voltage expected, impulse voltage was increased in steps of 5 kV until breakdown was achieved while applying a single impulse at each step to avoid long tests. Streamer signals were recorded at 240 kV as shown in figure 6.51. This further confirms that the streamers under positive polarity reach the 3rd mode of propagation initially, before branching out as they propagate towards the ground. This clearly represents the 3rd+2nd mode of propagation of streamers. The high intensity of streamers at the start suggest that the positive streamers are filamentary at the start, similar to the observations made under the needle-plane configuration. The time duration of the streamer signal is around 70us, owing to the larger voltage applied.
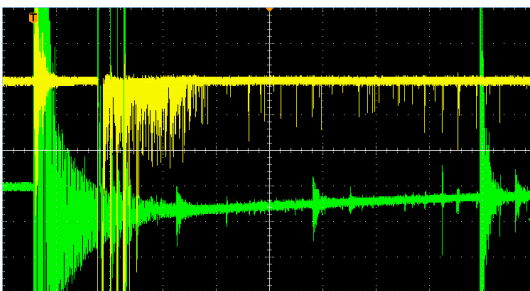
a)
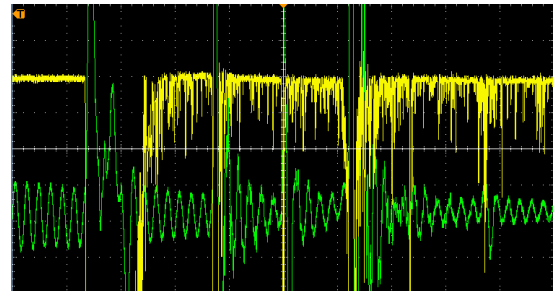
b)

Figure 6. 51: a) Streamer signals +240 kV (light signal- 50mV/division, shunt signal- 2V/division, time-10μs/division) b) Streamer signals +240 kV (light signal- 50mV/division, shunt signal- 2V/division, time-1μs/division)

Breakdown for this gap was observed at 340 kV as shown in figure 6.52(b). It can be seen from figure 6.52(a) that the time duration of the breakdown process was approximately 2us, with the streamer signal growing in amplitude before the PMT saturates. The shunt was disconnected at high voltages to prevent any damage to the ooscilloscope.

a)   b)

Figure 6. 52: a) Breakdown of transformer winding set up in ester +340 kV (light signal- 50mV/division, time-1μs/division) b) Tail chopped LI waveform during breakdown

Streamers observed in this set up could be due to the discharges on the surface of the wooden block as seen for the negative polarity. In order to further investigate this, spacer was introduced between the winding and the ground electrode to resemble real life winding arrangement. Figure 6.53 shows the streamer light signals recorded close to the streamer inception voltage under positive polarity. Streamer signals of large amplitude and light intensity representing the filamentary positive streamers are observed at the beginning, followed by smaller light signals at discrete time intervals. The number of pulses recorded are significantly lower than the streamer signals observed under negative polarity with spacer as expected. Moreover, the time duration of the streamer signals are much higher, suggesting that the filamentary streamers at the beginning propagate for a longer duration of time before they start to branch out.

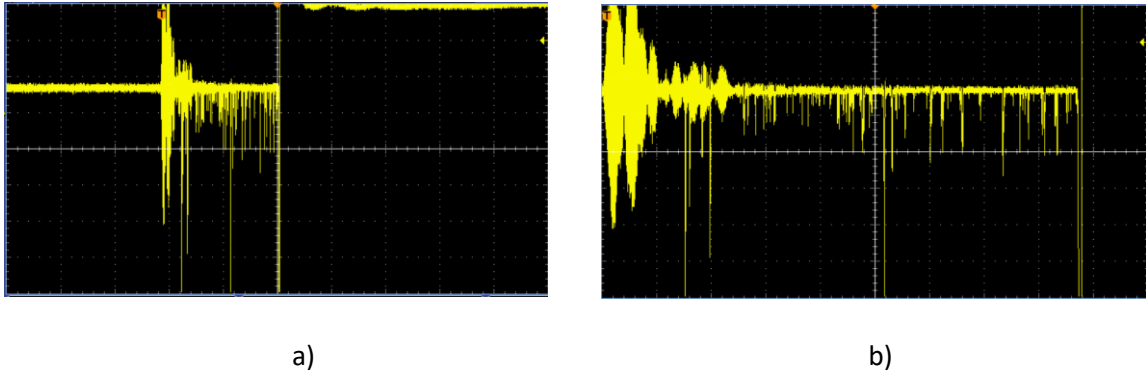a)   b)

Figure 6. 53: a) Streamer light signal with spacer +115 kV (light signal- 50mV/division, time-10μs/division) b) a) Streamer light signal with spacer +120 kV (light signal- 50mV/division, time-10μs/division)

On increasing the voltage level, the streamer signals resembled the ones observed during the presence of the wooden blocks. The intensity of the streamer signals increased at the start, suggesting that the streamers are propagating further to the ground electrode. Though the frequency of the signals did not change, the amplitude of the light signals recorded were higher, Moreover, light signal was recorded after 90us, which could possibly be due to the secondary reverse phenomenon under positive polarity.

a)   b)

Figure 6. 54: a) Streamer light signal with spacer +125 kV (light signal- 100mV/division, time-20μs/division) b) a) Streamer light signal with spacer +130 kV (light signal- 200mV/division, time-20μs/division)

Breakdown under positive polarity was observed at 135 kV. The streamer light signal recorded high intensity pulses at the beginning, before a train of discrete pulses were observed for a particular time duration. However, large pulses were recorded before the breakdown suggesting the propagation of higher modes of streamers before the breakdown process occurs. The magnitude of the light pulses are higher than the ones recorded during negative streamers as shown in figure 6.55. Higher number of positive streamers originating from winding are recorded when compared to the positive streamer signals from the needle. This could be due to the fact that there are multiple streamer initiating sites in the winding-spacer arrangement. However, this also suggests that the positive streamers originating from the winding are more branched, which could thereby affect the breakdown voltage.

a)   b)

Figure 6. 55: a) Streamer light signal with spacer +135 kV (light signal- 200mV/division, time-4μs/division) b) Streamer light signal with spacer +135 kV (light signal- 200mV/division, time-1μs/division)

6.5.2 Mineral oil

In order to evaluate the performance of ester as a transformer insulation, it is important to understand the streamer phenomenon in the traditional insulation such as mineral oil.

Previous sections have already discussed the difference in streamer characteristics under needle-PB configuration between ester and mineral oil. For the first time, streamers originating from transformer winding are compared between ester and mineral oil. In mineral oil, the winding-spacer configuration was investigated as this set up is most relevant to the real life electrode configurations. The tank with ester was properly cleaned before filling it with mineral oil. The windings used were impregnated in mineral oil before testing.

Streamer signals under negative polarity in mineral oil were significantly different from those observed in ester. This can be seen in figure 6.56 which shows the light signal detected during streamer activity at lower voltages close to the streamer inception. The number of pulses recorded are significantly lower when compared to the streamer light signals in ester. However, similar to the signal recorded in ester, a train of discrete pulses is seen. The negative streamers in mineral oil are significantly less thicker and have less offshoots as the streamer activity recorded are lesser in number. This is similar to the results analysed in the previous sections with the needle-PB-plane arrangement. Streamers originating from mineral oil are more hindered in their propagation when compared to ester. Moreover, the amplitude of the light signals recorded are much lower in case of mineral oil. The noise from the impulse generator resulted in large oscillations in the current signal and hence was not analysed for during these measurements.

a)   b)
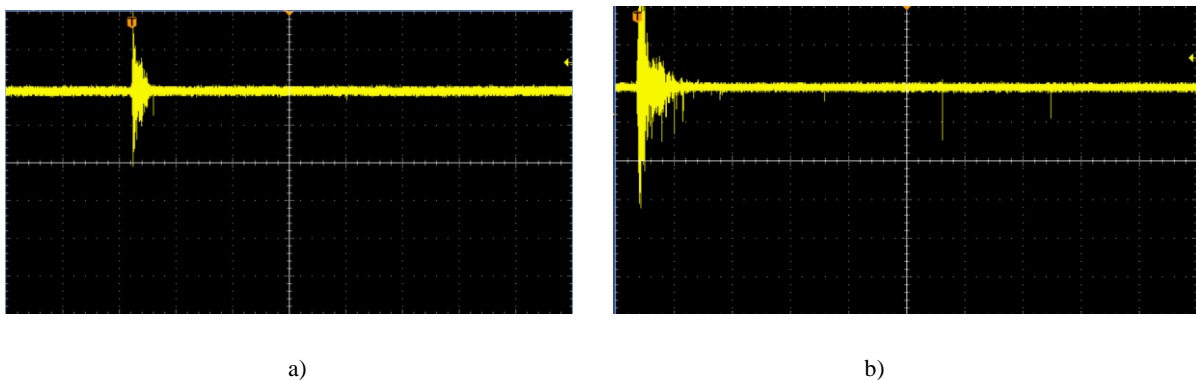
Figure 6. 56: a) Streamer light signal with spacer in mineral oil -95 kV (light signal- 50mV/division, time-10μs/division) b) Streamer light signal with spacer in mineral oil -100 kV (light signal- 50mV/division, time-4μs/division)

On increasing the voltage level, the light signal did not show significant variation. However, larger amplitudes of the streamer light signals were observed after several us, which could indicate the higher modes of streamer propagation in mineral oil. However, the streamer signal recorded was significantly less intense when compared to the ones recorded in ester.
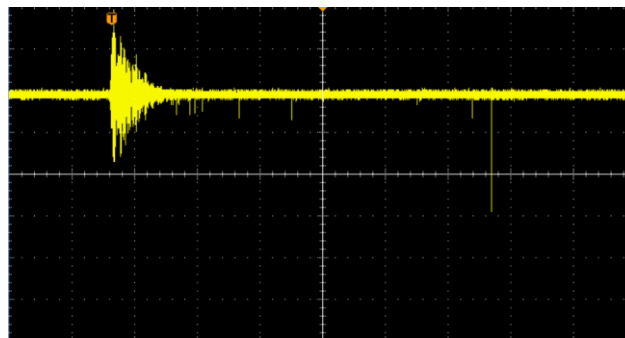
Figure 6. 57: Streamer light signal with spacer in mineral oil -105 kV (light signal- 50mV/division, time-4μs/division)

126

An interesting observation was that though the streamer activity in mineral oil was more hindered, the breakdown voltage was recorded at similar levels to that of ester. Though this could be due to the positioning of the spacer and the geometry of the winding used, it could also suggest that under more real life electrode arrangements, ester and mineral oil have similar breakdown voltages. The presence of the spacer could lower the acceleration voltage of mineral oil and promote the propagation of fast streamers which lead to breakdown. Since the time duration between each impulse was 30s, the accumulation effect could also be responsible for lowering the breakdown voltage of the mineral oi. However, more investigations have to be performed at larger gaps and different spacer dimensions to better understand the difference in streamer activity between ester and mineral oil. Figure 6.58 shows the streamer activity during breakdown at 112 kV. Unlike the signals observed in ester, very few pulses are recorded in mineral oil before large amplitudes of light signal are seen. These pulses could represent the fast streamers in mineral which immediately lead to breakdown. The time duration for breakdown was approximately 3.4us.

a)   b)
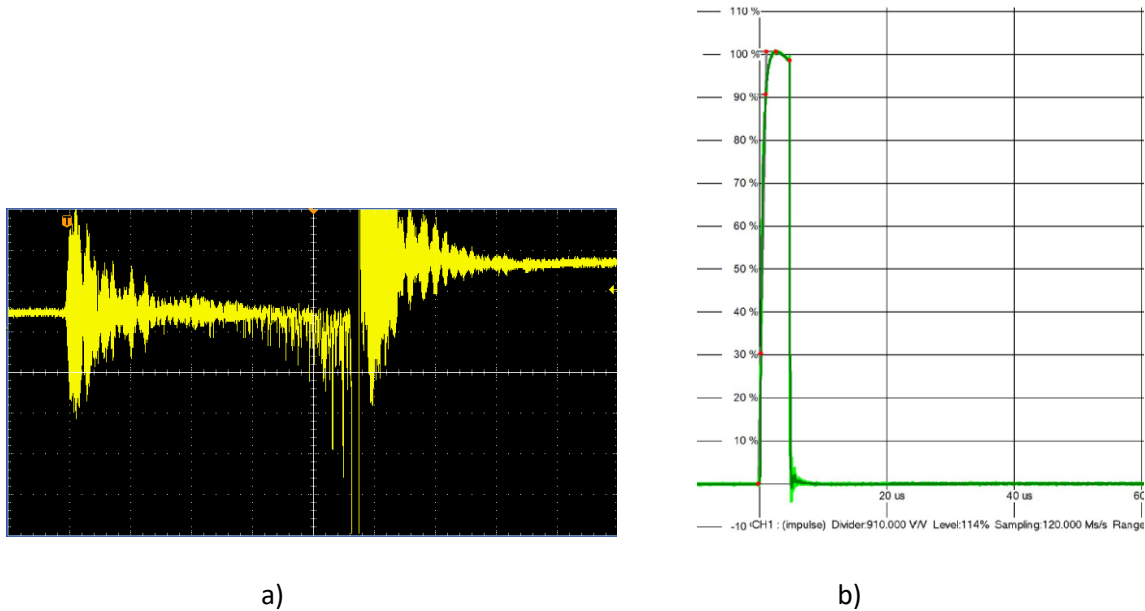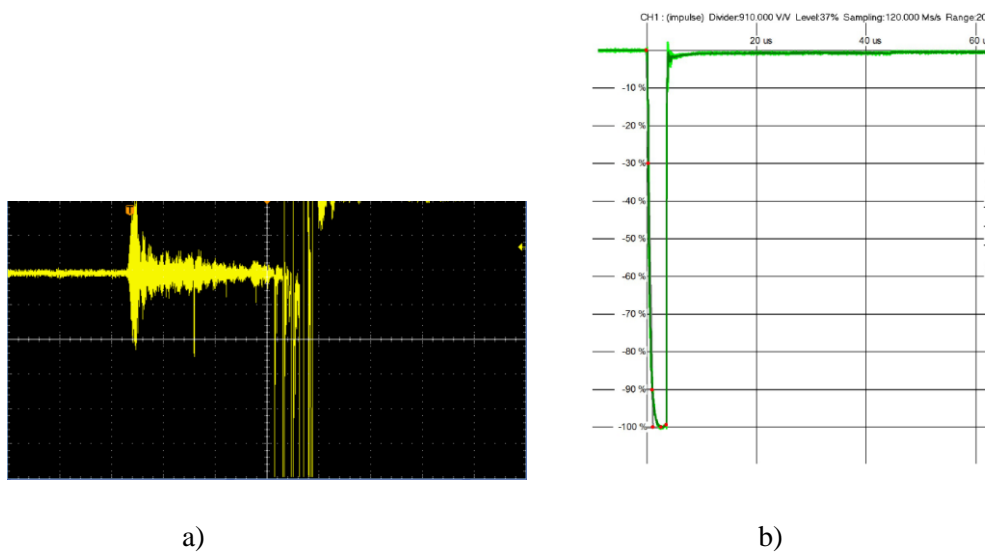
Figure 6. 58: a) Breakdown of transformer winding set up in mineral oil -112 kV (light signal- 50mV/division, time-1μs/division) b) Tail chopped LI waveform during breakdown

At lower voltages close to the inception voltage, the streamer signals recorded under positive polarity was similar to the negative streamers. However, on increasing the voltage level, the streamer signals grew in intensity initially before displaying smaller discrete pulses. This was similar to the observation made in ester, where large streamer signals were observed at the start. However, the number of pulses were higher in number in mineral oil but the corresponding light signal were lower in amplitude. This suggests that the positive streamers in mineral oil originating from windings in the presence of spacer are slightly more branched when compared to those in ester. The use of high speed cameras can provide a more clear picture on these observations.
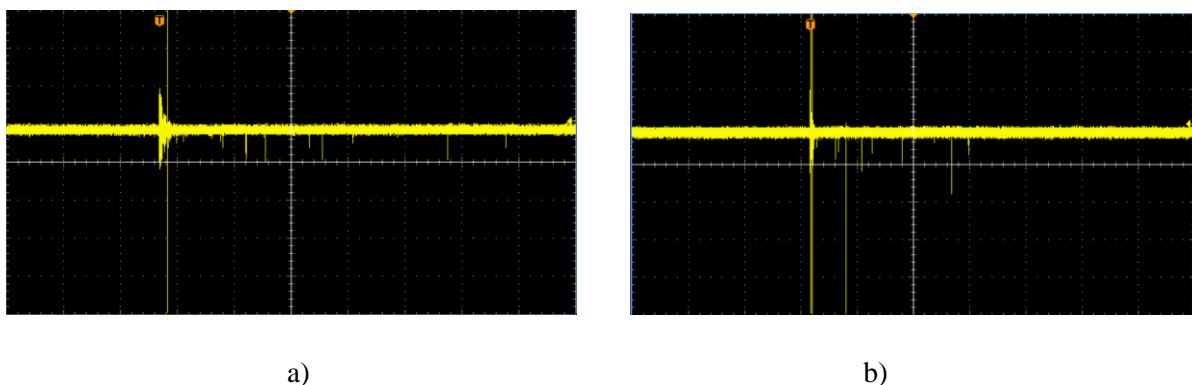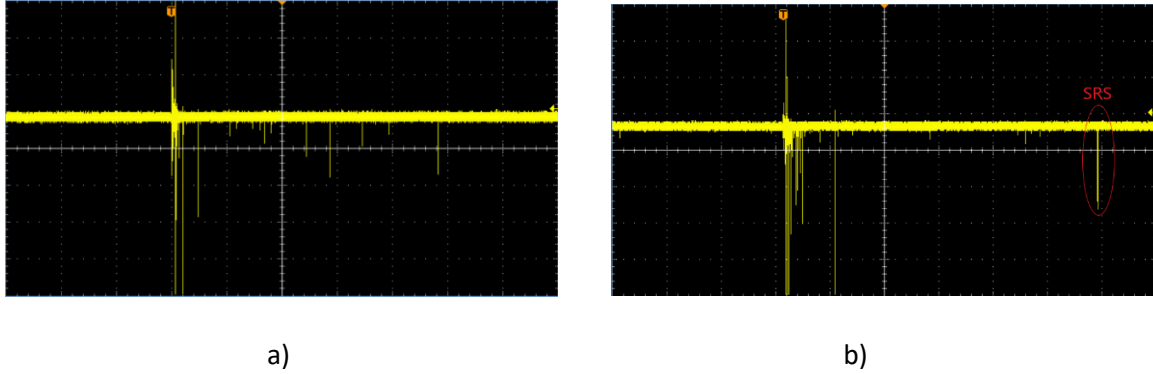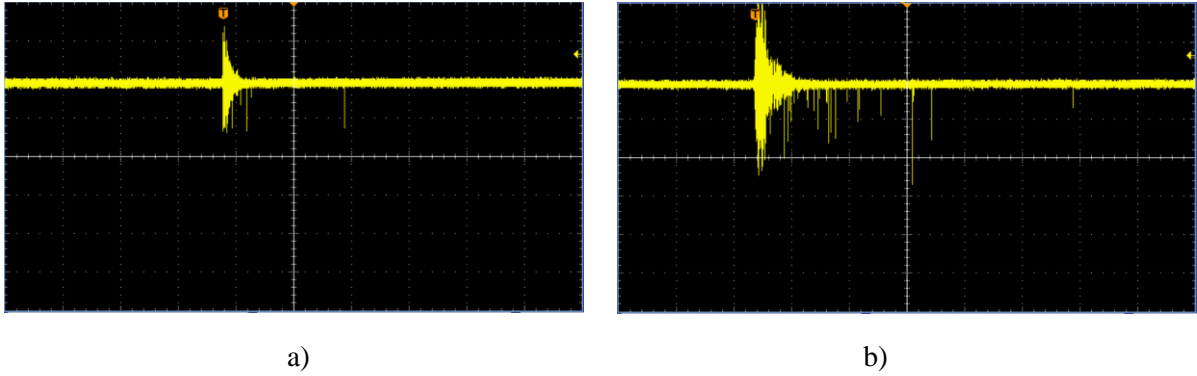
Figure 6. 59: a) Streamer light signal with spacer in mineral oil +80 kV (light signal- 50mV/division, time-4μs/division) b) Streamer light signal with spacer in mineral oil +90 kV (light signal- 50mV/division, time-4μs/division)

On increasing the voltage level close to breakdown, the intensity of the light signals recorded at the start was much higher. Unlike the signals observed under negative polarity, the light signal became more continuous rather than discrete pulses, seen in figure 6.60(a), suggesting that the positive streamers were more brighter and had higher intensity. This was different to the signals recorded in ester, indicating that the positive streamers in ester are more filamentary when compared to those under mineral oil. The presence of spacer could be influencing the streamer propagation in both these liquids differently. On approaching voltage levels right before breakdown, light signals corresponding to possible fast streamers of higher modes of propagation are observed as shown in figure 6.60(b).
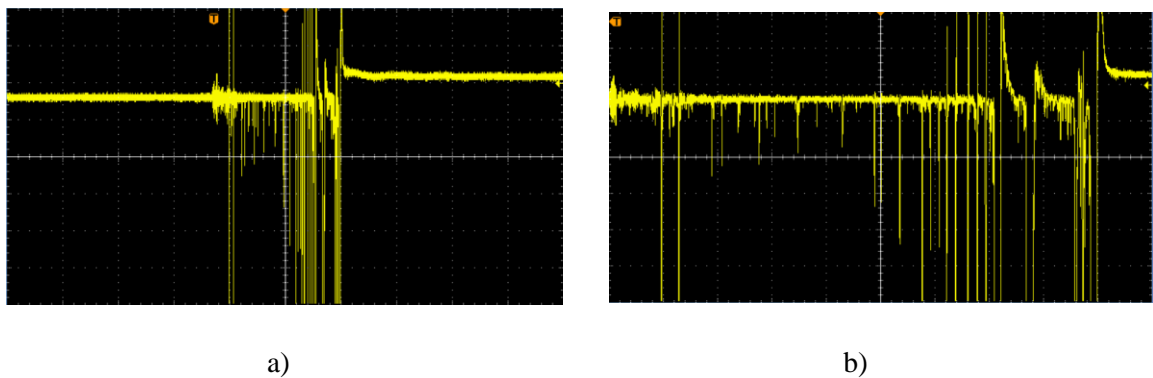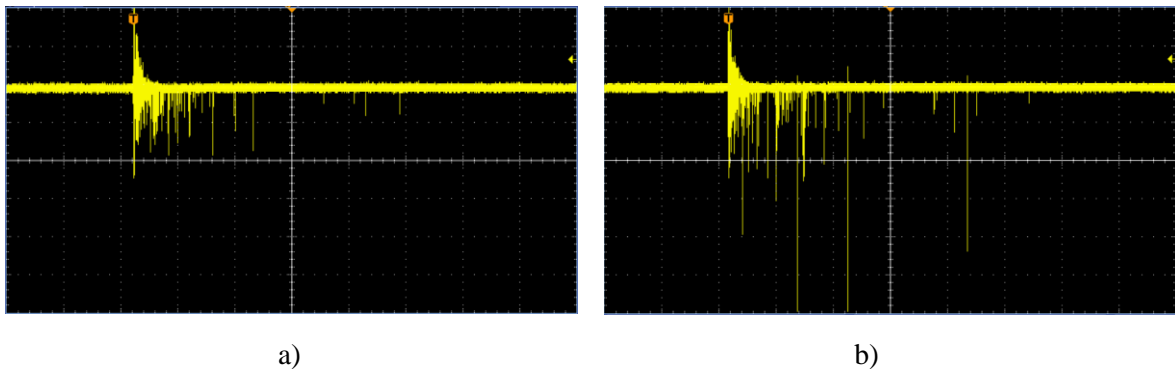

Figure 6. 60: a) Streamer light signal with spacer in mineral oil +100 kV (light signal- 50mV/division, time-4μs/division) b) Streamer light signal with spacer in mineral oil +105 kV (light signal- 50mV/division, time-4μs/division)

Breakdown voltage under postive polarity in mineral oil was at a similar level when compared to ester. Moreover, positive breakdown voltage was very close to the negative breakdown voltage. As previously mentioned, the positoining of the spacer and the exact distance between the windinng and the electrode could play important roles in determinming the breakdown voltage. However, the effect of the spacer itself on the breakdown voltage and the study of the accumulation effect in this electrode arrangement at different gaps would provide a better insight to the difference in streamer properties in mineral oil and ester. The postive streamer breakdown was accompamined by high intensity light signals with the total duartion of the breakdow process being 16us as shown in figure 6.61.
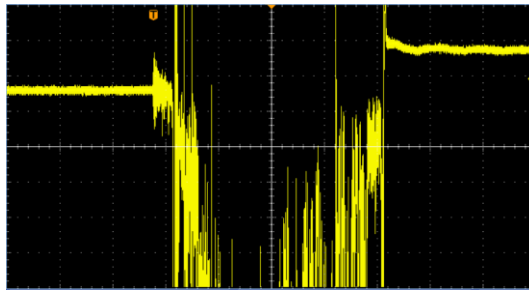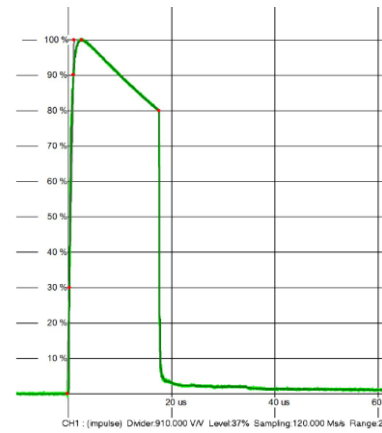
a)   b)

Figure 6. 61: a) Breakdown of transformer winding set up in mineral oil +112 kV (light signal- 100mV/division, time-4μs/division) b) Tail chopped LI waveform during breakdown

6.6 Statistical analysis- streamers under LI stress

Measurements were carried out 7 times in steps of 5 kV till breakdown to obtain statistics and repeatability of data during tests with the needle-PB-ground configuration. Appropriate amount of weighting time was given between each step as well as each test. Table 6.3 provides an approximate calculation of the number of pulses observed in the current signal for both liquids under negative polarity on an average as the pulses are more discrete when compared to the positive polarity. As indicated previously, steamer propagation occurs in steps where each step corresponds to a current and light pulse. Due to the high sensitivity of the PMT, the number of current pulses recorded are calculated for analysis and discussion. The time duration of streamer activity is analyzed with the help of light signals as the response from the PMT is more sensitive to the streamer phenomenon.

Voltage level(kV)	Ester -Number of pulses	Mineral Oil- Number of pulses	Ester -Time duration of light signal(us)	Mineral Oil- Time duration of light signal(us)
NEGATIVE POLARITY				
50	20-23	15-17	15-16	10-12
55	25-27	20-23	18-20	16-18
60	30-35	25-30	20-22	20-22
65	35-40	25-30	23-26	22-23
70	>45	25-30	25-27	24-26

Table 6. 3: Streamer signal analysis under impulse voltage for the needle-plane configuration - mineral oil and ester

129

From the table, it is evident that the streamer channel for ester has a significantly higher activity thereby indicating the presence of larger number of distinguished branches and offshoots. For both the liquids, the streamer duration increases with increase in applied voltage up to breakdown. The breakdown voltage levels are compared in figure 6.62 Though the streamer duration is lower for mineral at low voltages, it rises rapidly with the increase in voltage. This suggests that the stopping length of the streamer increases with higher voltages. Though the stopping length of the streamers could be higher at lower voltages for ester, on increasing the voltage, the streamer length for both liquids are similar for the given set up. Previous researchers have studied that the breakdown voltage, especially under negative polarity, is higher for mineral oil under divergent field set up in the absence of PB and this is observed during the measurements in Lodz University. The use of PB for the studies done in this thesis simulates a more likely situation in power transformers where both oil and PB is used as insulation. The higher difference in permittivity between the PB and mineral oil plays a crucial role in streamer properties and breakdown voltage as the creep stress over the PB impregnated with ester is lower. This is indicated in figure 6.62 from which it is clear that the breakdown voltage levels are similar for ester and mineral oil Here, the mean breakdown voltage of ester under negative polarity is 74.3 kV and under positive polarity is 50 kV. Mineral oil show similar results with mean BD voltage level of 50.8 kV under positive polarity and 75.7 kV under negative polarity. As expected, positive breakdown level is significantly lower for both liquids.
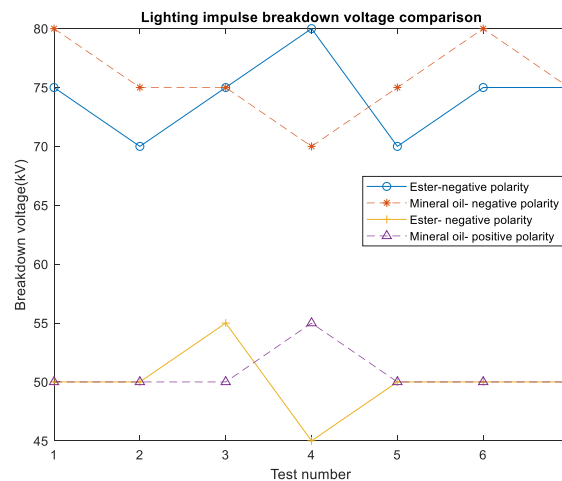
Figure 6. 62: LI breakdown voltage comparison between ester and mineral oil under needle-plane configuration

Another reason for the similar negative breakdown voltage levels between mineral oil and ester could be the accumulative effect on the negative streamers at the mineral oil/PB interface. Since the PB was not changed after each shot, the accumulation of pre stresses during the voltage rise before breakdown could have resulted in the lower breakdown levels of mineral oil than the expected levels. Thus, the acceleration voltage was likely reduced due to the effect of the PB as well as the accumulation effect of the impulses in case of mineral oil. It was also seen that the standard deviation of the BD levels under positive polarity is higher of mineral oil when compared to ester.

Figure 6.63 provides a graphical representation of the time duration to breakdown under different voltages for both polarities during 7 tests in the needle-plane configuration.
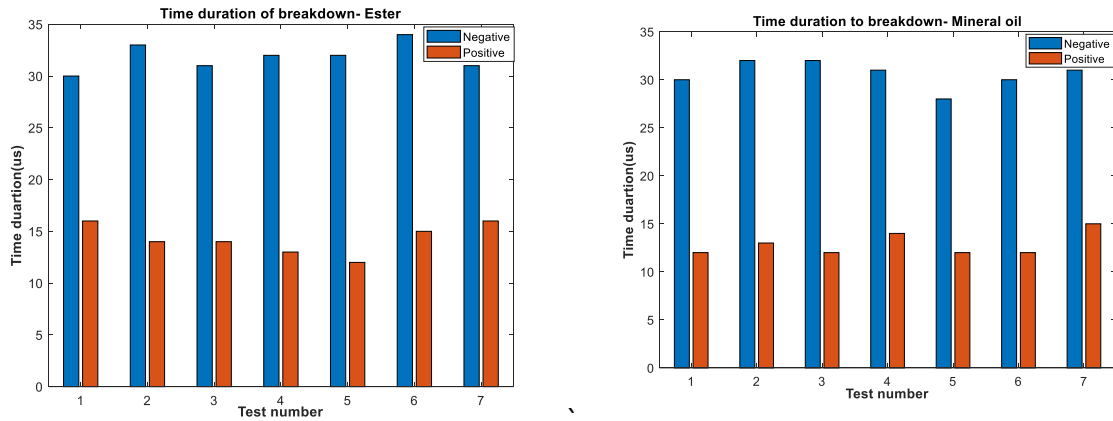
Figure 6. 63: a) Time duration to breakdown under both polarities for needle-plane configuration - ester b) Time duration to breakdown under both polarities for needle-plane configuration - mineral oil

The above figure provides further clarification about the filamentary nature of the positive streamer channel which lead to breakdown at lower voltages. For both liquids, the positive streamers result in breakdown much faster than the negative streamers. This could indicate that the positive streamers propagate at much higher velocities, resulting in a fast breakdown process. The lower breakdown levels under positive polarity suggests that the streamer length under positive polarity is longer and higher voltage has to be applied under negative polarity to reach similar stopping lengths. Lesser streamer signals are observed under the positive streamers because of the lesser number of branches and offshoots during propagation. The duration of time to breakdown is seen to be at similar levels for both liquids under both polarities. On further calculation, it can be seen that the standard deviation of the breakdown duration under positive polarity is slightly higher for ester.

During the propagation of streamers originating from the tip of the needle, significant increase in the amplitude of the streamer signal indicates a higher mode of propagation in the insulation. Figure 6.64 provides a clear picture of the maximum current magnitudes of the streamers observed under negative polarity after the first few us of streamer propagation in both liquids.
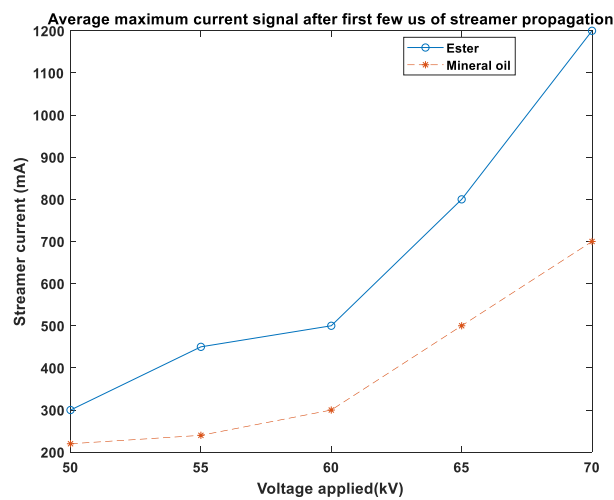
Figure 6. 64: Variation of streamer current signal with applied voltage for ester and mineral oil under needle-plane configuration

131

It is evident from the graph that the streamer current amplitudes are much higher in ester than mineral oil. Esters showed a significant increase in current magnitude with rising voltage suggesting that the streamers were branching out more frequently with higher number of offshoots. The higher amplitudes of current signal also indicates the faster modes of propagation of streamers. This means that the transition to higher modes of propagation is easier in esters when compared to the mineral oil, thereby increasing the probability to breakdown under esters. Streamers under mineral oil show significantly larger magnitude of currents during the first few us of streamer activity followed by a train of pulses with much lower amplitude. Negative streamers under ester grow in amplitude as the streamer propagates indicating that the streamer propagation is less hindered while propagating in ester. These large magnitudes of current signal seen during the final stages of the entire streamer signal indicate that the transition to higher modes of propagation is easier in ester. However, the presence of the PB resulted in similar breakdown levels for mineral oil and ester as mentioned previously.

Secondary reverse streamers were observed for both liquids under both polarities. However, the probability of occurrence of SRS was much higher in ester as shown in figure 6.65. The graph represents the number of times SRS were captured under negative polarity for different impulse voltages. Though SRS were recorded under positive polarity as well, the positive streamer inception was very close to the breakdown value, limiting the data available for analysis.
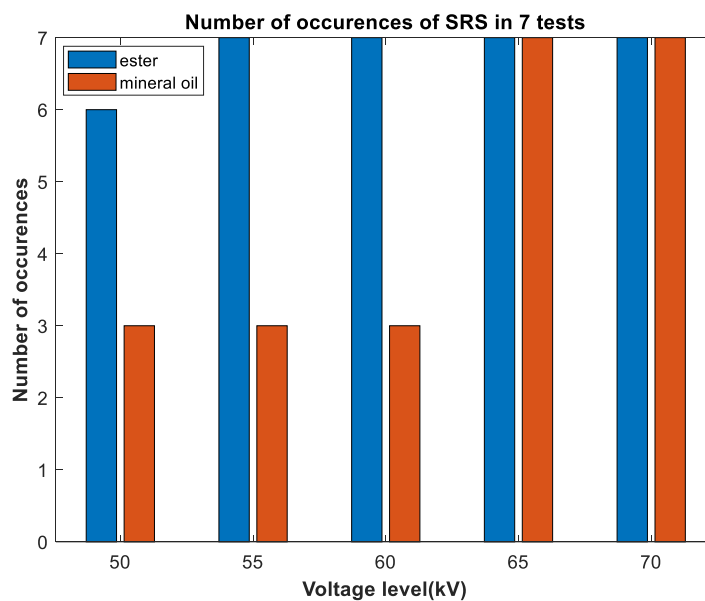
Figure 6. 65: Occurrence of SRS is ester and mineral oil under negative polarity for the needle-plane configuration

Secondary reverse streamers are recorded greater number of times at lower voltages under ester when compared to mineral oil. As mentioned before, the process of secondary reverse streamers involves the formation of a gaseous channel as well as space charge accumulation. The higher viscosity of ester could result in the slower dissipation of the gaseous channel after each impulse shot. Moreover, the electronegative molecules in ester aid the accumulation of space charges and hence, the difference in occurrence of SRS between both the liquids is noticed. In general, the occurrence of secondary reverse streamers is less frequent than what is seen during the experiments performed for this

thesis. This could be due to the presence of PB in these tests which could further enable the accumulation of space charges and aid the process of secondary reverse streamers.

The number of steps between the streamer inception voltage(SIV) and breakdown voltage for the winding-spacer configuration is shown in figure 6.67. Each step corresponds to a voltage of 5 kV. It can be seen that the streamers are recorded at similar voltage levels below the breakdown voltage under positive polarity and negative polarity for both liquids. Though the breakdown voltage itself could vary depending upon the winding used and the exact placement of the spacer, the difference between the streamer inception and breakdown suggests that positive streamers have a similar inception voltage when compared to negative streamers in this test configuration. This observation is contrary to the normal behavior of positive streamers which have an inception voltage very close to its breakdown voltage. This suggests that the presence of spacer between the winding and ground electrode plays a crucial role in streamer propagation in transformer insulation. Moreover, the presence of the spacer can also result in multiple sites for streamer initiation, thereby increasing the streamer activity. The presence of spacers could result in the higher number of offshoots during the positive streamer propagation, and increase the breakdown voltage level. However, it was seen that with the presence of the wooden blocks initially, streamers under positive polarity immediately lead to breakdown. This could possibly be due to the inability of the fiber cable to capture light from the ends of the winding. Also with the presence of the wooden blocks, the gap between the winding at the point of contact with the blocks and ground was much higher, resulting in a different field.
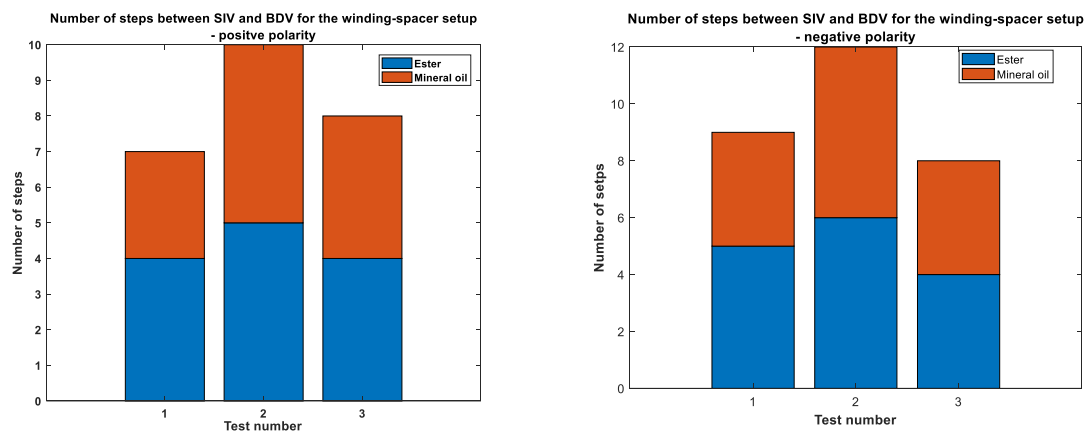
Figure 6. 66: a) Number of steps between SIV and BDV- positive polarity b) Number of steps between SIV and BDV- negative polarity

6.7 Summary

This chapter presents and analyzes the various results of the investigations performed to detect streamers in dielectrics using electrical and optical techniques. After several diagnostic analysis, suitable measurement set up was installed for the investigation of streamer phenomenon under DC and impulse voltages. Experiments performed in Lodz University of technology are also described in this chapter as they were very important in understanding the streamer detection process using optical method. Results obtained during the measurements performed in TU Delft provided useful information about the characteristic of streamers such as steamer current, intensity, shape in ester and mineral oil. Statistical analysis of the results during impulse tests are presented at the end of the chapter to provide

more insight about the difference between streamer propagation in ester and mineral oil. The chapter also describes the streamer signal originating from transformer winding in ester insulation and mineral oil. The effect of placing spacers between the winding and ground electrode is examined under both polarities. It was found that the spacers play a major role in increasing the streamer activity and reducing the breakdown voltage for both liquids. The breakdown voltage for the winding spacer configuration was similar under both liquids for both polarities suggesting that esters show similar impulse characteristics to mineral oil under real life electrode arrangements. These measurements and results will be very crucial for further testing with different electrode arrangements. The successful detection of streamers using these techniques will help in performing the tests involving more real-life electrode arrangements.

7. Conclusion and future work

This chapter summarizes the important results of the thesis obtained after several experiments and analyses. The findings of this thesis will prove to be crucial during the investigation of streamers and partial discharge with different electrode arrangements. Possible future work regarding the detection of streamers in more real-life samples have been discussed along with recommendations for improving the testing procedure.

7.1 Main conclusions

The primary goal of this thesis was the detection of pre-breakdown phenomenon in ester and mineral oil through electrical and optical techniques under impulse voltage. This section presents the important conclusions to the research questions formulated at the start of the thesis in two parts.

1. **Selection of right sensors for electrical and optical detection**
   Significant amount of work was performed during the course of this thesis to determine which optical and electrical sensor would give the best results for the detection of streamers. Though previous work on the optical detection of streamers exist, there are no existing guidelines on how to choose optical sensors for recording pre-breakdown phenomenon in dielectrics. Different parameters such as wavelength range, quantum efficiency, rise time, gain, SNR, dark current, cost, delivery time had to be studied before choosing the optical sensor. Based on these factors as well as other reasons such as ease of communication with the manufacturer, Thorlabs PMT 1001/M was purchased for the streamer detection. The choice of fiber bundle also involved several days of research to ensure that as much light emitted by the streamers was captured. Though investigations were conducted with different fiber bundles, the fiber bundle from FiberCable Connect, Germany was used for the final investigations in this thesis. With the help of experiments performed under the supervision of Professor Rozga and his team in Lodz university of Technology, the positioning of the optical fiber bundle and other details regarding the test set up were obtained. Streamer detection, especially under impulse voltages, using electrical sensors is a relatively newer field. Therefore, several experiments had to be performed before deciding the optimum measurement set up as presented in chapter 4. Measurements were initially carried out under DC before testing under impulse voltages. The electrical detection method was able to record the streamers effectively, although the optical detection technique proved to be more sensitive to the weaker streamer signals. The high sensitivity of the PMT resulted in the clipping of light signal during large streamer activity, the streamer current signal from the electrical detection was crucial to for analyses. The electrical detection also provided the polarity of the streamer signals.

2. **Difference in streamer activity between ester and mineral oil in needle-plane set up**
   Testing under DC as well as lighting impulse provided important information about streamer activity in ester and mineral oil. Difference in streamer signals under lightning impulse studies was slightly larger than those under DC tests. Since the

primary goal of this thesis was to detect streamers in ester, a divergent field set up was created in order to allow easy streamer propagation. Pressboards are commonly found in transformers and discharges produced in the transformers propagate along its surface due to tangential field. Surface discharges along a pressboard were simulated to understand the streamer activity at triple points under lightning impulse. After several tests, it was seen that streamers in ester propagate more easily and are more branched, especially under negative polarity, than in mineral oil. Tests performed using the rising voltage method up to breakdown suggested that the presence of PB had a greater effect on mineral oil than ester. Though it was expected that the breakdown voltage would be lower for ester, approximately same breakdown voltages were observed for both liquids. The PB reduced the acceleration voltage of mineral oil, although it did not have any effect on the streamer phenomenon itself. However, under non uniform fields, streamers propagating in ester are more likely to lead to breakdown when compared to mineral oil. The phenomenon for secondary reverse streamers was also captured during the tests. These streamers have a reverse polarity when compared with the primary streamers. The SRS phenomenon was more prominent in ester and was most likely induced due to the space charges in the oil. The presence of PB also aided this phenomenon.

3. **Detection of streamers originating from transformer winding under LI voltage in ester**

For the first time, a test set up for investigating streamer signal originating from windings insulated by paper in ester has been proposed in this thesis. Streamers were successfully detected optically and electrically under both polarities. Though the high sensitivity of the PMT resulted in its saturation during streamers in extremely divergent fields, it proved be advantageous during the detection of streamers in the winding configuration used in this thesis. The weaker streamer signals generated in this arrangement would limit the light signals emitted and hence were better detected by the PMT used in this thesis. However, the presence of noise signals during the current and light detection should be further investigated and eliminated. Investigations in ester under LI voltages suggested that streamers under negative polarity are more branched and propagate with lesser energy when compared to the positive streamers. While positive streamers are more filamentary during the initial stages of propagation, they gradually develop offshoots as the streamers propagate towards the opposite electrode. The presence of wooden blocks and spacers proved to be crucial in the generation of streamers suggesting that the streamers are most likely to develop at the triple point in different electrode arrangements. In most real life electrode arrangements as seen in figure 1.5, spacers are installed between the windings. Further studies with such arrangements could provide important details regarding the difference in streamer propagation between ester and mineral oil ,thereby affecting the breakdown process. When compared to the needle-PB-plane configuration, the secondary reverse streamer phenomenon observed under negative polarity was significantly different in the winding configuration. This was mainly due to the bigger geometry of the electrodes used in this set up when compared to needle-plane setup. On analyzing the streamer activity in mineral oil for the winding-spacer configuration, it was seen that fewer signals are recorded under negative polarity when compared to ester. Under positive polarity, mineral oil displays a slightly more branched streamer phenomenon when compared to ester. This indicates that streamers originating from windings propagate more easily in ester, especially under negative polarity. However, the breakdown voltage levels were similar for both liquids under both polarities indicating that the presence of spacers

between the windings affects the acceleration voltage of mineral oil more than that of ester. It was also observed that under the winding-spacer arrangement, the breakdown levels under both polarities were similar for both liquids.Positve streamer signals were recorded with higher number of signals when compared to the needle-plane configuration. The detection of streamers in ester and mineral under the winding configuration used in this thesis will prove to be crucial in understanding the difference in streamer activity between ester and mineral oil in more real-life electrode arrangements. The fiber bundle used in this thesis was successfully able to detect streamers at different locations on the winding and could be sensitive enough to detect streamers in larger real-life arrangements.

7.2 Future work and recommendations

In this thesis, streamer signals from windings on the surface of spacers were successfully detected. However, there were certain limitations to the investigations performed in this thesis. These limitations need to be addressed to ensure better results during future investigations.

- Though streamer signals could be detected using electrical techniques, the high sensitivity of the shunt hindered the measurements during large noise signals. The charging of the impulse generator and various other noise signals in the grid proved to be a problem during streamer detection under the winding configuration. Thus, proper shielding should be ensured for the shunt. Lower sensitivity of shunt can also be used, but it must be ensured that the electrical signals are free from oscillations.
- The PMT used in this thesis produced large amount of noise signals. Cooling the PMT down before use could eliminate these signals. Better SNR can be crucial in streamer detection under different winding arrangements.
- The presence of the spacer was important to understand the streamer difference in mineral oil and ester. However, it must be ensured the positioning of the spacer is more accurate during each test to better analyze the results obtained during different tests. The winding geometry should be as similar as possible for each test to ensure the gap between the winding and electrode is the same. Small gap differences could prove to be crucial in altering the streamer characteristics.
- The number of winding samples tested in this thesis is not enough to obtain a data spread. Higher number of windings are to be tested in order to have more conclusive results

Using this thesis as a guide, analysis of streamers in different electrode arrangement will be crucial for determining the viability of ester as transformer insulations. Research on the detection of streamers initiated from real-life winding configurations as shown in figure 1.5 has never been performed before and could be important in understanding the streamer characteristics in ester. Though streamers could be initiated due to protrusions on conductors, particles due to contamination, these scenarios are avoided as far as possible during the transformer design. Streamers initiated due to windings in such configurations represent a much more homogenous field which could alter its characteristics. The large size of the windings makes it harder to determine the exact initiation site for the streamers. Test set ups involving the Weidmann configuration could help in better validating the use of ester in power transformers. Studies done previously suggest that design modifications are necessary while using ester in transformers, but the extent of this could be determined by understanding the streamer initiation and breakdown process with different electrode arrangements. Investigations with different electrode arrangement involve different degrees

of inhomogeneity and therefore could be crucial in understanding the difference between streamer characteristics in ester and mineral oil. For example, experiments with tap changer contacts, as shown in figure 7.1, represent a more realistic electrode arrangement involving the divergent part of the transformer design. Study of streamer signals in these arrangements can help us understand the role of ester in promoting streamer propagation and validate its use as an alternate for transformer insulation.
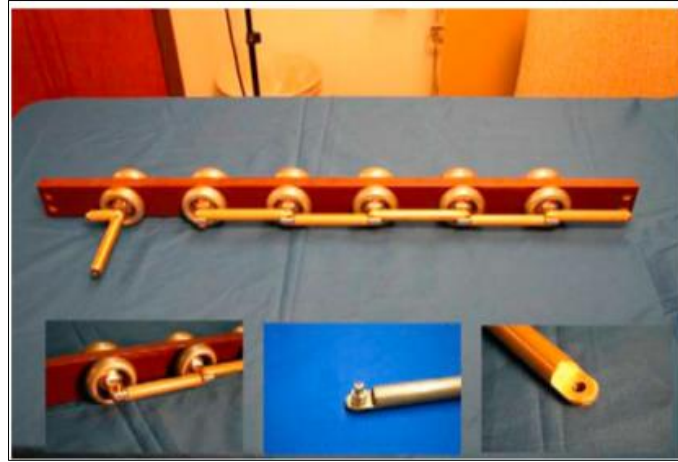
Figure 7. 1: Tap changer contacts used in transformers [46]

In order to effectively understand the streamer propagation in dielectrics, the use of high speed cameras play an important role. This enables us to better understand various characteristics such as stopping length, propagation velocity and streamer structure. The effect of spacer on different gaps between the winding and electrode have to be studied. Larger number of samples have to be tested to obtain more conclusive results. Accumulation effect has found to play a crucial role in the breakdown process especially for mineral oil. Tests involving multiple lightning impulse shots have to be analyzed in detail for the winding arrangements. The use of fluorescent polymer optical fiber (F-POF) could enable easier detection of discharges as they can be placed close to the set up without having to monitor the exact position of the fiber cable as in the case with the traditional fiber bundle. These fibers have previously been used to detect PD's in medium and high voltage applications. Fluorescent fibers are transparent in nature with the ability to absorb the light that fall through its cladding. A schematic diagram representing the working of the florescent fibers is shown in figure 7.2. Also, fiber optic interferometric sensors with intrinsic transducers situated along the length of the fiber can be used for the acoustic detection of discharges in transformer insulations.
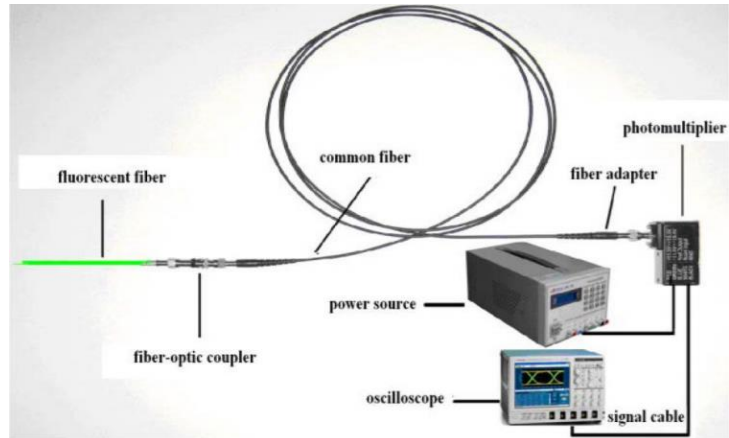
Figure 7. 2: Use of florescent fiber sensing for discharge detection [86]

As mentioned in chapter 1, test set ups have to also be investigated under different waveforms such as chopped impulse voltage and switching impulse voltage. Different duration of waveforms can also affect the breakdown strength of the insulation. The use of high speed imaging can provide more details on the primary propagation of streamers as well as the secondary reverse streamer phenomenon. Investigation with tail chopped impulse voltages have to be conducted to understand the mechanism of SRS phenomenon Polarity reversal and space charge effect should be further studied under different electrode configurations for application in HVDC transformers.

8. Bibliography

[1] E. Yuliastuti ,''Analysis of Dielectric Properties Comparison between Mineral Oil and Synthetic Ester Oil'', master thesis, TU Delft, 2010

[2] L.Lewand, "Laboratory evaluation of several synthetic and agricultural-based dielectric liquids", Doble Intern. Client Conf., Boston, US, paper.5E, 2001.

[3] Q. Liu and Z. D. Wang, "Streamer characteristic and breakdown in synthetic and natural ester transformer liquids with pressboard interface under lightning impulse voltage," in *IEEE Transactions on Dielectrics and Electrical Insulation*, vol. 18, no. 6, pp. 1908-1917, December 2011. doi: 10.1109/TDEI.2011.6118629

[4] Prevost, "Dielectric Properties of Natural Esters and their Influence on Transformer Insulation System Design and Performance," *2005/2006 IEEE/PES Transmission and Distribution Conference and Exhibition*, Dallas, TX, 2006, pp. 30-34. doi: 10.1109/TDC.2006.1668448

[5] Frotscher, R & Vukovic, Dejan & Jovalekic, M & Tenbohlen, Stefan & Harthun, J & Perrier, C & Schäfer, M. (2012)." Behaviour of ester liquids under dielectric and thermal stress - From laboratory testing to practical use." *44th International Conference on Large High Voltage Electric Systems* 2012.

[6]'' *Power transformers - Part 3: Insulation levels, dielectric tests and external clearances in air*' 'IEC 60076-3, December 2013

[7]: N. B. Timpe, "Partial Discharge Measurements in Distributed Parameter Systems: Cables", *Engineering Dielectric., Vol. I, Corona Measurements and Interpretation*, ASTM Special Tech. Publ. 669, pp. 134-175, 1979

[8] Batalović, Mirza & Sokolija, Kemo & Hadzialic, Mesud & Batalović, Nejra. (2016) ''Partial discharges and IEC standards 60840 and 62067: Simulation support to encourage changes''. 23. 589-598. 10.17559/TV-20141118124625.

[9][Online] Available: https://www2.le.ac.uk/departments/engineering/research/electrical-power/images/Electrical%20Tree.jpg/image_view_fullscreen [Accessed 10-Oct-2018]

[10] . H. Kreuger, "Partial Discharge", *Industrial High Voltage* Volume 2, Delft university Press, pg 117-157, 1992.

[11] T. W. Dakin, H. M. Philofsky and W. C Divens, "Effect of Electric Discharges on the Breakdown of Solid Insulation", *AIEE Trans.*, Vol. 73, pt. I, pp. 155-162, 1954.

[12] E. Kuffel,W.S. Zaengl,J. Kuffel, ''High Voltage Engineering- Fundamentals'' ISBN 0 7506 3634 3

[13] MHapeez, M. S., Abidin, A. F., Hashim, H., Hamzah, M. K., & Hamzah, N. R. (2013)."Analysis and classification of different types of partial discharges by harmonic orders.'' *Elektronika ir Elektrotechnika*, *19*(9), 35-41. DOI: 10.5755/j01.eee.19.9.2545

[14] D. Zmarzły, Ł. Nagi, S. Borucki, and T. Boczar, "Analysis of Ionizing Radiation Generated by Partial Discharges," *Acta Physica Polonica. A*, vol. 125, no. 6, pp. 1377–1379, Jun. 2014.

[15] Prawit Petchphung , Monthon Leelajindakrairerk, Norasage Pattanadech , Pearawut Yutthagowith , Kraision Aunchaleevarapan,''The comparison study of PD measurement with conventional method and unconventional method'' *2008 International Conference on Condition Monitoring and Diagnosis,* 21-24 April 2008

[16] El-Faraskoury, Adel & Mokhtar, Mostafa & Mehanna, Mohamed & , Ossma & Gouda, O.E.. (2012). ''Conventional and un-conventional partial discharge detection methods in high voltage XLPE cable accessories.''*Advances in Electrical Engineering Systems (AEES)* - 2167 - 633 X. 1.

[17] Tenbohlen, Stefan & Gulski, Edward & , Koltunowicz. (2016). ''Guidelines for partial discharge detection using conventional (IEC60270) and unconventional methods.'' *Electra.* 25-29.

[18] M. Ren, J. Zhou, B. Song, C. Zhang, M. Dong and R. Albarracin, "Towards Optical Partial Discharge with Micro Silicon Photomultiplier", *MDPI Sensors*, 2017.

[19] W. Chen, X. Chen, S. Peng, and J. Li, "Canonical correlation between partial discharges and gas formation in transformer oil paper insulation," *Energies*, vol. 5, no. 4, pp. 1081–1097, 2012.

[20] M. Yaacob, M & A. Alsaedi, M & Rashed, Jabbar & Dakhil, Adel & F. Atyah, S. (2014). ''Review on partial discharge detection techniques related to high voltage power equipment using different sensors.'' *Photonic Sensors.* 4. 10.1007/s13320-014-0146-7.

[21] A. Mukhtaruddin, M. Isa, M. R. Adzman, S. I. S. Hasan, M. N. K. H. Rohani and C. C. Yii, "Techniques on partial discharge detection and location determination in power transformer," *2016 3rd International Conference on Electronic Design (ICED)*, Phuket, 2016, pp. 537-542.doi: 10.1109/ICED.2016.7804703

[22] W. Hauschild and E. Lemke, ''High-Voltage Test and Measuring Techniques''.Springer, 2014.

[23] Z. Yin, R. Zhang, J. Tong, and X. Chen, "An all-fiber partial discharge monitoring system based on both intrinsic fiber optic interferometry sensor and fluorescent fiber," *International Conference on Optical Instrument and Technology: Optical Sensors and Applications,* 2013, vol. 9044, p. 904414.

[24] Z. Gacek, M. Szadkowski, G. Malitowski, F. Witos, and A. Olszewska, "Anusual Application of Partial Discharges to Diagnose of High Voltage Power Transformers," *Acta Phyica. Polonic A*, vol. 120, no. 4, pp. 609–615, 2011.

[25] Dr JP Holtzhausen Dr WL Vosloo. '' High Voltage Engineering Practice and Theory'' ISBN: 978 - 0 - 620 - 3767 - 7

[26] R. Tobazcon, "Prebreakdown phenomena in dielectric liquids," in *IEEE Transactions on Dielectrics and Electrical Insulation*, vol. 1, no. 6, pp. 1132-1147, Dec. 1994. doi: 10.1109/94.368650

[27] L. E. Lundgaard, D. Linhjell and G. Berg, "Streamer/leaders from a metallic particle between parallel plane electrodes in transformer oil," in *IEEE Transactions on Dielectrics and Electrical Insulation*, vol. 8, no. 6, pp. 1054-1063, Dec. 2001. doi: 10.1109/94.971465

[28] Pawel Rozga,'' Streamer Propagation and Breakdown in a Very Small Point-Insulating Plate Gap in Mineral Oil and Ester Liquids at Positive Lightning Impulse Voltage'' *Energies* 2016

[29] O. Lesaint, P. Gournay, A. Saker, R. Tobazeon, J. Aubin and M. Mailhot, "Streamer propagation and breakdown under AC in mineral oil for gaps up to 80 cm," *ICDL'96. 12th International Conference on Conduction and Breakdown in Dielectric Liquids*, Roma, Italy, 1996, pp. 251-254. doi: 10.1109/ICDL.1996.565450

[30] Farouk A.M. Rizk, Giao N. Trinh, '' High Voltage Engineering'', *CRC Press*, 2017

[31][Online] Available: https://en.wikipedia.org/wiki/Photomultiplier [Accessed 14-Nov-2018]

[32][Online] Available https://www.hamamatsu.com/resources/pdf/etd/PMT_handbook_v3aE-Chapter2.pdf [Accessed 10-Oct-2018]

[33] [Online] Available https://www.azooptics.com/Article.aspx?ArticleID=548 [Accessed 20-Jan-2019]

[34] G. Hudson, Gilbert & B. Loeb, Leonard. (1961),''Streamer Mechanism and Main Stroke in the Filamentary Spark Breakdown in Air as Revealed by Photomultipliers and Fast Oscilloscopic Techniques''. *Physical Review - PHYS REV X*. 123. 29-43. 10.1103/PhysRev.123.29.

[35] O. L. Hestad, S. Ingebrigsten and L. E. Lundgaard, "Streamer initiation in cyclohexane, Midel 7131 and Nytro 10X," *IEEE International Conference on Dielectric Liquids, 2005. ICDL 2005.*, Coimbra, Portugal, 2005, pp. 123-126. doi: 10.1109/ICDL.2005.1490042

[36] D. Martin and Z. D. Wang, "Statistical analysis of the AC breakdown voltages of ester based transformer oils," in *IEEE Transactions on Dielectrics and Electrical Insulation*, vol. 15, no. 4, pp. 1044-1050, August 2008. doi: 10.1109/TDEI.2008.4591226

[37] S. Chandrasekar and G. C. Montanari, "Analysis of partial discharge characteristics of natural esters as dielectric fluid for electric power apparatus applications," in *IEEE Transactions on Dielectrics and Electrical Insulation*, vol. 21, no. 3, pp. 1251-1259, June 2014. doi: 10.1109/TDEI.2014.6832272

[38] Q. Liu and Z. D. Wang, "Breakdown and withstand strengths of ester transformer liquids in a quasi-uniform field under impulse voltages," in *IEEE Transactions on Dielectrics and Electrical Insulation*, vol. 20, no. 2, pp. 571-579, April 2013. doi: 10.1109/TDEI.2013.6508761

[39] Y. Wang , Y.C. Chan , Z.L. Gui , D.P. Webb b, L.T. Li ,''Application of Weibull distribution analysis to the dielectric failure of multilayer ceramic capacitors'' *Material Science and Engineering: B* Vol 47, Issue 3, 1997, 197-203

[40][online] Available: https://www.weibull.com/hotwire/issue14/relbasics14.htm [Accessed 12-Nov-2018]

[41] R M Hill and L A Dissado ,''Theoretical basis for the statistics of dielectric breakdown'', *Journal of Physics C: Solid State Physics,* Volume 16, Number 11

[42] D. M. Mehta, P. Kundu, A. Chowdhury, V. K. Lakhiani and A. S. Jhala, "A review on critical evaluation of natural ester vis-a-vis mineral oil insulating liquid for use in transformers: Part 1," in *IEEE Transactions on Dielectrics and Electrical Insulation*, vol. 23, no. 2, pp. 873-880, April 2016. doi: 10.1109/TDEI.2015.005370

[43] T. A. Prevost, "Dielectric properties of natural esters and their influence on transformer insulation system design and performance — An update," *2009 IEEE Power & Energy Society General Meeting*, Calgary, AB, 2009, pp. 1-7. doi: 10.1109/PES.2009.5275167

[44] Cigre A2-35 '' Experiences in service with new insulating liquids''Working Group A2-35, 2010

[45] V. Dang, A. Beroual and C. Perrier, "Comparative study of streamer phenomena in mineral, synthetic and natural ester oils under lightning impulse voltage," *2010 International Conference on High Voltage Engineering and Application*, New Orleans, LA, 2010, pp. 560-563. doi: 10.1109/ICHVE.2010.5640765

[46] Mark Lashbrook, Attila Gyore, Russell Martin ''A review of the fundamental dielectric characteristics of ester-based dielectric liquids '', *Procedia Engineering 202* (2017) 121–129

[47] Z. Dianchun, W. Zhengwei, C. Chuntian and Y. Weiguo, "Discharge characteristics of streamer in liquid dielectric under lightning impulse voltage," *2013 Annual Report Conference on Electrical Insulation and Dielectric Phenomena*, Shenzhen, 2013, pp. 971-974. doi: 10.1109/CEIDP.2013.6748197

[48] Nijdam, S. (2011). ''Experimental investigations on the physics of streamers'' Eindhoven: *Technische Universiteit Eindhoven* DOI: 10.6100/IR693618

[49] Jianqi Qin and Victor P Pasko ''On the propagation of streamers in electrical discharges'' *Journal of Physics D: Applied Physics*, Volume 47, Number 43, 3 October 2014

50] Hongxin Ji, Yangchun Cheng, Chengrong li, Kai Chen, Chun Deng and Shaoyu Liu, "The developing rules of partial discharge in the inter-turn insulation of transformers under constant AC voltage," *2012 International Conference on High Voltage Engineering and Application*, Shanghai, 2012, pp. 219-224. doi: 10.1109/ICHVE.2012.6357025

[51] V. Sokolov, Z. Berler and V. Rashkes, "Effective methods of assessment of insulation system conditions in power transformers: a view based on practical experience," *Proceedings: Electrical Insulation Conference and Electrical Manufacturing and Coil Winding Conference (Cat. No.99CH37035)*, Cincinnati, OH, USA, 1999, pp. 659-667. doi: 10.1109/EEIC.1999.826289

[52] Carlos Gustavo Azcarraga Ramos, Andrea Cavallini, Ugo Plovan, '' A Comparison of the PDIV characteristics of ester and mineral oils'' *IEEE Insulation Magazine*, Sep-Oct 2014

[53] Z. D. Wang, Q. Liu, X. Wang, P. Jarman and G. Wilson, "Discussion on possible additions to IEC 60897 and IEC 61294 for insulating liquid tests," in *IET Electric Power Applications*, vol. 5, no. 6, pp. 486-493, July 2011. doi: 10.1049/iet-epa.2010.0209

[54] Xin Wang, ''Partial discharge behavior and breakdown mechanism of ester transformer liquids under AC stress'', PhD thesis, University of Manchester, 2011

[55] Othman, Nur & Zainuddin, Hidayat & Aman, A & Ab Ghani, Sharin & Ahmad Khiar, Mohd Shahril & Sutan Chairul, Imran & Talib, Mohd. ''Investigation on the degradation behavior of creepage discharge on pressboard immersed in palm fatty acid ester (PFAE) oil'' 2016, 78. 31-36. 10.11113/jt.v78.9759.

[56] X. Yi and Z. D. Wang, "Surface tracking on pressboard in natural and synthetic transformer liquids under AC stress," in *IEEE Transactions on Dielectrics and Electrical Insulation*, vol. 20, no. 5, pp. 1625-1634, Oct. 2013. doi: 10.1109/TDEI.2013.6633692

[57] Fernando Álvarez, Fernando Garnacho, Javier Ortego, and Miguel Ángel Sánchez-Urán ''Application of HFCT and UHF Sensors in On-Line Partial Discharge Measurements for Insulation Diagnosis of High Voltage Equipment'', *Sensors(Basel)*, Apr 2015 doi: 10.3390/s150407360

[58] T N Tran, I O Golosnoy, P L Lewin, G E Georghiou. ''Numerical modelling of negative discharges in air with experimental validation'' *Journal of Physics D: Applied Physics*, IOP Publishing, 2011, 44 (1), pp.15203

[59] M. Pompili and R. Bartnikas, "On partial discharge measurement in dielectric liquids," in *IEEE Transactions on Dielectrics and Electrical Insulation*, vol. 19, no. 5, pp. 1476-1481, October 2012. doi: 10.1109/TDEI.2012.6311489

[60] P. M. Mitchinson, P. L. Lewin, B. D. Strawbridge and P. Jarman, "Tracking and surface discharge at the oil-pressboard interface," in *IEEE Electrical Insulation Magazine*, vol. 26, no. 2, pp. 35-41, March-April 2010. doi: 10.1109/MEI.2010.5482553

[61] X. Yi and Z. Wang, "Creepage discharge on pressboards in synthetic and natural ester transformer liquids under ac stress," in *IET Electric Power Applications*, vol. 7, no. 3, pp. 191-198, 3 2013. doi: 10.1049/iet-epa.2012.0303

[62] H. Illias, Teo Soon Yuan, A. H. A. Bakar, H. Mokhlis, G. Chen and P. L. Lewin, "Partial discharge patterns in high voltage insulation," *2012 IEEE International Conference on Power and Energy (PECon)*, Kota Kinabalu, 2012, pp. 750-755.
doi: 10.1109/PECon.2012.6450316

[63] V. Rai, K. Pandey and K. Wadhwa, "Designing of multistage impulse voltage generator using ATP software," *2015 International Conference on Recent Developments in Control, Automation and Power Engineering (RDCAPE)*, Noida, 2015, pp. 276-279.doi: 10.1109/RDCAPE.2015.7281409

[64] Online Available: https://www.thorlabs.com/newgrouppage9.cfm?objectgroup_ID=2909
[Accessed November 1st, 2018]

[65] [Online] Available: https://en.wikipedia.org/wiki/Photomultiplier Accessed September 20, 2018

[66] [Online] Available https://www.hamamatsu.com/resources/pdf/etd/PMT_handbook_v3aE-Chapter2.pdf Accessed September 20,2018

 [67] [Online] Available https://www.azooptics.com/Article.aspx?ArticleID=548 [Accessed September 20,2018]

[68]*PMT 1000 Series Photomultiplier Tube User Guide,* Thorlabs Inc, August 1,2017

[69] Online Available: http://www.technobis.com/themes/fibre-optic-sensing/ [Accessed November 22, 2018]

[70]Online Available: https://www.fibrecableconnect.de/en/products-services/optical-fiber-bundle/ [Accessed November 22, 2018]

[71] R. Schwarz, M. Muhr and S. Pack, "Partial discharge detection in oil with optical methods," *IEEE International Conference on Dielectric Liquids, 2005. ICDL 2005.*, Coimbra, Portugal, 2005, pp. 245-248. doi: 10.1109/ICDL.2005.1490072

[72]Pawel Rozga, Marcin Stanek, Bartlomiej Pasternak,'' Characteristics of Negative Streamer Development in Ester Liquids and Mineral Oil in a Point-To-Sphere Electrode System with a Pressboard Barrier'' *Energies*, 28th April, 2018

[73] R. E. Hebner '' Measurement of Electrical Breakdown in Liquids'', pages 519–537. *Springer US*, Boston, MA, 1988.

[74] O. Lesaint and G. Massala. ''Positive streamer propagation in large oil gaps: experimental characterization of propagation modes.'' *IEEE Transactions on Dielectrics and Electrical Insulation*, 5(3):360–370, Jun 1998.

[75] O. Lesaint and G. Massala. ''Transition to fast streamers in mineral oil in the presence of insulating solids''. In Conference Record of the *1996 IEEE International Symposium on Electrical Insulation*, volume 2, pages 737–740 vol.2, 1996

[76] Jian Bin Ben Chen. ''Light Emission of Streamers in Dielectric Liquids'', Master Thesis, Norwegian University of Science and Technology, 2017

[77] R. E. Jorgenson, L. K. Warne, A. A. Neuber, J. Krile, J. Dickens, and H. Krompholz.'' Effect of dielectric photoemission on surface breakdown'': An LDRD report. 2003.

[78] G. Massala and O. Lesaint, "Positive Streamer Propagation in Large Oil Gaps'', *IEEE Transactions on Dielectric and Electrical Insulation* 5 (1998) 371-381

[79] D. Linhjell, L. Lundgaard and G. Berg, ''Streamer Propagation under Impulse Voltage in Long Point-plane Oil Gaps'', *IEEE Transactions on Dielectric and Electrical Insulation* 1 (1994) 447-458.

[80] J. Xiang, Q. Liu and Z. D. Wang, "Inception and breakdown voltages of insulating liquids under DC stress," *2016 IEEE International Conference on High Voltage Engineering and Application (ICHVE)*, Chengdu, 2016, pp. 1-4. doi: 10.1109/ICHVE.2016.7800894

[81] Xiang, J & Liu, Q ,''Current and emitted light characteristics of streamers in insulating liquids under ac voltages''. *The 19th International Symposium on High Voltage Engineering (ISH)*, Pilsen, Czech Republic, 23/08/15, in *host publication.* pp. 295, .

[82] Liu, Qiuming & Wang, Zhongdong. "Secondary reverse streamer observed in an ester insulating liquid under negative impulse voltage". *Journal of Physics D: Applied Physics.*, 2011, 44. 405203. 10.1088/0022-3727/44/40/405203.

[83] B. Lehouidj, S. Sahra, A. Nacer, H. Moulai and A. Beroual, "Streamer currents, emitted lights and energies into dielectric liquids submitted to DC stress," *2014 IEEE 18th International Conference on Dielectric Liquids (ICDL)*, Bled, 2014, pp. 1-4.doi: 10.1109/ICDL.2014.6893146

[84] O. Lesaint, P. Gournay, and R. Tobazeon, "Investigations on Transient Currents Associated with Streamer Propagation in Dielectric Liquids," *IEEE Transactions on Electrical Insulation,* vol. 26, pp. 699-707, 1991.

[85] Qiang Liu, ''Electrical performance of ester liquids under impulse voltage for application in power transformers'' ,PhD thesis, University of Manchester, 2011

[86] Jiabin Zhou, Shandong "Partial Discharge OpticalPulse Signal Characteristics for Corona Defect in Oil Immersed Transformer." *Research Journal of Applied Sciences, Engineering and Technology*: 3052-3056, 2013 ISSN: 2040-7459

[87] Haegele Stephanie, Vahidi Farzaneh, Tenbohlen Stefan, Rapp Kevin, Sbravati, Alan "Lightning Impulse Withstand of Natural Ester Liquid." *Energies.* , 2018, 11. 1964. 10.3390/en11081964.

[88] W. Lu, Q. Liu and Z. Wang, "Mechanisms of streamer leading to breakdown in synthetic ester liquid in uniform field," *2017 IEEE 19th International Conference on Dielectric Liquids (ICDL)*, Manchester, 2017, pp. 1-4. doi: 10.1109/ICDL.2017.8124651

Appendix A

A.1 ATP-EMTP software description

Electromagnetic Transient program, version Alternative transient program(EMTP-ATP) is a non- commercial digital simulation program used for analysing transients such as switching transients, overvoltage protection, relay settings, control systems especially in electrical power systems. Various models including rotating machines, transformers, transmission lines, cables, surge arrestors are available for transient and steady state analysis. EMTP was originally developed by H.W Dommel, who started his work in Munich Institute of Technology and later continued it in Bonneville Power Administration ,USA. EMTP is based on the application of trapezoidal rule to convert the differential 4 equations of the network components to algebraic equations. Non-zero conditions can be determined automatically by steady state or in some cases entered by the user for simpler components. EMTP allows symmetrical and unsymmetrical disturbances, making it ideal for analysing faults, lightning surges and switching actions. The FREQUENCY SCAN feature enables the frequency response of phasor networks. Modules such as TACS(Transient analysis of control systems) and MODELS(simulation language) enables modelling of control systems and components with non-linear characteristics such arcs and corona.

In this report, the ATP, which is the royalty-free version of EMTP is used for transient analysis. Electrical circuits have been modelled using interactive graphical pictures provided by ATPDraw, which is a graphical, mouse driven processor for ATP on Windows platform.

A.2 ATPdraw models used in this thesis

The ATPdraw models used in this thesis to simulate the lighting impulse waveform and the current signal detected by the shunt as seen in section 4.1.2.2 are presented below. Though 2 stages of the impulse generator is modelled, the output is taken from the first stage as shown in figure 8.1. The breakdown process is simulated with the help of a switch as shown in figure 8.2. The values of the resistors and capacitors used have been previously mentioned in chapter 4.
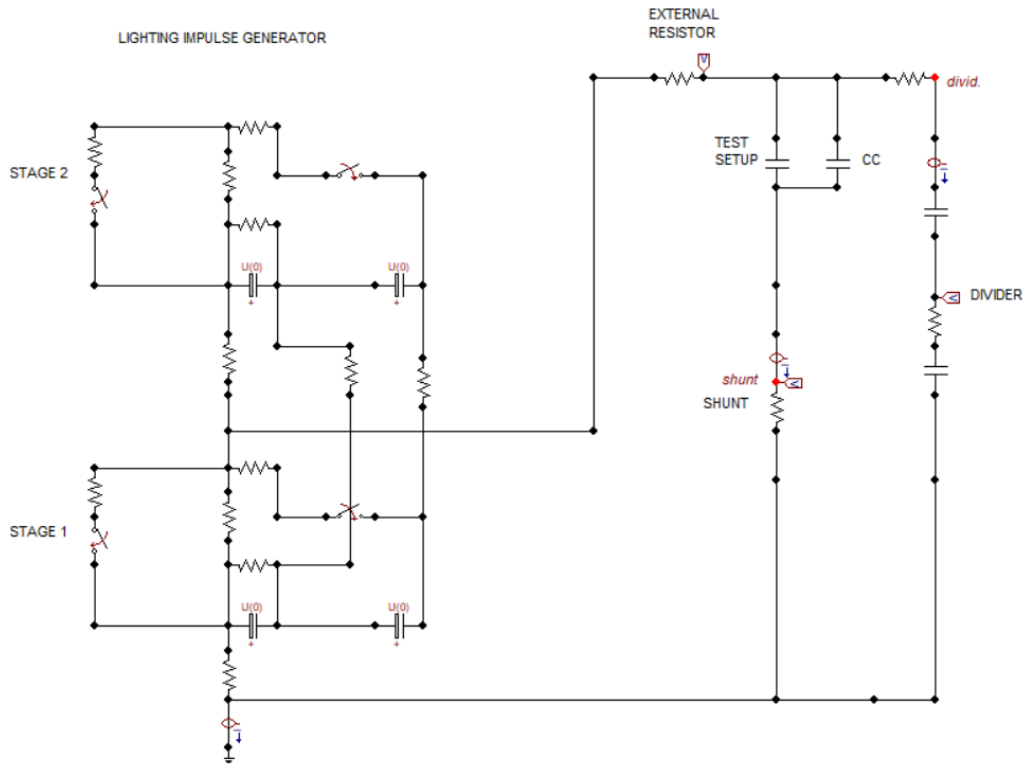
Figure A. 1: ATPdraw model to simulate electrical test set up used in this thesis under needle-plane arrangement
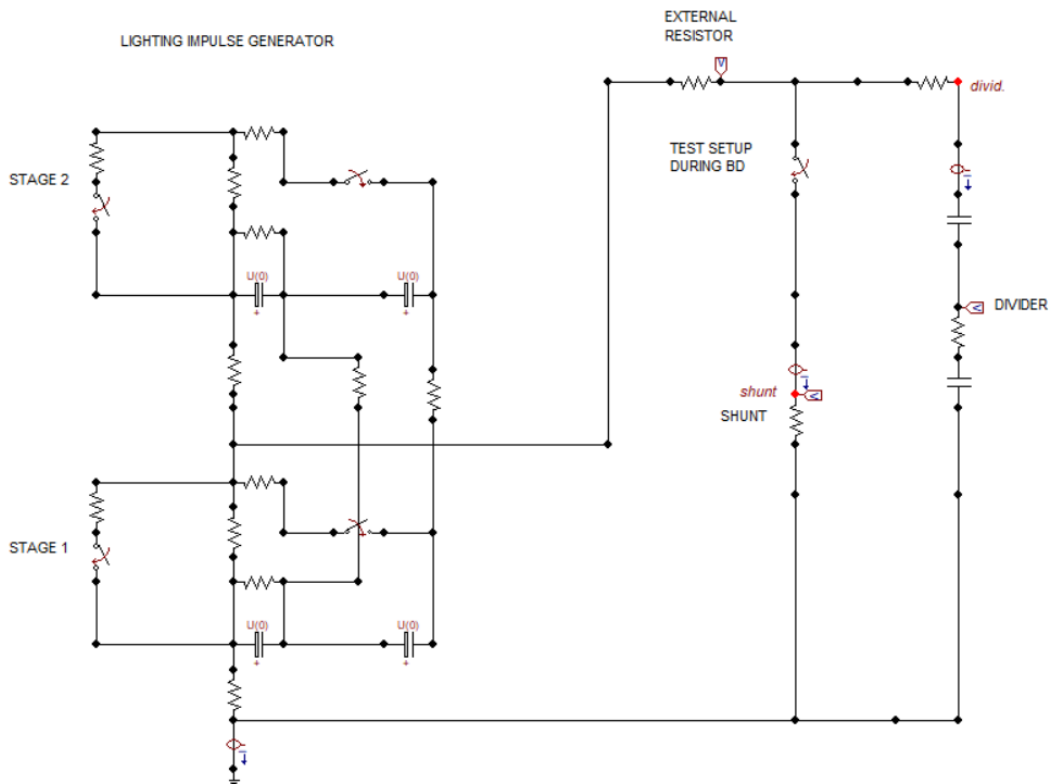

Figure A. 2: ATPdraw model to simulate BD in the electrical test set up used in this thesis under needle-plane arrangement

147